Biomaterials Science

ROYAL SOCIETY OF CHEMISTRY

REVIEW

View Article Online
View Journal | View Issue

Cite this: *Biomater. Sci.*, 2025, **13**, 2836

Osteoimmunomodulation by bone implant materials: harnessing physicochemical properties and chemical composition

Mehdi Sanati, *[a] Ines Pieterman,[b] Natacha Levy,[c,d] Tayebeh Akbari,[e] Mohamadreza Tavakoli,[f] Alireza Hassani Najafabadi[g] and Saber Amin Yavari *[a,d]

Received 6th March 2025,
Accepted 21st April 2025

DOI: 10.1039/d5bm00357a

rsc.li/biomaterials-science

Chronic inflammation at bone defect sites can impede regenerative processes, but local immune responses can be adjusted to promote healing. Regulating the osteoimmune microenvironment, particularly through macrophage polarization, has become a key focus in bone regeneration research. While bone implants are crucial for addressing significant bone defects, they are often recognized by the immune system as foreign, triggering inflammation that leads to bone resorption and implant issues like fibrous encapsulation and aseptic loosening. Developing osteoimmunomodulatory implants offers a promising approach to transforming destructive inflammation into healing processes, enhancing implant integration and bone regeneration. This review explores strategies based on tuning the physicochemical attributes and chemical composition of materials in engineering osteoimmunomodulatory and pro-regenerative bone implants.

1. Introduction

Bone tissue has a remarkable ability to regenerate, but critical-sized bone defects often require medical intervention.[1] While autograft bone transplantation has been the gold standard, it has notable drawbacks, particularly at the donor site.[2] As an alternative, bone implants provide scaffolds that support tissue healing by offering biological signals, physical support, and delivering bioactive molecules or cells. They also help mobilize the body's cells to the injury site.[3,4] In this context, bone tissue engineering with carefully designed bioactive implant materials has gained significant interest. These implants go beyond merely serving as load-bearing structures or drug delivery systems; they leverage the regenerative properties of bone tissue to effectively address bone defects.[5]

The bone healing process begins with an inflammatory response, which is crucial for initiating regeneration. However, this inflammation must be precisely regulated in both intensity and duration. If not properly controlled, excessive or prolonged inflammation can disrupt subsequent healing stages and hinder bone regeneration.[1,6] Excessive inflammatory responses to implanted bone materials can lead to complications such as fibrous encapsulation and aseptic loosening of the implant.[7,8] Therefore, the development of immunomodulatory bone implant materials offers a promising strategy to convert these excessive inflammatory reactions into pro-healing signals. This approach not only enhances implant osseointegration but also strengthens the bone's intrinsic healing capacities.[9–11] Research has clearly shown that the physicochemical properties, such as the shape and size of released particles, stiffness, topography, hydrophilicity, and surface potential, as well as the chemical composition of materials, including both biodegradable and non-biodegradable metals and natural and synthetic polymers, significantly influence local immune responses at the implantation site.[12–14] This review provides an updated analysis of the latest advancements, advantages, and limitations of osteoimmunomodulatory biomaterials while exploring current strategies for optimizing their properties. Compared to existing studies, this work not only offers a comprehensive and comparative assessment of biomaterials, delivering deeper insights, but also covers a broader range of polymers essential for synthesizing novel bone implants. In conjunction with existing literature, this review serves as a valuable resource for guiding future strategies in immunomodulatory material design.

[a]*Department of Orthopedics, University Medical Center Utrecht, Utrecht, The Netherlands. E-mail: m.sanati@umcutrecht.nl, s.aminyavari@umcutrecht.nl*
[b]*Utrecht Institute for Pharmaceutical Sciences, Faculty of Science, Utrecht University, Utrecht, The Netherlands*
[c]*Metabolic Diseases Pediatrics Division, University Medical Centre Utrecht, Utrecht, The Netherlands*
[d]*Regenerative Medicine Centre Utrecht, Utrecht University, Utrecht, The Netherlands*
[e]*Department of Microbiology, Islamic Azad University, North Tehran Branch, Tehran, Iran*
[f]*Department of Pharmaceutical Nanotechnology, Faculty of Pharmacy, Tehran University of Medical Sciences, Tehran, Iran*
[g]*Terasaki Institute for Biomedical Innovation, Los Angeles, CA, USA*

2. Contribution of the immune system to tissue regeneration

The immune system plays a crucial role in coordinating inflammatory processes to defend against threats and restore homeostasis. Following tissue injury, damage-associated molecular patterns (DAMPs) and pathogen-associated molecular patterns (PAMPs) effectively activate the immune system and trigger local inflammation, prompting resident immune cells in the tissue to produce inflammatory molecules. These molecules then recruit additional immune cells from the bloodstream to the site of injury.[15–17] The innate immune response to tissue injury involves monocytes, neutrophils, and macrophages; nevertheless, when insufficient, the adaptive immune response, which includes B and T lymphocytes, is activated to eliminate the remaining threats.[18] Beyond their conventional role in eliminating damaged cells and pathogens, immune cells actively regulate tissue healing by modulating cell growth, differentiation, and angiogenesis, thereby facilitating regeneration. However, prolonged immune activation can sustain inflammation and disrupt the healing process (Fig. 1).[13,19,20] This section briefly outlines both the positive and negative impacts of various immune cell responses on tissue repair.

2.1. Neutrophils

Neutrophils, the first immune cells migrating to damaged tissue, detect DAMPs and PAMPs through their pattern recognition receptors, regulating their polarization. The inflammation triggered by DAMPs and PAMPs leads to vasodilation and increases the permeability of local blood vessels, facilitating neutrophil migration to the site of injury.[21,22] Neutrophils easily squeeze through narrow spaces between tissue cells and the extracellular matrix (ECM); once they arrive at the injury site, they eliminate pathogens by releasing potent antimicrobials and forming neutrophil extracellular traps (NETs). NETs are web-like structures composed of proteins assembled on a scaffold of decondensed chromatin, which effectively trap, neutralize, and destroy various pathogens.[23–25] NETs are primarily released through a cell death pathway known as NETosis; however, it requires careful regulation, as the non-specific cytokines secreted by neutrophils can cause tissue damage and hinder the healing process.[24,26,27] For instance, epithelial healing and wound closure were accelerated in neutropenic mice compared to normal controls.[28] Consistently, neutrophil apoptosis helped resolve inflammation and promote tissue repair.[29,30] Moreover, regulatory T cells (Tregs) contribute to resolving local inflammation, crucial for tissue healing, by upregulating interleukin (IL)-10 and transforming growth factor-beta (TGF-β) expression while suppressing pro-inflammatory IL-6 production by neutrophils.[31,32]

At the injury site, neutrophils release interferons, such as IFN-γ, which recruit macrophages and other immune cells through the toll-like receptor 9 (TLR9) pathway.[33–35] In turn,

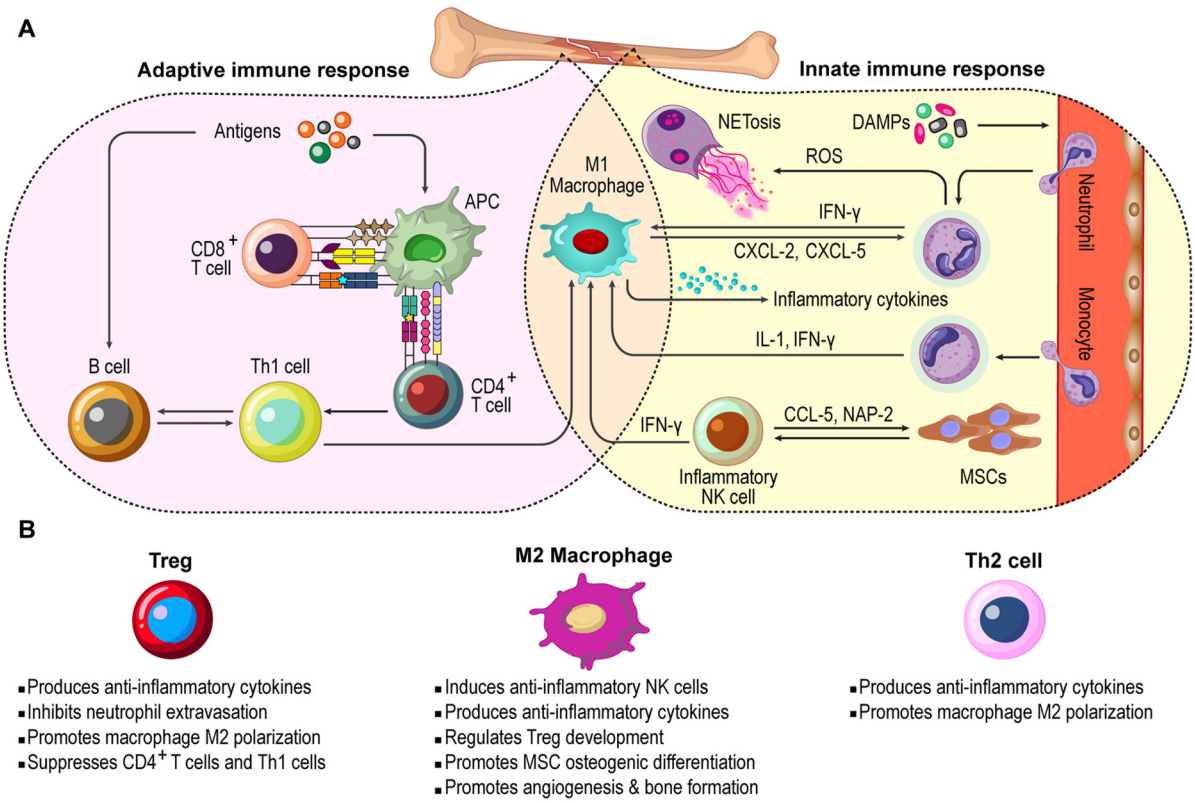

Fig. 1 Immune system, inflammation, and bone regeneration. (A) Schematic representation of inflammatory innate and adaptive responses during bone lesions. (B) The participation of immune cells in reducing long-term inflammation at the bone injury site. For details, see text.

macrophages secrete neutrophil chemoattractants, like CXCL-2 and CXCL-5, *via* the TLR9-myeloid differentiation primary response gene 88 (MyD88) pathway, drawing more neutrophils to the lesion site.[36] While the accumulation of neutrophils might be seen as potentially harmful to tissue regeneration due to their role in sustaining inflammation, they also secrete proteases that can damage host tissue and delay healing.[37] However, neutrophils likely play a positive role in tissue repair by promoting angiogenesis, tissue cell proliferation, and ECM remodeling. They achieve this by secreting factors such as vascular endothelial growth factor (VEGF), various growth factors, and matrix metalloproteinases (MMPs).[37–39]

2.2. Monocytes and macrophages

Monocytes undergo phenotypic and functional changes at lesion sites to aid in inflammation and tissue repair.[40] Chemoattractant protein (MCP) and chemokine receptors (CCR-2 and CCR-5) attract inflammatory monocytes to lesions, where they differentiate into M1 macrophages and produce cytokines like IL-6 and tumor necrosis factor-alpha (TNF-α), thereby contributing to tissue cleanup and pathogen elimination, MSC recruitment and differentiation towards osteoblasts, and angiogenesis. However, prolonged M1 activation can impede bone regeneration by inducing chronic inflammation and triggering MSC apoptosis.[41–43] Conversely, anti-inflammatory monocytes differentiate into M2 macrophages to resolve inflammation and promote tissue repair through secreting IL-10, which regulates Treg development, and TGF-β, which supports bone healing by influencing endothelial and osteogenic cells.[42,44–47] Numerous studies have highlighted the mentioned beneficial effects of M2 macrophage polarization on bone regeneration.[48–50]

2.3. T cells and other immune cells

Various T cells play different roles in tissue regeneration. $CD8^+$ T cells hinder osteogenic processes by stimulating osteoclasts and promoting mesenchymal stem cells (MSCs) apoptosis.[51,52] Various subsets of $CD4^+$ T cells play distinct roles in tissue healing. Type 1 T helper (Th1) cells promote inflammation through secreting IFN-γ, which negatively affects bone formation, while Th2 cells release IL-4 and IL-13, which promote M2 polarization of tissue-resident macrophages.[53,54] Regulatory T cells (Tregs) help reduce inflammation by inhibiting neutrophil extravasation and IL-6 production, encouraging neutrophil apoptosis, downregulating inflammatory monocyte activity, upregulating M2 macrophages, and suppressing $CD8^+$ T cells and Th1-mediated inflammation.[55–64] Another important player in bone healing is γδ T cells, which secrete IL-17 and stimulate the proliferation of mesenchymal progenitor cells, facilitating osteoblastic differentiation.[65]

Osteoclasts, known for bone resorption, exhibit immune-responsive properties. Pro-inflammatory cytokines, such as TNF-α, produced by immune cells, enhance osteoclast activity, whereas their inhibition reduces bone loss in osteoporosis models.[66,67] Regarding the literature, T cells play a significant role in regulating osteoclasts differentiation and function. Activated T cells express receptor activator of nuclear factor kappa-B ligand (RANKL) to promote osteoclast differentiation, while Tregs suppress osteoclast formation through cytokines like IL-10 and TGF-β as well as direct cell–cell interactions *via* cytotoxic T-cell associated protein 4 (CTLA-4) binding to CD80/86 on osteoclast precursors.[68–70] Th1 and Th2 cells also release factors that stimulate B cell differentiation, leading to the production of mediators like TNF-α and TGF-β. These mediators affect osteoclast differentiation process, thereby contributing to the regulation of bone metabolism.[10]

NK cells respond to inflammation following tissue damage and contribute to bone repair by clearing necrotic tissue and secreting neutrophil-activating protein 2 (NAP-2) and CCL-5 to recruit MSCs.[71] MSCs can mutually enhance NK cell-mediated inflammation and IFN-γ and TNF-α release during the early stage of tissue injury.[72,73] However, MSCs suppress NK cell proliferation and cytokine secretion and induce their polarization into anti-inflammatory phenotypes during the healing phase.[73–75] Additionally, MSC-derived TGF-β and IL-6 promote NK cell senescence, which in turn enhances MSC-driven VEGF expression, facilitating tissue regeneration.[73] Similarly, under the influence of M2 macrophage-derived IL-10 and TGF-β, most NK cells acquire a regulatory phenotype, contributing to tissue repair and regeneration. It is also worth mentioning that NK cells can modulate M1 and M2 macrophage polarization based on the immune response phase.[76]

Other immune cells also play roles in tissue healing. Generally speaking, B lymphocytes aid tissue regeneration by regulating neutrophil infiltration, increasing growth factors, and reducing MMP-2 activity.[77] However, in bone tissue, B lymphocytes may have different effects. Activated B lymphocytes inhibit osteoblastogenesis in bone MSCs by activating Notch signaling.[78] Memory B lymphocytes promote alveolar bone degradation and osteoclastogenesis during periodontitis by inducing cytokine expression and the proliferation of Th1 and Th17 cells.[79] Mature B lymphocytes influence osteoclastogenesis by producing RANKL and osteoprotegerin.[80] Dendritic cells (DCs) can also interfere with tissue regeneration by producing IFN-γ and promoting inflammation.[81] Mast cells have dual roles: they attract monocytes to injury sites and promote inflammation but also produce anti-inflammatory cytokines to reduce inflammation.[82,83] This information underscores the importance of understanding immune cell functions in tissue regeneration. Immunomodulatory strategies, therefore, hold significant promise for enhancing tissue healing, including bone regeneration.

3. The foreign body reaction (FBR): immune cells react to implant materials

The host immune responses to bone implants determine their quality of integration and function. The acute sterile inflammatory reaction, also called foreign body reaction (FBR),

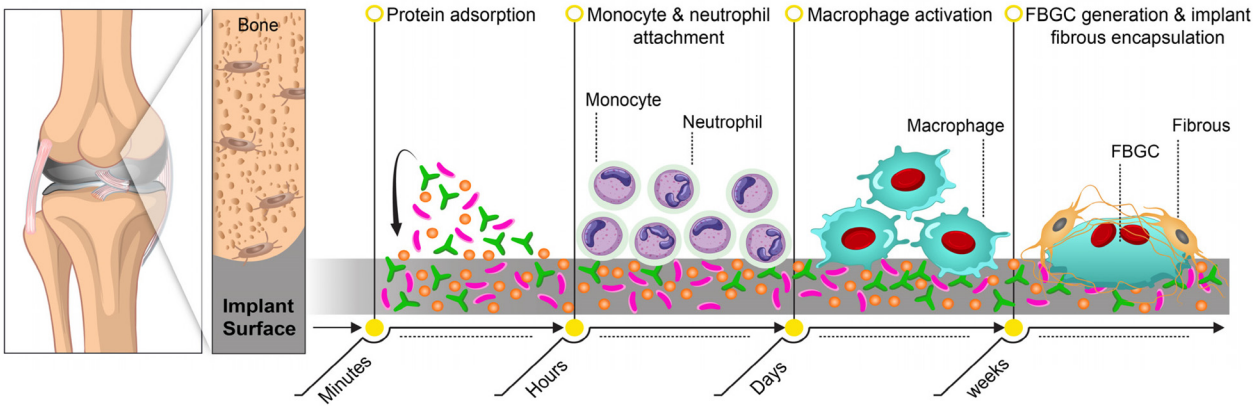

Fig. 2 Schematic representation of FBR to bone implant materials.

renders implant fibrotic encapsulation, limiting its interaction with the host tissue (Fig. 2).[8] Implantation damages local blood vessels, leading to plasma protein adsorption (albumin, fibronectin, vitronectin) that facilitates immune cell adhesion.[84] The resulting exudate contains platelets and coagulation factors, forming clots that release TGF-β, CXCL-2, and CXCL-8, attracting neutrophils.[85] These neutrophils bind to protein-coated implants *via* integrins, become activated, and amplify inflammation, recruiting more immune cells. Persistent neutrophil activation and CXCL-8 secretion sustain inflammation, delaying healing.[86,87] Activated neutrophils release NETs to target implants, but excessive NET formation can sustain fibrosis, leading to a dense matrix that hinders tissue-implant integration.[88] They also secrete CCL-2 and CCL-4, recruiting inflammatory monocytes that adhere to implant proteins and differentiate into M1 macrophages.[87] Chemotactic factors from blood clots further amplify monocyte recruitment, increasing the M1 macrophage population.[89,90] These macrophages release inflammatory chemokines, reactive oxygen species (ROS), and degrading enzymes, exacerbating tissue damage.[91,92] Due to the implant's size, macrophages undergo frustrated phagocytosis and transition to an anti-inflammatory M2 phenotype. This shift promotes macrophage fusion into foreign body giant cells (FBGC), which persist on the implant surface, leading to fibrous encapsulation and hindering integration.[93,94] Inflammatory T cells further enhance macrophage adhesion and fusion.[95,96]

Evidence suggests that DCs play a role in this process, with implant protein composition shaping their immune interactions. Plasma proteins activate DCs *via* TLRs; for example, albumin induces IL-10 production, reducing inflammation and supporting regeneration, while vitronectin interactions may enhance inflammatory CD4+ T cell responses.[97] Various implant surface characteristics, such as chemistry, roughness, and topography, can alter the protein layer composition, leading to different immune reactions.[98–100] These insights highlight the importance of surface engineering in implants to foster favorable immune responses for bone regeneration.

4. Engineering immunomodulatory implants for bone regeneration

Extensive research has demonstrated the significant impact of the immune system on tissue healing.[101,102] Beyond minimizing adverse immune reactions, there is increasing interest in designing implants that actively regulate local immune responses to promote bone regeneration.[103,104] This section explores bone implant materials with intrinsic immunomodulatory properties that support both integration and bone healing. Strategies to regulate immune cell polarization and behavior include modifying physicochemical properties at the material-host interface and optimizing chemical composition (Fig. 3).

4.1. The impact of physicochemical features of implants

The physicochemical properties of bone implants, including particle size and shape, surface topography, potential, stiffness, and hydrophilicity, play a crucial role in regulating local immune cell function and inflammatory responses upon implantation.[105–107] Understanding this provides a valuable opportunity to develop immunomodulatory bone implants, which help minimize the FBR, improve implant integration, and steer immune responses toward bone healing (Table 1).

4.1.1. Shape and size of released particles. The size and shape of particles released from metallic implants or incorporated into engineered implants are critical factors when evaluating their immunomodulatory effects. Nano-sized hydroxyapatite particles (HAPs) have been shown to promote bone healing by improving implant mechanical properties, supporting bone mineralization, and assisting in the elimination of residual tumor cells after osteosarcoma surgery.[108–110] Lebre *et al.* demonstrated that HAPs influence innate immune responses in mice by modulating NLRP3 inflammasome activation and IL-1β secretion, depending on their size and shape. Small (0.1 and 5 μm) needle-shaped HAPs induced greater cytokine release and inflammatory responses compared to smooth, spherical particles of the same size or larger particles

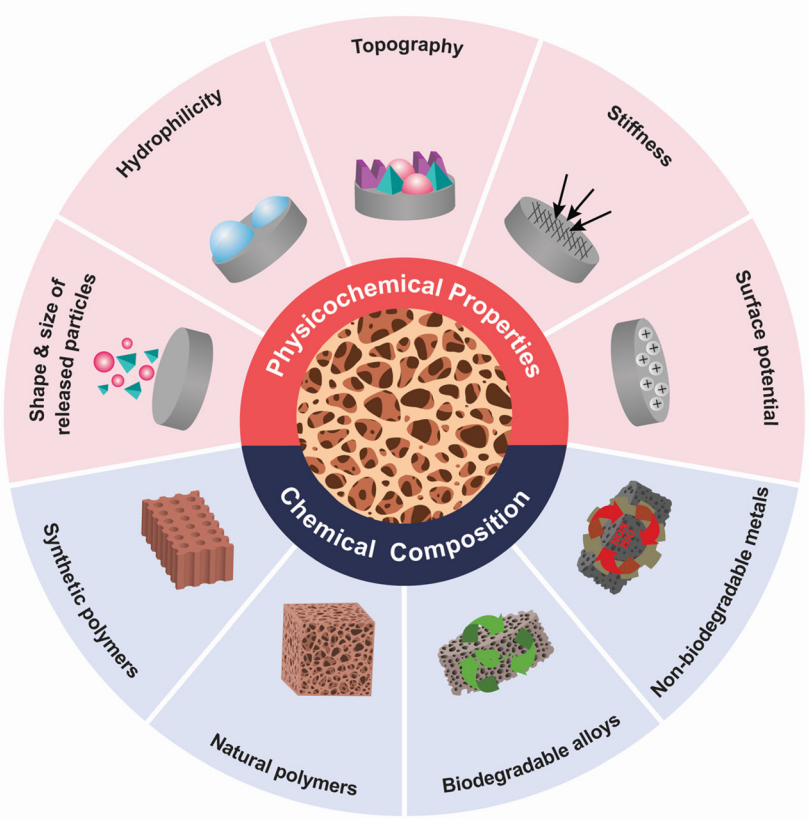

Fig. 3 Critical factors affecting the immunomodulatory function of bone implant materials.

(100 μm). This was linked to increased neutrophil and eosinophil recruitment by needle-shaped HAPs. These results suggest that adjusting HAP properties could help modulate immune responses after implant insertion.[111] Another study in dogs found that inflammation resolved more quickly at the implant site of round HAPs in buccal soft tissue compared to sharp-edged particles.[112] The effects can be attributed to the characteristics of HAPs, where irregular or sharp shapes provide a larger surface area for protein absorption, triggering stronger tissue responses.[113] Additionally, particles with rough surfaces can destabilize lysosomal and phagosomal membranes, triggering inflammasome activation.[114]

Considering particle size, smaller particles probably tend to induce stronger pro-inflammatory immune responses. Gil *et al.* found that among irregularly shaped titanium (Ti) particles from dental implants, smaller particles (5 and 10 μm) significantly increased pro-inflammatory markers like TNF-α and IL-1β compared to larger particles (15 and 30 μm). Interestingly, 15 μm particles also upregulated anti-inflammatory markers such as TGF-β and IL-10 more than the control or smaller particles. This is particularly important in dentistry, as procedures used in oral implantology to eliminate bacterial biofilm from the implants' surface, *e.g.*, milling the Ti surface or employing rough Ti implants, often result in a considerable release of particles.

Smaller particles tend to induce stronger pro-inflammatory immune responses. Gil *et al.* found that irregularly shaped titanium (Ti) particles from dental implants, particularly smaller ones (5 and 10 μm), significantly increased pro-inflammatory markers like TNF-α and IL-1β compared to larger particles (15 and 30 μm). Interestingly, 15 μm particles upregulated anti-inflammatory markers such as TGF-β and IL-10 more than smaller particles or control.[115] This is relevant in dentistry, where procedures like milling or using rough Ti implants often release particles that affect immune responses.[115,116] The size effect is likely due to the increased surface area of smaller particles, which enhances protein attachment and immune cell activation compared to larger particles.[114]

Generally, irregularly shaped particles induce stronger inflammatory responses than spherical ones, with smaller, rougher particles more likely to provoke inflammation than larger, smoother ones. However, irregular particles with high curvature or needle-like shapes are particularly effective at activating inflammasomes (*i.e.*, intracellular multiprotein complexes of the innate immune system that trigger inflammatory responses) due to frustrated phagocytosis, ROS leakage, and inflammasome activation.[114] This highlights the substantial influence of implants-released particle size and shape. However, given that the chemical composition of implants is also a crucial factor, a comparative analysis of various implants

Table 1 The impact of physicochemical properties of bone implants on their osteoimmunomodulation

Properties	Material	Type of study	Value	Immunomodulation	Ref.
Shape & size of release particles	HAPs	*Ex vivo*	0.1 and 5 μm needle-shaped	Provoked cytokine release and inflammation in comparison to smooth spherical particles of the same size or bigger particles (100 μm).	111
		In vivo	Round-shaped	Inflammation resolved faster at the implantation site compared to sharp-edged particles.	112
	Ti particles	*In vitro*	5 and 10 μm	Upregulated pro-inflammatory markers (TNF-α and IL-1β) compared to larger particles (15 μm) that upregulated anti-inflammatory markers (TGF-β and IL-10).	115
Stiffness	GelMA	*In vitro*	1.5 kPa	Upregulated ROS production and pro-inflammatory factors (CXCL-10 and TNF-α) released by neutrophils compared GelMA with higher stiffness (5.7 kPa) that induced an anti-inflammatory phenotype in neutrophils.	118
			10 and 29 kPa	Induced macrophage M1 polarization and upregulated pro-inflammatory cytokines (TNF-α and IL-6) compared to surfaces with lower stiffness (2 kPa).	122
	PDMS	*In vitro*	8–32 kPa	Promoted NETosis and induced the secretion of pro-inflammatory factors (IL-10, TNF-α, CCL-2, CCL-3, and CCL-5) compared to PDMS surfaces with lower stiffness.	119
			>100 kPa	Upregulated IL-2 generation and CD4+ and CD8+ T cell multiplication and expanded IFN-γ-producing Th1-like cells in comparison to substrates with much higher stiffness (>2 MPa).	131
	Polyacrylamide	*In vitro*	34.88 ± 4.22 kPa	Induced macrophage M2 polarization compared to hydrogels with low (2.55 ± 0.32 kPa) or high (63.53 ± 5.65 kPa) stiffness.	121
			2.55 ± 0.32 kPa	Induced macrophage M1 polarization compared to hydrogels with medium (34.88 ± 4.22 kPa) or high (63.53 ± 5.65 kPa) stiffness.	
			70 kPa	Induced macrophage M2 polarization compared to hydrogels with lower (10 kPa) stiffness.	124
			323 kPa	Enabled M1 macrophage polarization compared to gels with less stiffness (11 and 88 kPa) that primed macrophage M2 polarization.	126
			50.6 ± 15.1 kPa	Upregulated pro-inflammatory IL-2 production by Jurkat T cells compared to the softer hydrogel (7.1 ± 0.4 kPa).	130
			7.5–140 kPa	Treg induction augmented with greater material stiffness.	132
			100 kPa	Potentiated TCR-induced CD4+ T lymphocyte migration, proliferation, and morphological shift.	129
	Culture plates	*In vitro*	64 kPa	Upregulated macrophage M2 polarization compared to culture plates with low stiffness (0.2 kPa).	176
	Transglutaminase cross-linked gelatin	*In vitro*	60.54 ± 10.45 kPa	Polarized macrophages into the M1 phenotype and upregulated IL-1β, TNF-α, and iNOS expression compared to low-stiffness gelatin (1.58 ± 0.42 kPa) that upregulated M2 polarization.	125
Topography	Zn plates	*In vitro*	Rough surface with micro-topographies	Attenuated inflammatory macrophage polarization.	139
	Ti implant	*In vitro*	Smooth surface	Upregulated M1 inflammatory macrophages as well as IL-1β, IL-6, and TNF-α expression compared to hydrophilic rough Ti that upregulated M2 anti-inflammatory macrophages and IL-4 and IL-10 expression.	137
				Induced neutrophil inflammatory responses, provoking pro-inflammatory macrophage polarization compared to the rough Ti surface.	140
			Surface micro/nano topographies	Stimulated macrophage polarization towards the pro-healing M2 phenotype.	149
				Provoked RAW264.7 macrophage M2 polarization and IL-10 expression and downregulated IL-1β compared to Ti surfaces with micron or nano topographies.	147

Table 1 *(Contd.)*

Properties	Material	Type of study	Value	Immunomodulation	Ref.
		In vitro & in vivo		Reduced DC inflammatory responses compared to Ti surfaces with only micro-topographies.	177
		In vitro	HC-like surface structures	Nano-scale surface structures expanded the M2 macrophage population, upregulated anti-inflammatory cytokines (IL-4 and IL-10) and lowered pro-inflammatory cytokines (IL-1β and TNF-α) compared to micro-scales and the un-patterned Ti surface.	150
		In vivo	Surface 30 nm nanotubes	Enhanced macrophage recruitment and regulated their polarization and cytokine profiles towards anti-inflammatory responses compared to larger nanotubes (50, 70, and 100 nm).	152
		In vitro	Micro/sub-micro hierarchical surface structure	The biomimetic surface structure hindered inflammatory reactions mediated by M1 macrophages by repressing the TLR2/NF-κB signaling.	158
	TPS-Ti	*In vitro*	Surface nanowires	Caused non-activated or LPS-activated macrophages to adopt a less inflammatory profile.	153
	Hydroxyapatite ceramics	*In vitro & in vivo*	Surface nano-topographies (~100 nm)	Promoted macrophage M2 polarization and attenuated pro-inflammatory cytokine secretion compared to surfaces with micro-topographies (~500 nm).	145
	Fibrous membranes		Surface latticed topography	Upregulated M2 macrophage marker genes compared to other random and aligned surface topographies.	151
	PLA membranes	*In vitro*	Bone topography mimicking surface structure	COL1 and hydroxyapatite-modified membranes with natural bone-mimicking surface topography induced a sequential and synergistic polarization of M1 and M2 macrophage.	159
Hydrophilicity	Ti implant	*In vitro*	Heparin and fibronectin-functionalized hydrophilic surface	Showed a lower capacity in provoking pro-inflammatory cytokines (TNF-α, MCP-1, and IL-1β) secretion compared to Ti surfaces with lower hydrophilicity.	161
			Hydrophilic-modified SLA-treated surface	Induced M1 to M2 macrophage phenotypic alteration and decreased inflammatory genes (TNF, IL-1β, CXCL-8) expression levels compared to the SLA-treated surface that upregulated M1 macrophages.	163
			Graphene oxide-coated SLA-treated surface	The graphene oxide coating enhanced surface hydrophilicity and promoted macrophage M2 polarization compared to the SLA-treated surface.	165
			Hydrogenated surface Ti dioxide nanotubes	Showed enhanced surface wettability, thereby eliciting macrophage M2 polarization, upregulating anti-inflammatory cytokines (IL-10, BMP-2, and TGF-β1) and downregulating LPS-induced pro-inflammatory cytokines (TNF-α, MCP-1, and IL-6).	166
			Rough and hydrophilic surface	Reduced pro-inflammatory cytokine and enzyme generation and inhibits NETosis compared to neutrophils cultured on rough Ti surfaces.	140
				Increasing surface roughness and wettability elicited a Th2 pro-wound-healing phenotype and resolved inflammation.	167
	PET base biomaterials	*In vivo*	Hydrophilic and anionic surfaces	Reduced monocyte adhesion and macrophage fusion into FBGC while also causing harmful macrophages to undergo apoptosis.	178
Surface potential	Ti implant	*In vitro & in vivo*	Polydopamine-coated surface	The coated surface exhibited less negative potential and a greater tendency to switch macrophages towards the M2 phenotype, which provoked pro-healing cytokine secretion.	171
	Polyether urethane	*In vivo*	Sulphonate substituted negative surface	20% sulphonate substitution caused less neutrophil infiltration compared to 10% or 30% sulphonate substitution.	172
	PEO-coated gold nanorods	*In vitro*	Carboxyl or amino-modified surfaces	Negatively charged carboxyl groups could push macrophages toward the M1 phenotype, whereas positively charged amino surface groups could push them toward the M2 phenotype.	174

Abbreviations: HAPs; hydroxyapatite particles, Ti; titanium, TNF-α; tumor necrosis factor-alpha, IL; interleukin, TGF-β; transforming growth factor-beta, GelMA; gelatin methacrylate, ROS; reactive oxygen species, CXCL; (C–X–C motif) ligand, PDMS; polydimethylsiloxane, CCL; C chemokine ligand, TCR; T cell receptor, iNOS; inducible nitric oxide synthase, DC; dendritic cell, HC; honeycomb, TLR; toll-like receptor, NF-κB; nuclear factor kappa B, LPS; lipopolysaccharide, PLA; poly-L-lactic acid, COL1; type I collagen, MCP-1; monocyte chemoattractant protein, SLA; sand-blasted, large-grit, acid-etched, BMP-2; bone morphogenetic protein 2, PET; polyethylene terephthalate, FBGC; foreign body giant cells, PEO; polyethylene oxide.

under identical conditions, considering these parameters, could offer a more precise understanding of the phenomenon.

4.1.2. Stiffness. Matrix stiffness has garnered significant attention in bone regeneration mechanobiology, as it plays a critical role in osteogenic processes by regulating immune responses to implanted materials.[107,117] More rigid matrixes might develop anti-inflammatory and pro-healing neutrophils through activating the Janus kinase-1 (JAK1)/signal transducer and activator of transcription 3 (STAT3) signaling.[118] Neutrophils cultured in 3D gelatin methacrylate (GelMA) hydrogel with low stiffness (1.5 kPa) showed increased ROS production and higher secretion of pro-inflammatory chemokines (*e.g.*, CXCL-10) and cytokines (*e.g.*, TNF-α). In contrast, neutrophils cultured in the hydrogel with higher stiffness (5.7 kPa) exhibited increased gene expression of CD206 (a marker of anti-inflammatory neutrophils) and CXCL-12 (which inhibits inflammatory cell migration) and elevated IL-10 secretion.[118] However, when seeded on polydimethylsiloxane (PDMS) surfaces with varying stiffness (0.2–32 kPa), neutrophils on stiffer surfaces (8–32 kPa) showed increased NETosis and higher secretion of pro-inflammatory cytokines and chemokines. This is driven by the activation of focal adhesion kinase (FAK), which regulates immune cell attachment and function through integrin-mediated interactions.[119]

Implant stiffness might also regulate macrophage polarization by affecting the ROS-initiated nuclear factor kappa B (NF-κB) pathway.[120] Chen *et al.* showed that bone marrow-derived macrophages (BMDMs) cultured on polyacrylamide hydrogels with medium stiffness (34.88 ± 4.22 kPa) expressed more M2 macrophage marker CD206 and secreted higher levels of IL-4 and TGF-β, compared to those on low (2.55 ± 0.32 kPa) or high (63.53 ± 5.65 kPa) stiffness hydrogels. Macrophages on low-stiffness hydrogels exhibited higher ROS production and M1 markers, such as CD86, IL-1β, and TNF-α. Morphologically, macrophages on medium-stiffness hydrogels had a spindle-like shape (M2), while those on low or high stiffness had a pancake-like shape (M1) (Fig. 4 and 5). Implantation studies in mice confirmed that hydrogels with medium stiffness attracted more M2 macrophages, while low stiffness attracted more M1 macrophages.[121] However, conflicting data exist. Zhuang *et al.* found that macrophages seeded on GelMA hydrogels with 10 and 29 kPa exhibited an M1 phenotype and higher secretion of pro-inflammatory cytokines (TNF-α and IL-6) compared to those on lower stiffness surfaces (2 kPa).[122] Liu *et al.* showed that high-stiffness biomaterials (64 kPa) increased the M2 macrophage population, promoting osteogenic differentiation of adipose-derived MSCs and secretion of immunomodulatory proteins (LBP and RBP4) to enhance bone healing.[123] Additionally, polyacrylamide hydrogels with 70 kPa stiffness induced platelet activation during hemostasis, which improved M2 macrophage polarization, angiogenesis of endothelial cells, and osteogenesis of bone marrow-derived MSCs (BMMSCs) compared to hydrogels with lower stiffness (10 kPa).[124]

Several studies suggest that macrophages tend to polarize towards the M1 phenotype on high-stiffness matrices. For example, macrophages on high-stiffness (60.54 ± 10.45 kPa) transglutaminase cross-linked gelatin exhibited M1 polarization, marked by increased expression of IL-1β, TNF-α, and inducible nitric oxide (iNOS), which negatively impacted osteogenic differentiation of BMMSCs. In contrast, macrophages on low-stiffness gelatin (1.58 ± 0.42 kPa) showed higher levels of CD206 and IL-10.[125] Mei *et al.* found that BMDMs cultured on polyacrylamide gels with high stiffness (323 kPa) exhibited M1 polarization through Piezo1/YAP signaling, while gels with lower stiffness (11 and 88 kPa) promoted M2 polarization.[126] Other studies also reported that macrophages on substrates with lower stiffness tend to adopt the M2 phenotype.[127,128]

T cells are also sensitive to mechanical cues, with material stiffness influencing T cell receptor-induced migration and morphological changes in $CD4^+$ T lymphocytes. However, their metabolism and cell cycle are only affected by very high stiffness levels, such as 100 kPa.[129] Consistently, Chin *et al.* demonstrated that Jurkat T cells cultured on a stiff polyacrylamide hydrogel (50.6 ± 15.1 kPa) produced significantly higher levels of the pro-inflammatory cytokine IL-2 compared to those on a softer hydrogel (7.1 ± 0.4 kPa).[130] Another study discovered that substrates with a stiffness lower than 100 kPa induce a four times higher IL-2 generation and human $CD4^+$ and $CD8^+$ T cell multiplication compared to substrates with a much higher stiffness (>2 MPa). When naive $CD4^+$ T cells were grown on softer substrates, there was a 3-fold expansion in the proportion of IFN-γ-producing Th1-like cells.[131] However, Tregs induction on polyacrylamide gels with stiffness ranging from 7.5 to 140 kPa was shown to be augmented with greater material stiffness, which involved a more significant use of oxidative phosphorylation (OXPHOS).[132] These findings highlight that material stiffness around 100 kPa may stimulate T cell-mediated inflammatory responses, while surfaces with lower stiffness promote Treg induction, aiding in inflammation resolution.

The conflicting data on material stiffness and immune cell-mediated bone regeneration highlight the need for studies using standardized bone defect models. This underscores the importance of considering multiple implant-mediated signals in osteoimmunomodulation and bone regeneration. It is also important to note that the mechanical strength of a bone scaffold should be comparable to that of the surrounding bone tissue. If the scaffold is excessively stiff, it can result in stress shielding and bone resorption, which may, in turn, trigger immune responses.[133] Dense metallic materials generally possess a substantially higher Young's modulus than natural bone, leading to stress shielding during implantation. To mitigate this effect, a key strategy in metallic implant design is to reduce stiffness by introducing a porous structure, thereby enhancing compatibility with the mechanical properties of natural bone. In this regard, fabrication techniques, such as powder metallurgy in combination with other methods, have been widely employed to develop porous metallic scaffolds, including those based on stainless steel, titanium alloys, and magnesium alloys.[134–136]

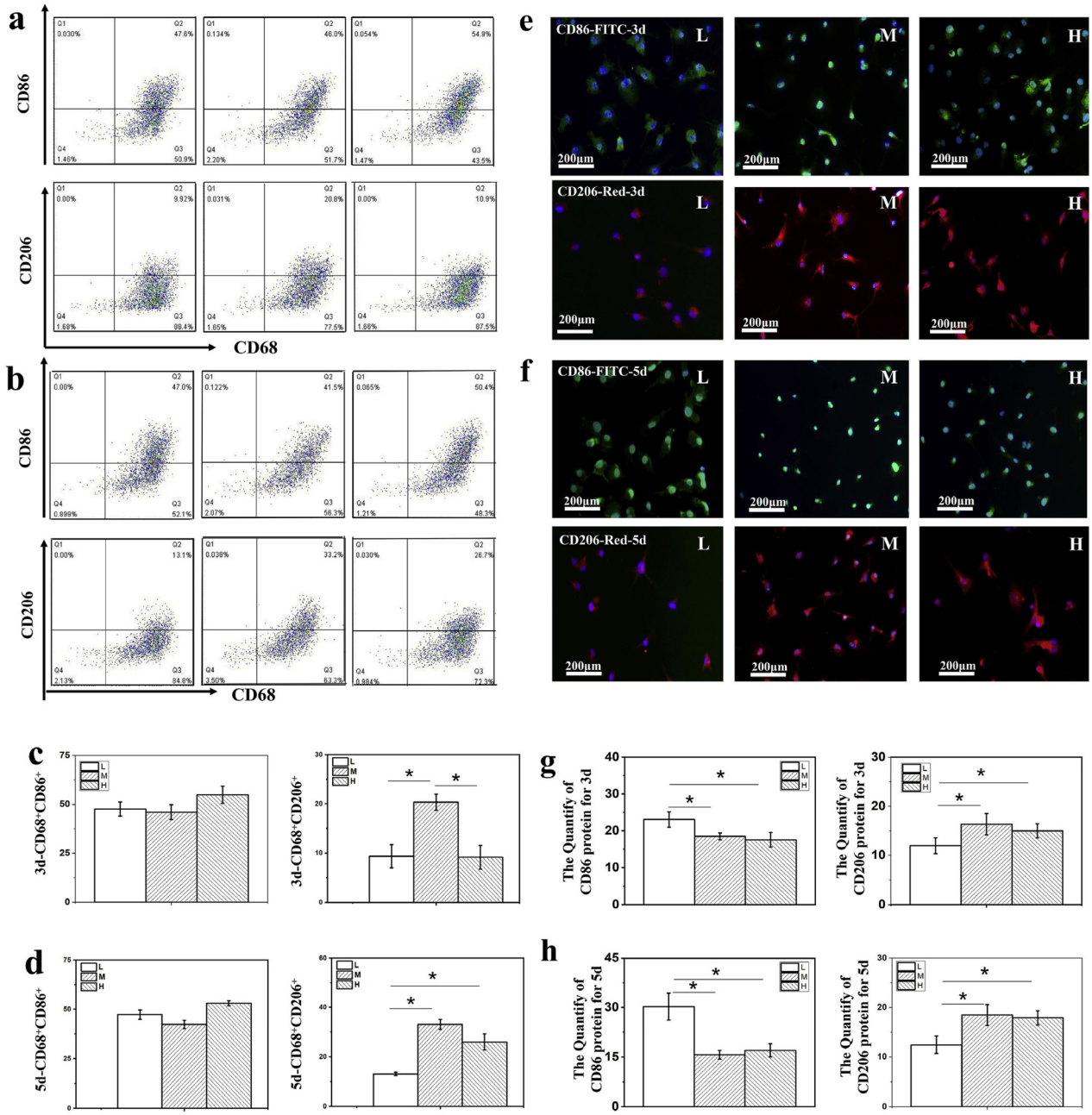

Fig. 4 Hydrogel stiffness affects CD86 and CD206 expression of BMDMs. Macrophages were incubated on polyacrylamide hydrogels with various stiffnesses. (a) and (b) Represent the expression analysis of $CD68^+CD86^+$ and $CD68^+CD206^+$ macrophages by flow cytometry assay after 3 and 5 days; (c) and (d) Show the quantitative analysis of $CD68^+CD86^+$ and $CD68^+CD206^+$ macrophages after 3 and 5 days; (e) and (f) Represent CD86 and CD206 expression of macrophages after 3 and 5 days by immunofluorescence staining; (g) and (h) Show quantitative analysis of $CD86^+$ and $CD206^+$ immunofluorescence density by Image J. L, M, and H: low, middle, and high stiffness, respectively. * $p < 0.05$. Reproduced under terms of the CC BY-NC-ND 4.0 license.[121] Copyright 2020, The Authors, published by Elsevier.

4.1.3. Topography

4.1.3.1. The impact of topography size and roughness. Increasing implant surface roughness enhances bone regeneration by promoting stem cell osteogenesis and M2 macrophage polarization through topography-dependent mechanisms.[106,137,138] Engineered zinc (Zn) plates with micro-topographies reduced M1 macrophage responses.[139] Similarly, rough, hydrophilic Ti surfaces promoted M2 macrophage polarization and IL-4 and IL-10 expression, while smooth Ti induced M1 inflammatory responses and IL-1β, IL-6, and TNF-α levels.[137] Neutrophils also respond to implant surface characteristics, with smooth surfaces inducing inflammation and NETosis, influencing macrophage polarization. Conditioned media from neutrophils on smooth Ti promoted pro-inflammatory macrophages,

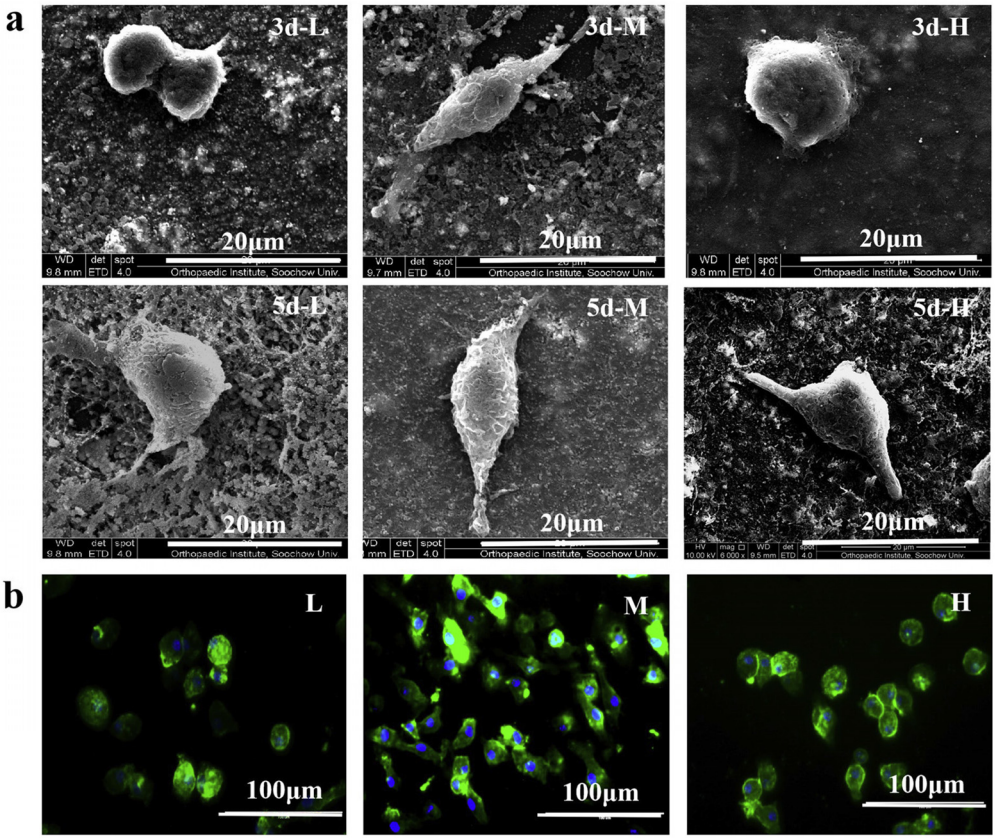

Fig. 5 The morphology and actin cytoskeleton of BMDMs incubated on polyacrylamide hydrogels with various stiffnesses. (a) The macrophage morphology after 3 and 5 days, illustrated by scanning electron microscope; (b) the F-actin cytoskeleton of macrophages after 5 days illustrated by the fluorescent microscope with phalloidin-FITC (in green) and DAPI (in blue) staining. L, M, and H: low, middle, and high stiffness, respectively. Reproduced under terms of the CC BY-NC-ND 4.0 license.[121] Copyright 2020, The Authors, published by Elsevier.

while rough Ti had the opposite effect, suggesting surface topography impacts macrophages directly and indirectly.[140]

While micro-rough patterns enhance implant surface area, boost the biomechanical interaction between bone and implant, and help attenuate inflammation,[141,142] nano topographies offer improvements in the surface energy of implants, cell adhesion, and implant interaction with the bone interface at cellular levels.[143,144] Wang *et al.* engineered hydroxyapatite ceramics with identical composition but varying surface topographies (~100–500 nm) and found that nano-sized topographies promoted M2 macrophage polarization. Larger topographies correlated with increased pro-inflammatory cytokine release and reduced M2 macrophage populations.[145] In order to combine the benefits of micro topographies and nano topographies, the Sun research group developed Ti disks with micro/nano topographies using SLA technology and alkali-heat treatment. These disks promoted M2 macrophage polarization, reducing IL-1β and increasing IL-10, which enhanced autophagy as well as osteoblast precursor proliferation and osteogenic differentiation. M2 macrophages also facilitated bone morphogenetic protein 2 (BMP-2) and VEGF secretion, improving osseointegration.[146,147] Ti implants with micro/nano topographies from SAH surface treatment exhibited optimal roughness and wettability, enhancing M2 macrophage polarization and suppressing osteoclast activity compared to microtopography-only implants.[148] Luu *et al.* also demonstrated that Ti surfaces with micro/nano-patterned grooves (400–500 nm) promote M2 macrophage polarization and IL-10 secretion by inducing cell elongation.[149] The data indicates that structures incorporating both micro- and nano-scale topographies are more effective in promoting pro-healing macrophage polarization than those with only micro or nano topographies.

4.1.3.2. The impact of topography architecture. The size and texture of implant surface topographies are crucial for modulating immune responses. Optimized textures are believed to enhance spatial properties and surface area.[150,151] Zhu *et al.* created honeycomb-like (HC) surface structures on Ti implants using monodispersed polystyrene spheres and a customized film transfer method. These structures, ranging from nanometer to micrometer scale (90, 500, 1000, and 5000 nm), influenced macrophage behavior. The HC-90 pattern, with a spacing smaller than the macrophage pseudopodium size, allowed for easier macrophage spreading, filopodia formation, and RhoA-associated protein kinase (ROCK) signaling activation. This led to an upregulation of M2 macrophages, with increased CD206, anti-inflammatory cytokines (IL-4, IL-10),

and BMP-2 levels, as well as decreased M1 markers like CCR-7 and pro-inflammatory cytokines (IL-1β, TNF-α), compared to other surface types. However, iNOS and oncostatin M (OSM) expression levels showed no significant differences across the surfaces (Fig. 6). HC-90 promoted osteogenic differentiation of MSCs *in vitro* and encouraged osseointegration *in vivo*.[150] Another study used electrospinning to create bone-regenerative fibrous membranes from PLGA, fish collagen, and HAPs with random, aligned, and latticed topographies. Subcutaneous implantation in mice triggered only a mild FBR. The latticed membrane, with its porous hierarchical structure and anisotropic fiber arrangement, mimicked native bone ECM and promoted cell attachment. It recruited more macrophages and significantly upregulated M2 macrophage markers, enhancing osteogenesis. This process also induced local hypoxia, activating HIF-1α signaling and VEGF gene expression to support angiogenesis. Ultimately, the latticed membrane demonstrated superior osteogenic activity in a murine calvarial bone defect model.[151]

Studies have shown that nano-porous Ti surfaces, created through etching and anodizing to form nanotubes, promote macrophage M2 polarization and enhance bone formation. Implants with 30 nm nanotubes improved macrophage recruitment and shifted polarization towards anti-inflammatory responses while inhibiting osteoclast differentiation by suppressing FAK phosphorylation and MAPK activation.[152] Additionally, Liu *et al.* developed Ti implants with titania nanostructures (nanowires, nanonests, and nanoflakes), which enhanced protein adsorption, integrin binding, and macrophage responses, leading to improved BMMSC osteogenic differentiation and superior osseointegration compared to traditional Ti implants.[153]

Recently, a bioceramic (calcium phosphate)-based bone graft called MagnetOs has been developed as a commercial product, incorporating NeedleGrip™ technology—a submicron, needle-shaped surface topography—to enhance traction for pro-healing M2 macrophages. It has been suggested that MagnetOs can promote bone growth even in soft tissues and is designed to repair critical-size bone defects, such as those found in the posterolateral spine.[154–156] Notably, a randomized controlled clinical trial demonstrated the superiority of MagnetOs Granules over autograft, which is considered the optimal graft material for spinal fusion.[157] These findings suggest that specific surface architectures, such as nanowires, nanotubes, and latticed or HC-like patterns, could enhance the design of immunomodulatory bone implants.

4.1.3.3. The importance of mimicking natural bone topography. While surface topography-based strategies have successfully induced macrophage M1/M2 switching and promoted bone regeneration, they fail to precisely replicate natural bone topography. Dai *et al.* fabricated micro and sub-micro hierarchical surfaces on Ti implants mimicking bone architecture. *In vitro*, the modified implant suppressed M1-mediated inflammation *via* TLR2/NF-κB inhibition, promoting BMMSC osteogenic differentiation and reducing osteoclastogenesis. *In vivo*, it integrated seamlessly into bone tissue.[158] In addition, mimicking natural bone topography could optimize sequential M1/M2 activation for bone repair. M1 macrophages initiate angiogenesis and osteogenesis early but must transition to M2 to reduce inflammation and support healing. Researchers used soft lithography to create poly-L-lactic acid (PLA) membranes mimicking bovine femur bone topography, enhanced with COL1 and hydroxyapatite to replicate the bone microenvironment. These membranes sequentially and synergistically polarized M1 and M2 macrophages, highlighting their potential for bone tissue engineering.[159] As described, paying attention to the size, roughness, and architecture of bone implant topographies is critical to attaining a desired immune response to promote osseointegration and improve bone regeneration. It is worth noting that simultaneous consideration of these principles would be a winning approach for future investigations.

4.1.4. Hydrophilicity. Implant surface wettability influences protein adsorption. Hydrophilic surfaces reduce protein attachment, while hydrophobic surfaces can increase immunogenicity by triggering immune recognition of hydrophobic elements.[160] Li *et al.* enhanced Ti implant hydrophilicity by functionalizing surfaces with heparin and fibronectin, which contain hydrophilic groups. This modification reduced pro-inflammatory cytokine secretion (TNF-α, MCP-1, IL-1β) compared to less hydrophilic Ti surfaces.[161] The highly hydrophilic surfaces of bone implants could promote macrophage M2 polarization compared to hydrophobic surfaces.[137,162] On hydrophilic surfaces, integrin β1 binds to fibronectin, likely activating PI3K/Akt signaling to induce M2 polarization. In contrast, on hydrophobic surfaces, integrin β2 binds to fibrinogen, triggering NF-κB signaling and M1 polarization.[162] For example, hydrophilic-modified SLA Ti surfaces induced M1 to M2 phenotypic alteration of macrophages, thereby alleviating inflammation by downregulating inflammatory genes (IL-1β, TNF, and CXCL-8). This induced TGF-β/BMP signaling in osteoblasts and promoted osteogenesis compared to SLA Ti surfaces.[163,164] Consistently, Li and colleagues demonstrated that improving the hydrophilicity of SLA Ti surfaces *via* graphene oxide coating improves the macrophage's M2 polarization and osteogenic differentiation of BMMSCs.[165] Another investigation by Gao *et al.* also demonstrated that hydrogenation of Ti dioxide nanotubes on Ti surfaces produces a superhydrophilic substrate with significantly enhanced wettability, given the generation of oxygen vacancies in the nanotubes. The produced hydrophilic surface elicited the M2 macrophage polarization, upregulated anti-inflammatory cytokines (IL-10, BMP-2, and TGF-β1), and reduced the lipopolysaccharide (LPS)-induced pro-inflammatory cytokines (TNF-α, MCP-1, and IL-6) secretion.[166]

Moreover, the surface hydrophilicity of bone implants might affect neutrophil-mediated inflammatory responses. The culture of neutrophils on rough and hydrophilic Ti implant surfaces reduced pro-inflammatory cytokine and enzyme generation and inhibited NETosis compared to neutrophils cultured on rough Ti surfaces.[140] The contribution of the adaptive immune system in tuning inflammatory responses to

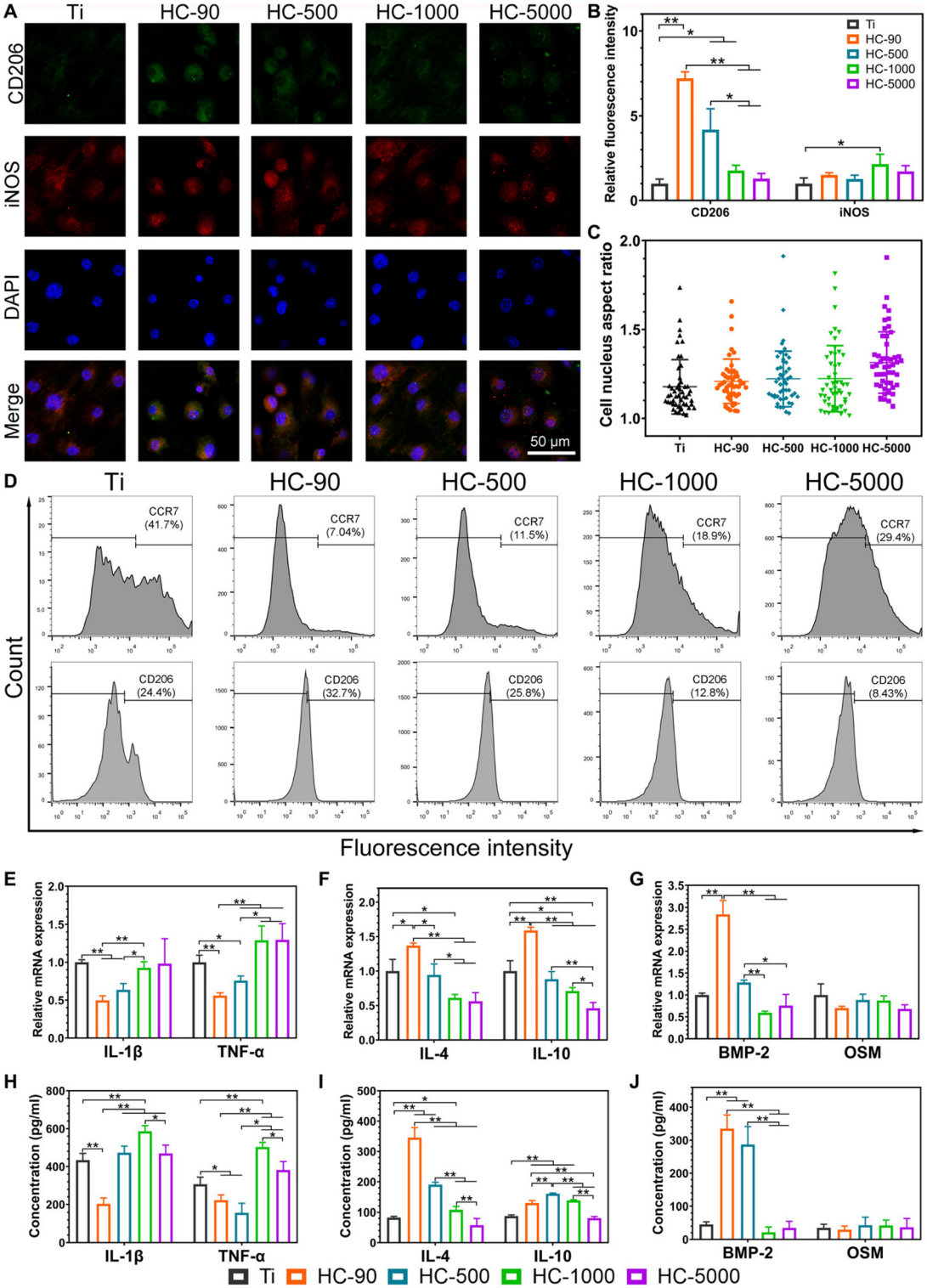

Fig. 6 Macrophage-mediated immune responses on diverse nanostructures. (A) Fluorescence microscopy of CD206, iNOS, and nucleic staining of macrophages; (B) quantitative measurement of CD206 and iNOS fluorescence intensity of macrophages; (C) quantitative measurement of cell nucleus aspect ratio regarding the fluorescence microscopy images; (D) macrophage polarization assessment based on the CCR7 and CD206 expression for M1 and M2 macrophages, respectively, using flow cytometry; (E) and (F) relative mRNA expression levels of M1 (IL-1β and TNF-α) and M2 (IL-4 and IL-10) macrophage-related genes, respectively; (G) relative mRNA expression level of BMP-2 and OSM; (H), (I), and (J) ELISA analyses of pro-inflammatory cytokines (IL-1β and TNF-α), anti-inflammatory cytokines (IL-4 and IL-10), and osteogenic cytokines (BMP-2 and OSM), respectively. * $p < 0.05$ and ** $p < 0.01$. Reproduced under terms of the CC-BY-NC 4.0 license.[150] Copyright 2021, The Authors, published by Science.

implant surface characteristics has also been established. Research conducted by Hotchkiss *et al.* has shown that increasing Ti surface roughness and wettability could shift adaptive immune responses towards the Th2 pro-wound-healing phenotype. This, in turn, speeds up inflammation resolution and increases stem cell and macrophage recruitment on the implant surface.[167] Overall, improving the surface hydrophilicity of bone implants can contribute to alleviating inflammation by tuning innate and adaptive immune responses. Nevertheless, significant surface hydrophilicity might remarkably reduce protein adsorption, diminishing interactions with immune cells and immunomodulatory impacts.[168,169] Consistent with these preclinical findings, a randomized clinical trial demonstrated that a patented bone bioactive liquid, consisting of a phosphate saline solution with calcium chloride and magnesium chloride, enhances the stability of Galaxy TS dental implants and promotes bone formation. These effects are likely mediated by improved implant surface wettability and the modulation of inflammatory markers in human primary macrophages.[170]

4.1.5. Surface potential. There is limited data on how the surface potential of implants might influence the fate of immune cell recruitment towards either bone regeneration or resorption. Introducing diverse coatings and functional groups might alter the surface potential of implants, thereby altering the immune microenvironment around them. Li *et al.* utilized polydopamine coatings to reduce the negative surface potential of Ti surfaces. When cultured on these surfaces, bone marrow-derived monocytes showed a greater tendency to switch towards M2 macrophages both *in vitro* and *in vivo*.[171] Another study by Hunt *et al.* developed poly(ether)urethanes with 10, 20, and 30% sulphonate substitution to achieve a range of negative surface charges. Two weeks after intramuscular implantation of substrates in mice, the 20%-charged polymer caused fewer neutrophil infiltration than other polymers.[172] Positive surface charges are believed to promote tissue regeneration by enhancing protein adsorption, which influences immune cell attachment and recruitment. However, the charge value is critical, as higher surface potential can impact cell proliferation and filopodia formation. In contrast, negative surface potential may provoke inflammatory reactions.[105,173] For example, negatively charged carboxyl groups can push macrophages toward an M1 phenotype, whereas positively charged amino surface groups can push them toward an M2 phenotype.[174] However, inconsistent data exist, such as the study demonstrating that negatively charged surface carboxyl groups might eliminate macrophage-mediated inflammation.[175] The nature of functional groups and other surface properties of biomaterial interfaces might contribute to the observed outcome. Accordingly, there is a pressing need to take a more serious look at the issue of surface potential.

4.2. The impact of the chemical composition of implants

The chemical composition of bone implants plays an important role in modulating FBR, immune cell behavior, and osseointegration. This section highlights the impact of commonly used materials in implant fabrication and their immunomodulatory effects on bone healing. Table 2 presents engineered implants designed with these materials to enhance immune compatibility and regeneration. Some immunomodulatory biomodification strategies are highlighted in Table 3.

4.2.1. Non-biodegradable metallic implants. Non-biodegradable metallic implants offer excellent mechanical strength but face challenges due to corrosion. Corrosion byproducts, such as metal ions, can affect biocompatibility and trigger inflammatory responses, particularly through macrophage interactions. This issue is especially critical for metal-on-metal (MOM) implants, where significant corrosion is linked to high revision rates.[179–182]

4.2.1.1. Stainless steel alloy. Stainless steel (SS 316L) is valued for its strong mechanical properties in biomedical applications. However, its corrosion in the inflammatory environment of bone lesions can exacerbate local inflammation, further accelerating implant degradation and hindering bone regeneration. Li *et al.* investigated the impact of SS 316L localized corrosion on macrophage function and polarization. They found that RAW264.7 cells reduced the implant's pitting corrosion resistance by consuming glucose and disrupting the biomolecule-adsorbed layer. This corrosion released high local concentrations of Cr^{3+} and Ni^{2+}, which decreased macrophage viability and induced M1 polarization, as indicated by increased CD86, TNF-α, IL-6 expression, and intracellular ROS (Fig. 7). Additionally, Fe^{2+} and Cr^{3+} from the implant, combined with macrophage-generated ROS, created a synergistic effect that elevated ROS levels and produced toxic Cr^{6+}, further exacerbating implant corrosion and inflammation.[183] Heise and colleagues consistently revealed that macrophages cultured on SS 316L disks produced considerably more NO than control, generated macrophage-sized surface corrosive pits, and caused a marked Cr^{3+}, Fe^{2+}, and Ni^{2+} release.[184] Eventually, relatively high concentrations of metallic ions released by SS 316L alloy corrosion might cause BMMSCs to experience oxidative stress and membrane depolarization, impairing their osteogenic capacity.[185]

Various strategies have been employed to reduce SS 316L corrosion. Incorporating 10.5% Cr promotes the formation of a protective Cr oxide layer, improving corrosion resistance. Additionally, optimizing the carbon content to 0.03% enhances both yield strength and corrosion resistance.[186,187] Various coating materials have been applied to improve SS 316L corrosion resistance. A Nb pentoxide thin film provides a protective barrier, reducing corrosion and inflammation in gingival cells.[188] Similarly, Ferreira *et al.* demonstrated that nanostructured Nb and carbon coatings significantly enhance corrosion resistance.[189] Another approach involves Cu-substituted hydroxyapatite/functionalized multi-walled carbon nanotube composites.[190] Ongoing research continues to explore coating strategies, though their effects on local immune responses require further investigation.[191–193]

4.2.1.2. Cobalt–chrome–molybdenum (CoCrMo) alloy. Given its hardness and tribological properties, the CoCrMo alloy is among the promising orthopedic materials.[194] After implan-

Table 2 The osteoimmunomodulatory and osteogenic impacts of engineered bone implants

Category	Base implant material	Engineered implant	Type of study	Immunomodulation	Impact on bone tissue	Ref.
Non-biodegradable metals	Ti	Ti–5Cu alloy	*In vitro*	Induced RAW264.7 macrophage polarization towards the M2 phenotype.	Improved MC3T3-E1 cell multiplication and osteogenic differentiation.	343
		Strontium-zinc phosphate-coated Ti	*In vitro* & *in vivo*	Upregulated macrophage M2 polarization and suppressed inflammation.	Induced pro-osteogenic factors production and rat BMMSC osteogenesis.	344
		Hydroxyapatite-coated Ti–29Nb–13Ta–4.6Zr alloy	*In vivo*	The alloy with 70–90 μm thickness attenuated inflammation by suppressing TNF-α production.	Improved implant osseointegration and osteogenesis.	345
		Ti6Al4V–6Cu	*In vitro*	Repressed the activation, proliferation, and pro-inflammatory cytokine secretion of macrophages.	Showed no negative impact on osteoblasts and increased the angiogenesis of HUVECs in favor of alveolar bone regeneration.	346
	Stainless steel	SS 316L–5Cu	*In vivo*	Upregulated CD206-positive M2a macrophages as the primary source of PDGF-BB.	Promoted the generation of type H vessels during bone regeneration.	347
		Hydrothermal surface-treated SS 316L	*In vitro* & *in vivo*	Exhibited low metal ion release and good anti-inflammatory properties as shown by surrounding fibrous capsule membrane with low thickness.	Showed good protein adsorption and osteoconductivity, given its superhydrophilicity.	348
Biodegradable metals	Mg	Mg–10Gd alloy	*In vitro*	Reduced TNF-α and IL-1β secretion and increased OSM and BMP-6 secretion by macrophages.	Facilitated the osteogenic differentiation of HUCPV and provided a beneficial microenvironment for bone regeneration.	349
		SF-PEDOT:PSS-coated ZE21C Mg alloy	*In vitro*	Upregulated M2 macrophages evidenced by IL-4, IL-10, and TGF-β1 upregulation and IL-6 and TNF-α downregulation.	Accelerated bone mineralization through enhancing ALP, COL1, and OCN release.	350
	Zn	Surface-engineered Zn plates with microscale topography	*In vitro*	Surface roughness of the micro-texture attenuated the M1 inflammatory immune response.	Showed enhanced adhesion, considerable self-renewal, and improved osteogenic differentiation of bone cells.	139
		Ca–Zn–P-coated Zn	*In vitro* & *in vivo*	Induced macrophage M2 polarization.	Promoted implant osseointegration and osteogenesis.	351
Natural polymers	Collagen	Mineralized collagen	*In vitro* & *in vivo*	Tuned the adrenomedullin secretion by macrophages, creating a suitable bone immune microenvironment.	Promoted rat mandibular defect repair by fostering the osteogenic differentiation, proliferation, and migration of bone BMMSC adhesion.	352
		Hierarchical intrafibrillarly mineralized collagen	*In vitro* & *in vivo*	Induced CD206 + Arg1 + M2 macrophage polarization.	Promoted bone regeneration by provoking BMMSC adhesion, proliferation, and osteogenic differentiation.	353
	Hyaluronic acid	Nanofibrous FmocFF/hyaluronic acid hydrogel	*In vitro* & *in vivo*	Upregulated M2 macrophages dispersed through the regenerating tissue.	Reinforced osteogenic differentiation of MC3T3-E1 pre-osteoblasts, resulting in about 93% bone restoration.	354
	Chitosan	Chitosan/agarose/nanohydroxyapatite	*In vitro*	Induced macrophage M2 polarization as evidenced by increased levels of anti-inflammatory cytokines (IL-4, IL-10, and IL-13).	Enhanced the osteogenic ability of BMMSCs and human osteoblasts.	355
		3D porous chitosan/hydroxyapatite scaffold	*In vitro*	Upregulated anti-inflammatory cytokines (IL-4, IL-10) production.	Induced the osteogenic differentiation of human MSCs towards osteoblast phenotype, evidenced by elevated ALP and OCN expression.	356
		Sulfated chitosan	*In vitro*	Induced a moderate pro-inflammatory macrophage response initially followed by a shift toward an anti-inflammatory response.	Enhanced crosstalk between immune cells and stem cells and facilitated BMMSC chemoattraction and osteogenic differentiation.	357

Table 2 *(Contd.)*

Category	Base implant material	Engineered implant	Type of study	Immunomodulation	Impact on bone tissue	Ref.
Synthetic polymers	PEG	Short-chain chitosan and nano-sized HAPs-integrated tetra-PEG	*In vitro*	Promoted M2 and suppressed M1 polarization of macrophages *via* repressing the TLR4/NF-κB signaling.	Improved osteogenic capacity and hindered osteoclast formation and resorption.	358
	PMMA	Mineralized collagen-modified PMMA	*In vivo*	Attenuated macrophage proliferation and fusion around the implant.	Promoted implant osseointegration and decreased fibrous tissue generation.	299
		PCS-reinforced PMMA	*In vitro* & *in vivo*	Exhibited antioxidant effects and considerably suppressed inflammation.	Promoted neobone generation and bone ingrowth at the surface and inside the cement by promoting osteogenic proteins and angiogenesis.	359
	PEEK	Hydroxyapatite composited PEEK with a 3D porous surface	*In vitro*	Inhibited macrophage M1 polarization and downregulated NO generation.	Enhanced osteogenic OSX and ALP gene expressions and reduced osteolytic MMP-9 and MMP-13 gene expressions.	319
		Polyelectrolyte multilayered nanoporous films-modified PEEK	*In vitro*	Induced macrophage M2 polarization and attenuated acute inflammatory responses.	Attenuated fibrous encapsulation of implant and provided a favorable milieu for osteogenic differentiation of human BMMSCs.	360
		Chitosan-coated Mg bioactive glass nanoparticles-surface modified PEEK	*In vitro* & *in vivo*	Induced macrophage M2 polarization and decreased the expression of inflammatory factors.	Improved the BMMSC osteogenic differentiation *in vitro* and promoted implant osseointegration *in vivo.*	361
Bioceramics	BGs	Ce-doped MBGNs	*In vitro*	Suppressed pro-inflammatory cytokines (TNF-α, IL-1β, and IL-6) in macrophages.	Showed pro-osteogenic activities by suppressing pro-osteoclastogenic responses.	340
	CPs	β-TCP	*In vitro*	Induced M2 macrophage polarization, upregulated anti-inflammatory genes (IL-10 and IL-1rα), and downregulated pro-inflammatory genes (IL-1β and IL-6).	Upregulated BMP-2 that provoked osteogenic differentiation of BMMSCs.	329

Abbreviations: Ti–5Cu; titanium–5 wt% copper, BMMSCs; bone marrow-derived mesenchymal stem cell, Ti–29Nb–13Ta–4.6Zr; Ti–29 wt% niobium–13 wt% tantalum–4.6 wt% zirconium, TNF-α; tumor necrosis factor-alpha, Ti6Al4V–6Cu; Ti–6 wt% aluminium–4 wt% vanadium–6 wt% copper, HUVECs; human umbilical vein endothelial cells, SS 316L–5Cu; stainless steel 316 low–5 wt% copper, PDGF-BB; platelet-derived growth factor BB, Mg–10Gd; magnesium–10 wt% gadolinium, IL; interleukin, OSM; oncostatin M, BMP-6; bone morphogenetic protein 6, SF-PEDOT:PSS; silk fibroin-poly(3,4-vinyldioxythiophene):poly(styrene sulfonate), TGF-β1; transforming growth factor-beta 1, ALP; alkaline phosphatase, OCN; osteocalcin, COL1; type I collagen, Ca–Zn–P; calcium zinc phosphate, Arg1; arginase 1, FmocFF; fluorenylmethyloxycarbonyl-diphenylalanine, PEG; polyethylene glycol, HAPs; hydroxyapatite particles, TLR4; toll like receptor-4, NF-κB; nuclear factor kappa b, PMMA; polymethyl methacrylate, PCS; poly(citrate-silicon), PEEK; polyether-ether-ketone, NO; nitric oxide, OSX; osterix, MMP; matrix metalloproteinase, BGs; bioactive glasses, MBGNs; mesoporous bioactive glass nanoparticles, CPs; calcium phosphates, β-TCP; β-tricalcium phosphate.

tation; the CoCrMo alloy generates bioactive wear particles that, at high concentrations, promote ROS accumulation and trigger NLRP3-dependent macrophage pyroptosis. This process leads to the release of pro-inflammatory cytokines, such as IL-18 and IL-1β, which accelerate osteoclastogenesis.[195] There is also evidence suggesting the participation of macrophages in accelerating CoCrMo alloy corrosion by promoting inflammation.[196] Mathew's research team found that CoCrMo wear particles induced phenotypic changes in monocytes, leading to upregulation of TNF-α, iNOS, and STAT6 and downregulation of CD86 and arginase 1 (Arg1). These altered macrophages secreted higher levels of TNF-α, IL-1β, IL-6, IL-8, and IL-10 than M1 and M2 macrophages and exhibited intermediate ROS levels. The ROS and inflammatory cytokines may trigger electrochemical changes on the alloy surface, accelerating corrosion and contributing to implant failure.[180] Mihalko *et al.* also showed that macrophages could ingest Co and Mo metal ions on CoCrMo implants, thereby affecting their surface with pitting damage to the oxide surface layer.[197] Moreover, macrophages rendered superior damage to the oxide layer of CoCrMo implants in the existence of lymphocytes and local inflammation induced by the addition of IFN-γ and LPS.[198]

The presence of 28% Cr in CoCrMo alloy enhances the formation of a protective Cr oxide layer, increasing its resistance to corrosion, improving biological compatibility, and promoting better bone tissue integration.[199] Several surface modifications have been applied to CoCrMo implants to enhance corrosion resistance, reduce inflammation, and promote osteogenesis. Lin *et al.* showed that hydrophilic hydrogenated CoCrMo surfaces improved biocompatibility, reduced free radical production, and supported bone formation *in vitro* and *in vivo*.[200] Lohberger *et al.* demonstrated that Ti nitride coat-

Table 3 Several potential biomodification strategies for developing immunomodulatory bone implants

Implant material	Potential biomodification	Modification method	Type of study	Immunomodulation	Ref.
Ti	GL13K	Surface linking using CPTES as a linker.	*In vitro*	Inhibited M1 macrophages and was compatible with M2 macrophages. Downregulated TNF-α and IL-1β in M1 macrophages and upregulated IL-10 and TGF-β3 in M2 macrophages.	362
Ti	BMP-2pp	—	*In vitro* & *in vivo*	Precluded Ti particle-induced M1 macrophage polarization by deactivating the NF-κB signaling and encouraged M2 macrophage differentiation.	363
CSZP coated Ti	IL-4	—	*In vitro* & *in vivo*	Promoted M2 macrophage polarization and osteogenesis of BMMSCs.	364
PEG	RGD	Photopolymerizing acrylate-PEG-YRGDS and the base macromer mixture.	*In vitro*	Attenuated the gene expressions of TNF-α and IL-1β in macrophages seeded onto the PEG.	92
PEEK	DOPA4/BMP-2p	Coating through immersing PEEK in the PBS solution of Azide-DOPA4 or BMP2p.	*In vitro* & *in vivo*	Caused a synergistic effect with $Foxp^{3+}$ iTreg cells to promote osteogenesis.	365
SPEEK	A-485	Coating with A-485-loaded MBG nanoparticles through placing SPEEK in the coating solution and freeze-drying.	*In vitro* & *in vivo*	Attenuated immune responses, implant fibrous encapsulation, and osteoclastogenesis, and promoted osteogenesis.	366
PPB	LL-37	Grafting through immersing PPB discs into LL-37 peptide solution.	*In vitro* & *in vivo*	Induced osteogenic differentiation of MSCs and was conducive to the M2 macrophage polarization.	367
β-TCP	S1P	Coating through immersing the scaffold in S1P and calcium chloride solutions, respectively.		Downregulated inflammatory-related genes and upregulated osteogenic-related genes (OPN, OCN and RUNX2), thereby promoting osteogenesis.	368

Abbreviations: Ti; titanium, GL13K; an antimicrobial peptide, CPTES; 3-(chloropropyl)-triethoxysilane, TNF-α; tumor necrosis factor-alpha, IL; interleukin, TGF-β; transforming growth factor-beta, BMP-2; bone morphogenetic protein 2, NF-κB; nuclear factor kappa B, CSZP; calcium–strontium–zinc–phosphate, BMMSCs; bone marrow-derived mesenchymal stem cells, PEG; polyethylene glycol, PEEK; polyetheretherketone, A-485; a potent and selective catalytic inhibitor of p300/CBP, MBG; mesoporous bioactive glass, iTreg; induced regulatory T cell, SPEEK; sulfonated PEEK, PPB; baicalin-loaded core–sheath-structured fibrous scaffold, β-TCP; β-tricalcium phosphate, S1P; sphingosine 1-phosphate.

ings enhanced biocompatibility by preventing corrosion-induced particle release and reducing inflammation.[201] Ti Nb nitride coating also reduced metal ion release and improved compatibility with osteoblast-like cells.[202] Coatings like Ti Si nitride and Ti Zr nitride could also improve fretting corrosion resistance in orthopedic applications.[203] Overall, CoCrMo degradation at the bone lesion site, driven by local inflammation, leads to corrosion products that enhance macrophage inflammatory functions. The strategies discussed aim to interrupt this cycle, preventing inflammation-mediated implant failure and promoting better osseointegration.

4.2.1.3. Ti and Ti alloy. Ti alloys such as Ti–6Al–4V (TC4) have been incorporated into manufacturing bone implants, given their good mechanical strength and biocompatibility; however, their corrosion products (*i.e.*, particles and ions) were shown to be absorbed into the *peri*-implant tissues and trigger macrophage-mediated inflammatory responses that not only result in bone resorption but also accelerate implant corrosion and failure.[204–209] A study on *peri*-implant gingival tissues from patients with failed Ti dental implants found that Ti particles influenced macrophage polarization, leading to increased lymphocyte and macrophage infiltration. This was associated with elevated IL-1β, IL-8, and IL-18 levels, which contributed to local inflammation and impacted osteoblast and osteoclast activity, explaining implant osseointegration failure.[208]

Interestingly, several novel Ti alloys have been invented with exceptional corrosive resistance and immunomodulatory effects. The Ti–24Nb–4Zr–8Sn (Ti2448) alloy has gained attention for its low elastic modulus, high strength, excellent corrosion resistance, and strong osseointegration. Liu *et al.* studied its corrosion behavior and immunomodulation under oxidative stress, finding that Ti2448 showed better corrosion resistance than the TC4 alloy due to the formation of protective Ti dioxide and Nb pentoxide films. Additionally, Ti2448 reduced intercellular ROS levels, promoted macrophage M2 polarization, and increased the expression of pro-healing factors like IL-10 and BMP-2, compared to TC4.[210] Kurtz *et al.* reported the invention of Ti–29Nb–21Zr alloy with improved corrosive resistance under inflammatory conditions compared to conventional TC4 alloy.[211,212] Accordingly, fabricating Ti alloys with high corrosive resistance might be suitable for attenuating FBR and avoiding orthopedic implant failure.

Gudima *et al.* analyzed the transcriptome of pro-inflammatory and pro-healing macrophages on polished and porous Ti surfaces. Pro-healing macrophages exhibited a stronger response, likely due to overlap between Ti-induced and IFN-γ-driven inflammation. Ti surfaces downregulated acute inflammatory chemokines but promoted chronic inflammation and osteoclastogenesis by upregulating proteins like CHI3L1, CHIT1, CSF1, TNFSF14, and MMPs. No significant differences were found between macrophages on polished *versus* porous Ti.[213] This suggests that Ti's intrinsic properties primarily drive macrophage programming, though surface characteristics like roughness and hydrophilicity also influence immune responses, particularly *via* Wnt signaling. Blocking Wnt secretion reduced inflammatory cytokines on smooth and rough Ti and lowered IL-4 and IL-10 on rough-hydrophilic Ti.[214,215] $CD4^+$ and $CD8^+$ T cells responded differently to Ti

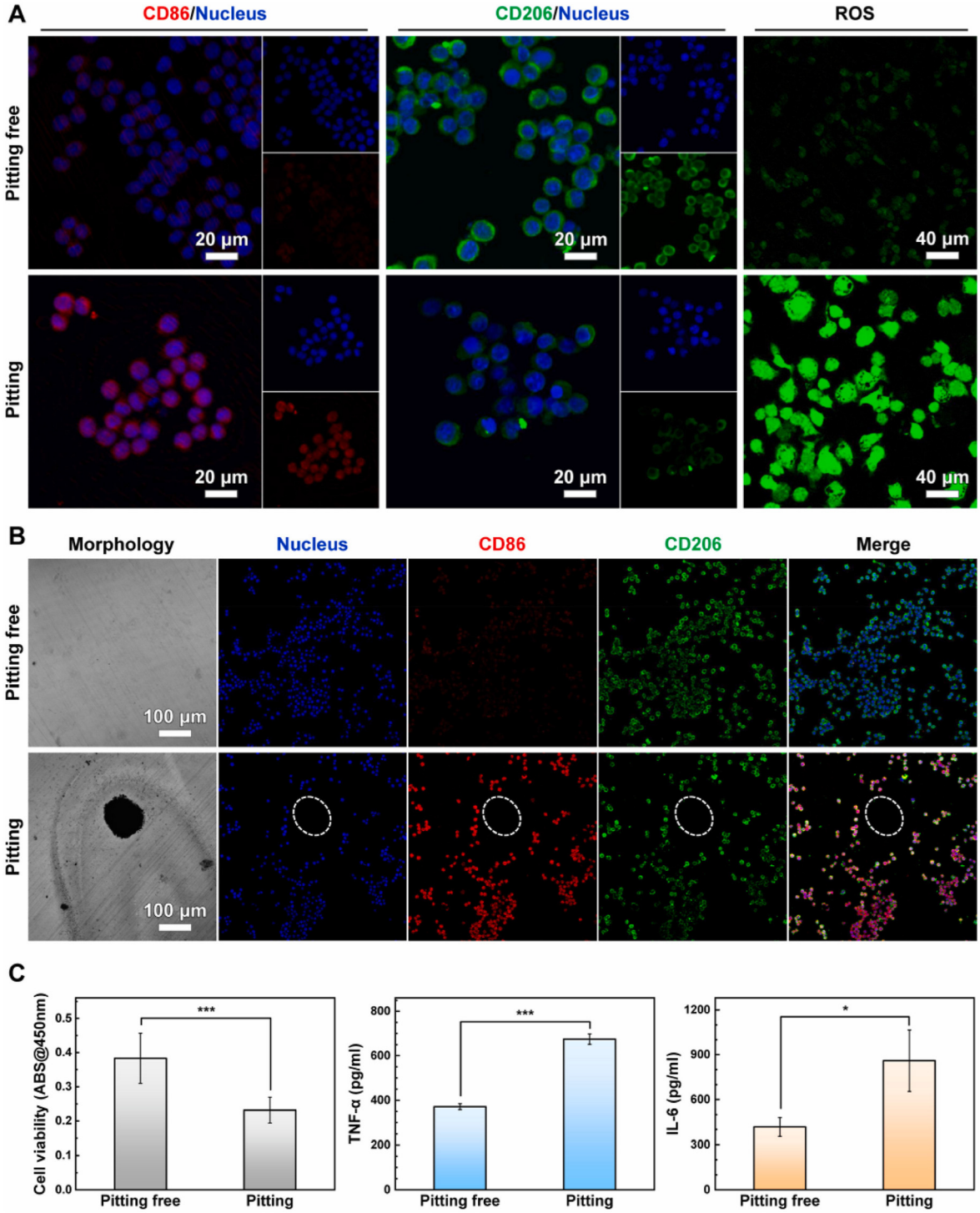

Fig. 7 Cell survival and polarization of RAW264.7 macrophages cultured on pitting and pitting-free 316L stainless steel implants for 24 hours. (A) Representation of CD86, CD206, and ROS fluorescence images; (B) confocal laser scanning microscopy images of corrosion morphology and CD86/CD206 co-staining; (C) CCK-8 assay measurement of cell survival and ELISA measurement of TNF-α and IL-6 expression. * $p < 0.05$, ** $p < 0.01$, and *** $p < 0.001$. Reproduced under terms of the CC-BY-NC 4.0 license.[183] Copyright 2024, The Authors, published by Elsevier.

surfaces, affecting macrophage polarization and MSC recruitment. Notably, $CD4^+$ T cell absence impaired pro-healing responses to rough-hydrophilic Ti, increasing inflammation and reducing bone formation.[216,217] These findings highlight the importance of tuning Ti surface attributes to optimize immune responses.

4.2.2. Biodegradable metallic implants. Biodegradable metals, *e.g.*, Mg, Fe, and Zn, are gaining more consideration as

advantageous candidates to the classic metallic materials for bone implants due to their propensity to break down over time to avoid removal surgery.[218] These metals and their degradation products have shown considerable effects in regulating local immune responses and bone healing processes.

4.2.2.1. Mg-based implants. Mg-based alloys are promising biodegradable orthopedic materials due to their bone-like mechanical properties, but their rapid corrosion limits clinical use. Rahman *et al.* emphasized that alloying and surface treatments can help regulate degradation.[219] Released Mg^{2+} fosters a pro-osteogenic immune environment, initially triggering inflammation but later promoting macrophage polarization for healing.[220–222] This immunoregulatory effect is linked to PI3K/Akt activation, ROS reduction, and NF-κB/MAPK suppression.[223–225]

Degrading Mg and the AZ31 Mg-based alloy improved the viability of LPS-primed pro-inflammatory macrophages; however, they regulated cells' ROS-reactive nitrogen species (RNS) balance.[225] Mg-based materials upregulated M2 macrophages, increased anti-inflammatory factors (IL-4, IL-6, and IL-10), decreased pro-inflammatory factors (TNF-α and IL-1β), and elevated the OSM and BMP-6 osteogenic factors expression.[10,223,226] Consistently, incorporating Mg into a Ti-based alloy (Ti–0.625Mg) demonstrated promising results in modulating macrophage polarization. Macrophages on Ti–0.625Mg initially exhibited M1 polarization on day 1 due to an elevated environmental pH (~8.03) but shifted to M2 polarization by day 5 as Mg ions accumulated within cells. Compared to pure Ti, Ti–0.625Mg induced more M1 and fewer M2 macrophages on day 1 but reversed this trend by day 5 (Fig. 8). *In vivo* studies further confirmed its superior anti-inflammatory response, enhanced osteogenesis, and reduced fibrous encapsulation.[227] Incorporating Mg into fibrinogen scaffolds also improved mechanical properties, upregulated M2 macrophages, and decreased inflammatory mediators (IFN-induced protein 10 (IP-10) and IL-1β) production *in vitro* and *in vivo*.[228]

It is worth mentioning that prolonged Mg^{2+} exposure over 3 days might overactivate NF-κB signaling in macrophages, promote osteoclastic-like cells, and slow bone maturation by inhibiting hydroxyapatite precipitation.[220] Additionally, excessive degradation particles from high-purity Mg implants drive macrophages toward the M1 phenotype, releasing pro-inflammatory cytokines that impair BMMSC osteogenic differentiation.[229] Therefore, the concentration, exposure duration, and elimination rate of Mg^{2+} must be carefully regulated to prevent adverse effects on implant osseointegration and bone regeneration.

Of note, the rapid degradation of Mg-based implants compromises their biomechanical integrity in clinical applications and generates gas bubbles that may induce local inflammation. In contrast, Mg alloys with a slower corrosion rate do not produce noticeable bubbles, as the released hydrogen gas gradually diffuses into surrounding tissues.[10,230] Zhang *et al.* demonstrated that their Mg–2Zn alloy, which has a lower degradation rate and superior mechanical strength compared to high-purity Mg, enhances skull bone repair by promoting M2 macrophage polarization and supporting BMMSC osteogenesis.[231] Implementing surface coatings, such as bioceramics or polymeric materials, is a further strategy to regulate the Mg-based implant degradation rate.[232] A Mg-based alloy coated with hydroxyapatite and bioactive glass exhibited a controlled degradation rate, preventing bubble formation and improving implant stability.[233] In a nutshell, Mg alloys and Mg-incorporated materials with controlled degradation rates show great potential as bone implants due to their osteoimmunoregulatory effects.

4.2.2.2. Fe-based implants. Fe and Fe-based alloys are promising for orthopedic applications due to their excellent mechanical properties, including high yield strength, elastic modulus, and ductility. However, their slow corrosion rate and corrosion products present challenges that need to be addressed.[234] Researchers have developed porous and degradable Fe-based bone implants to overcome their slow biodegradation.[235–237] Putra *et al.* created 3D-printed porous Fe matrix composites with silicate-based bioceramic particles, achieving a biodegradation rate 2.6 times higher than that of pure Fe with the same geometry.[237] Fe plays a significant role in immune regulation, but limited research exists on the immune response to Fe-based bone implants and their corrosion products.[238,239] Wegener *et al.* developed a cylindrical sponge-like Fe-based implant placed in the proximal tibia of Merino sheep. After 12 months, bone regeneration and mineralization occurred within the implant pores and at the bone–implant interface. Despite the presence of degraded alloy particles, no inflammatory response was observed in blood or histological analyses.[235,236] Meanwhile, Fe accumulation could affect immune responses by fostering macrophage M1 polarization and thereby provoking local inflammation.[240,241] Accordingly, the fate of the interaction of Fe-based implant degradation products with immune cells, particularly macrophages, remains an open question that needs to be answered before further advances in designing Fe-based bone tissue scaffolds.

4.2.2.3. Zn-based implants. Zn-based alloys are promising biodegradable orthopedic implants due to their strength, ductility, controlled degradation, and Zn^{2+} release. Zn^{2+} (11.25–45 μM) promotes bone remodeling and M2 macrophage polarization.[242–245] Ji *et al.* found that Zn–2Cu–0.5Zr alloy accelerated osteoporotic fracture healing by enhancing M2 polarization and BMMSC differentiation *via* Wnt/β-catenin signaling.[246] Qiang *et al.* developed a calcium phosphate-coated Zn–0.8Mn–0.1Li alloy, which improved M2 polarization, reduced inflammation, and enhanced BMP-2 expression. The coated alloy outperformed the uncoated version, emphasizing the benefits of calcium phosphate coatings in immune modulation and bone healing.[247–251]

The surface area and topographical cues of porous materials regulate macrophage behavior, while pore geometry influences degradation rates. Zn alloy degradation increases with scaffold porosity but decreases with larger pore sizes. Therefore, carefully designing biodegradable Zn-based porous

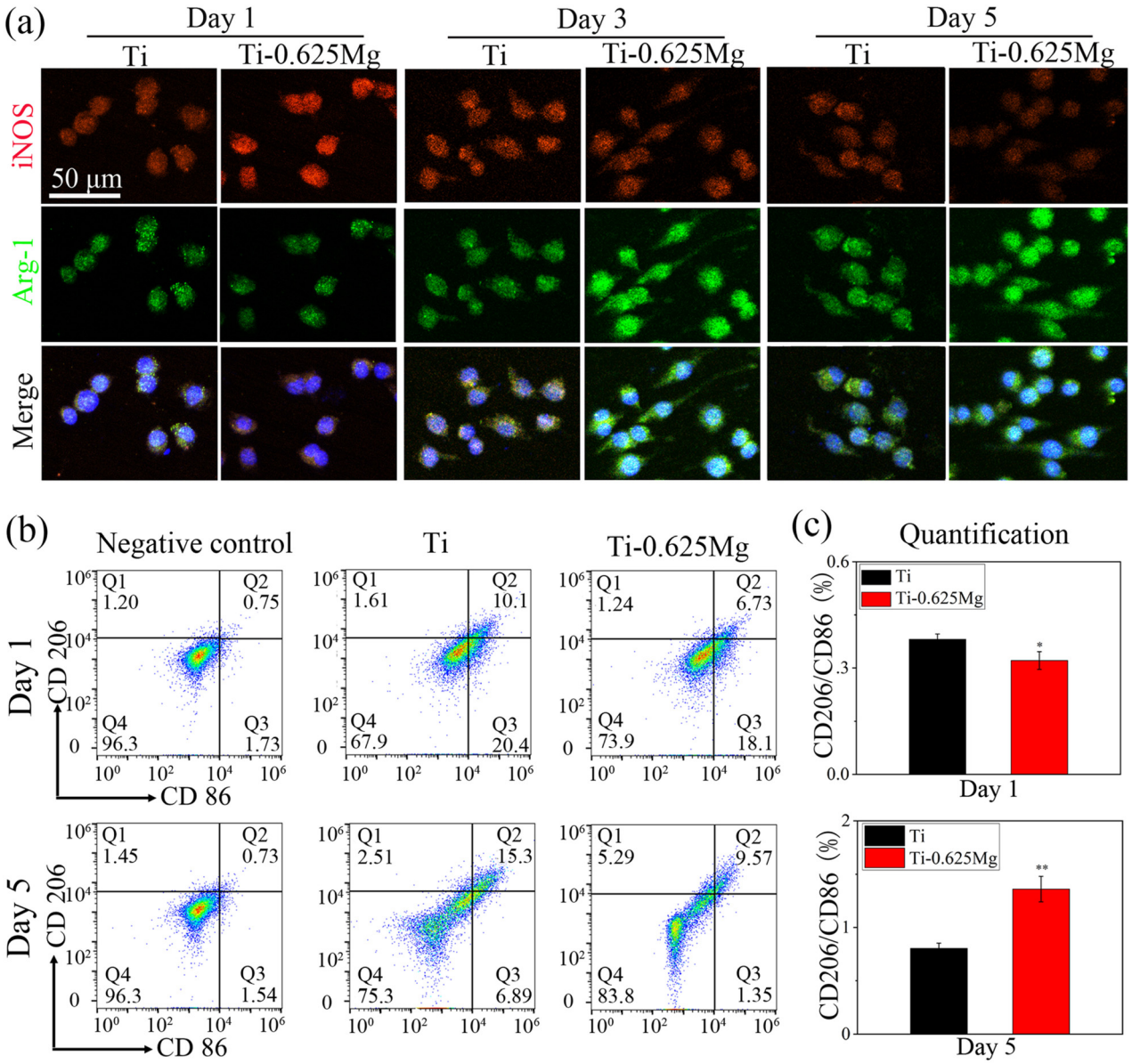

Fig. 8 Macrophage polarization on Ti alloys. (a) Immunofluorescent staining images representing iNOS and Arg1 expression as M1 and M2 macrophage markers in Ti and Ti–0.625Mg groups on days 1, 3, and 5; (b) flow cytometry analysis of macrophage CD206 (M2 marker) and CD89 (M1 marker) expression in Ti and Ti–0.625Mg groups on days 1 and 5; (c) the CD206/CD86 expression ratio by macrophages in Ti and Ti–0.625Mg groups on days 1 and 5. $*p < 0.05$, $**p < 0.01$. Reproduced under terms of the CC-BY 4.0 license.[227] Copyright 2022, The Authors, published by Science.

scaffolds can optimize immune responses and enhance bone healing.[252] Li *et al.* developed high-strength binary Zn–0.8Li alloy scaffolds with 90% porosity to control degradation and minimize Zn toxicity. They also designed gyroid (G) and body-centered cubic (BCC) pore structures to study the impact of pore geometry on scaffold degradation and bone repair. The simultaneous Zn^{2+} and Li^{+} release enhanced macrophage M2 polarization indicated by CD206, IL-4, IL-10, and Arg1 expression upregulation, as well as TNF-α, iNOS, and IL-1β expression downregulation. The alloy nanoscale wavy-like roughness enabled macrophage activation during early attachment. After one month, the G scaffold maintained uniform degradation and promoted anti-inflammatory macrophage polarization, leading to enhanced osteogenesis *via* JAK/STAT signaling, indicated by notable improvements in osteogenic markers like alkaline phosphatase (ALP) and osteocalcin (OCN), collagen deposition, and the formation of new bone, whereas the BCC scaffold accumulated degradation products, limiting tissue ingrowth (Fig. 9).[253] These findings highlight the significant immunomodulatory attributes of Zn-based implants, which may be improved by creating porous structures with suitable surface topographies.

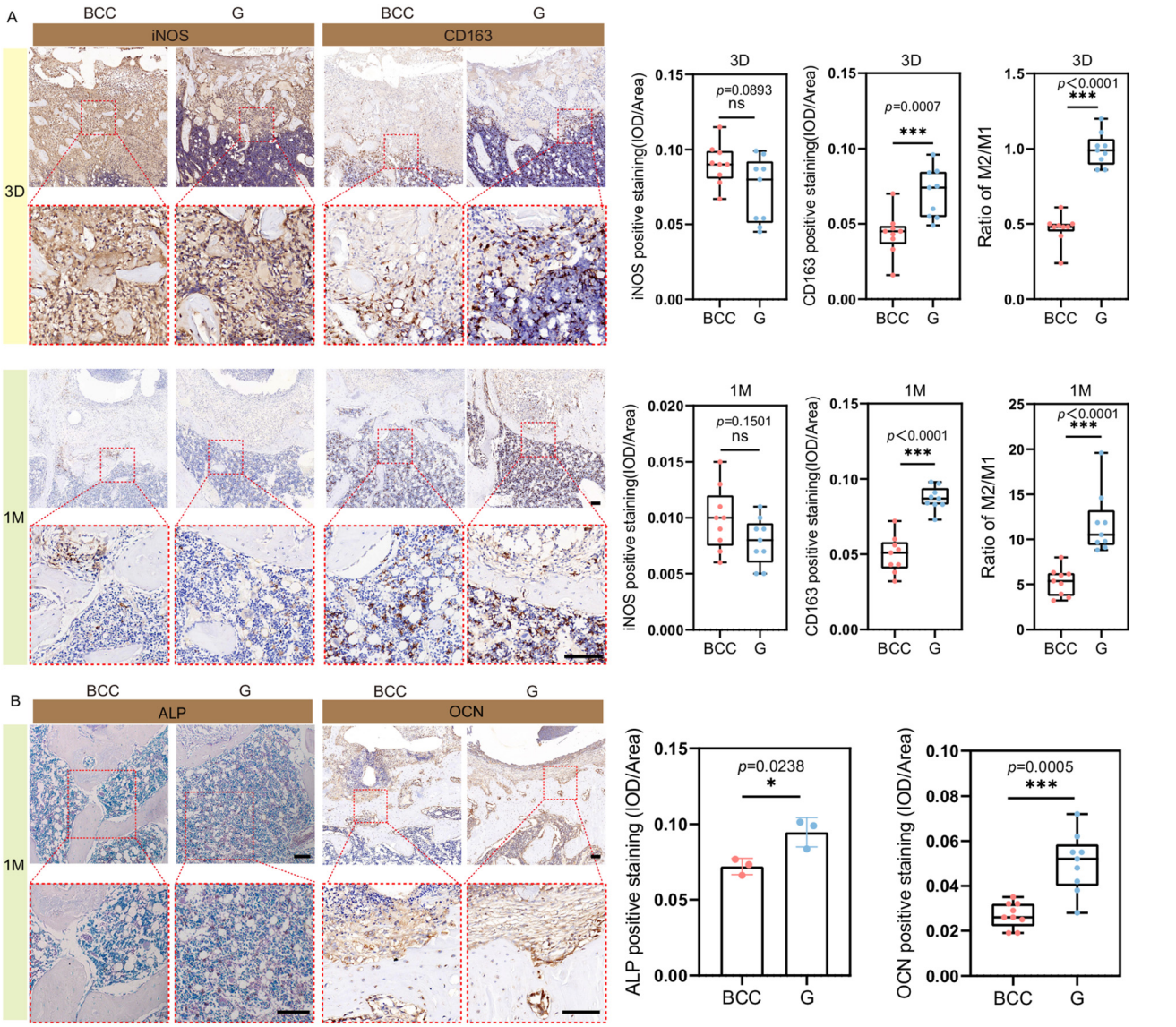

Fig. 9 Zn-based alloy scaffolds-mediated macrophage polarization and osteogenesis. (A) Qualitative representation and quantitative analysis of iNOS and CD163 (*i.e.*, M1 and M2 macrophage markers, respectively) immunohistochemistry staining of rat femur histological sections at 3 days and 1 month; (B) qualitative representation and quantitative analysis of ALP (osteoblastic lineage cell marker) and OCN (mature osteoblast marker) staining images in rat femur histological sections at 1 month. The scale bar = 100 μm. * $p < 0.05$, ** $p < 0.01$, and *** $p < 0.005$. Reproduced under terms of the CC-BY 4.0 license.[253] Copyright 2024, The Authors, published by Nature.

4.2.3. Polymeric implant materials

4.2.3.1. Natural polymers. Natural polymers are highly biocompatible, biodegradable, and rich in bioactive sites, making them ideal for tissue scaffolding. Certain natural polymers, such as collagen, hyaluronic acid, and chitosan, have demonstrated immunomodulatory effects, making them valuable in bone regenerative biomaterials.[254,255]

4.2.3.1.1.Collagen

Mineralized collagen (MC) is a promising tissue-engineering scaffold, as its nanostructure may regulate macrophage polarization, supporting bone regeneration. Implanting intrafibrillarly-MC (IMC), mimicking the surface chemistry and hierarchical topography of natural bone, in critical-sized rat mandible defects induced macrophage M2 polarization, formed more neobone, and enhanced the MSC recruitment compared to extrafibrillarly-MC (EMC) without a bone-like hierarchical nanostructure (Fig. 10). Small extracellular vesicles (*i.e.*, nanoscale membranous particles (<200 nm) like exosomes containing biomolecules, *e.g.*, proteins and nucleic acids, that enable extracellular communication) derived from IMC-treated macrophages promoted BMMSC osteogenic differentiation by upregulating key osteoblastic markers (BMP-2, bone gamma-carboxyglutamate protein (BGLAP), osterix (OSX), and COL1) and enhancing calcium nodule formation *via* the BMP-2/Smad5 pathway. IMC exhibited significantly higher water absorption than EMC, likely due to the absence of hydroxyapatite clusters,

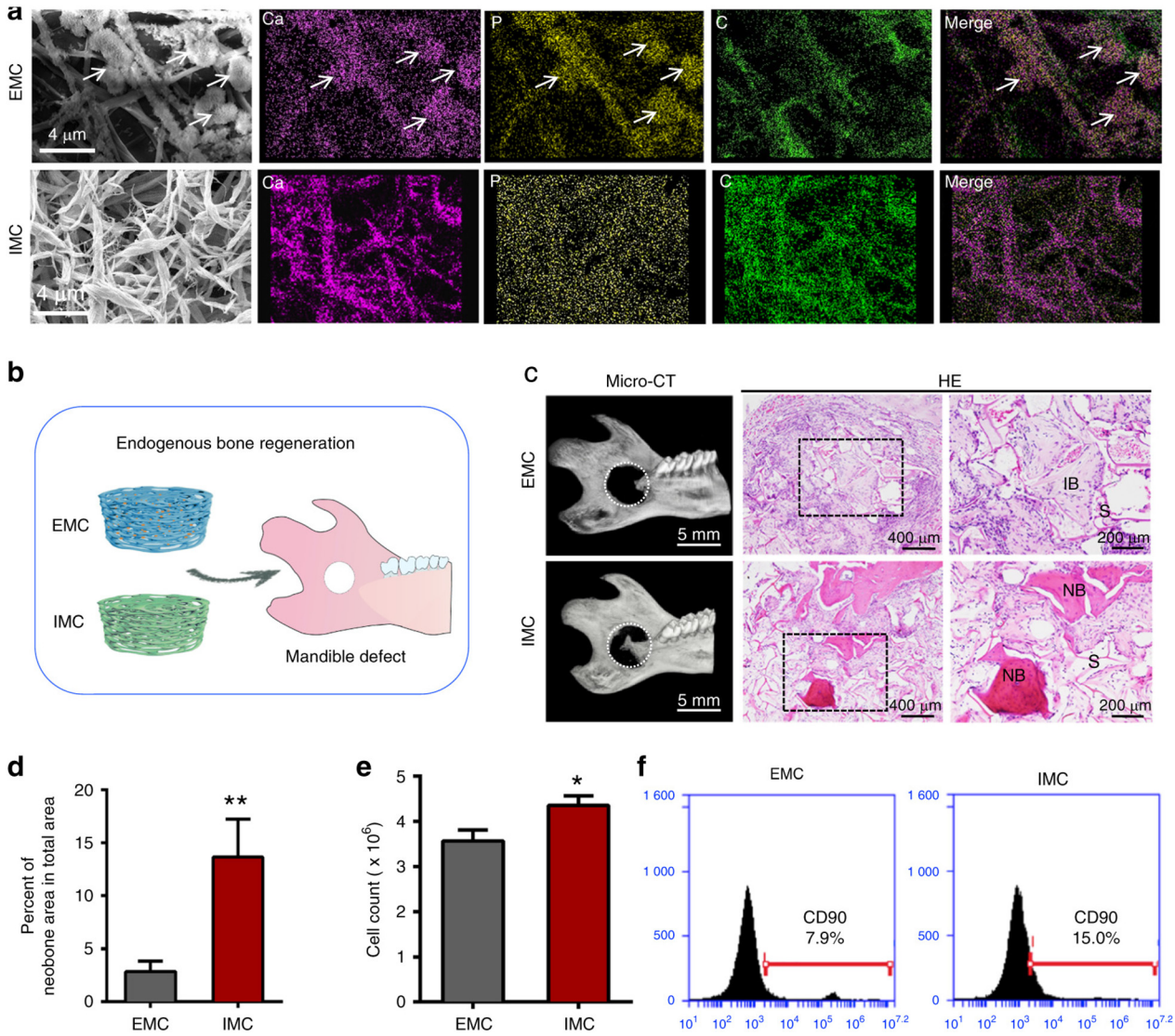

Fig. 10 Encouraging endogenous bone healing and MSC recruitment with IMC *in vivo*. (a) Scanning electron microscopy (SEM) and energy dispersive X-ray spectroscopy (EDS) mapping of IMC and EMC. Arrows demonstrate apatite clusters; (b) schematic representation of rat mandible defect and scaffold implantation; (c) micro-CT and H&E staining images of the neobone generation two weeks after EMC and IMC implantation. NB: new bone, IB: immature bone; (d) semi-quantification of the neobone area; (e) flow cytometry examination of cell counts one week after EMC and IMC implantation; (f) flow cytometry examination of $CD90^+$ cell counts in the EMC and IMC groups. ** $p < 0.01$ and * $p < 0.05$ compared to EMC. Reproduced under terms of the CC-BY 4.0 license.[256] Copyright 2020, The Authors, published by Nature.

as well as superior durability under cyclic loads, making it a promising scaffold for bone regeneration.[256,257] Sun *et al.* also confirmed that IMC triggered macrophage M2 polarization, upregulated IL-10 and Arg1 expression, and improved bone regeneration, while M1-like macrophages were upregulated on EMC, accompanied by the upregulation of iNOS and IL-6.[258] Incorporating MC as a coating material also benefits metallic implant osseointegration. Coating Ti implants with MC could instill macrophage M2 polarization by stimulating the integrin-related cascade and subsequently accelerate the MSC osteogenic differentiation.[259]

4.2.3.1.2.Hyaluronic acid

Hyaluronic acid, a highly hydrophilic polysaccharide, is widely used in tissue engineering due to its chemical versatility. Its incorporation into bone regeneration strategies and osteoinductive scaffolds has shown promising results.[260] Notably, hyaluronic acid regulates immune responses to implanted biomaterials by interacting with immune cells *via* CD44 receptors and TLRs, with its effects being dependent on molecular weight (MW).[261,262] High MW hyaluronic acid reduces inflammation by activating CD44 receptors; it enhances macrophage-mediated clearance of apoptotic cells, a function associated with anti-inflammatory macrophages. This is while low MW hyaluronic acid may trigger inflammatory responses *via* TLR activation.[263,264] Consistently, culture of macrophages with low MW hyaluronic acid (≤5 kDa) was shown to upregulate pro-inflammatory genes (NOS2, TNF, IL-12b, and CD80) and heightened NO and TNF-α release,

while high MW hyaluronic acid (>800 kDa) upregulated pro-resolving genes transcription (Arg1, macrophage mannose receptor-1 (MRC-1), and IL-10). In addition, macrophages treated with low MW hyaluronic acid and the TLR ligand (LPS) displayed a sustained and increased expression of inflammatory genes and mediators.[265] Some other investigations also recruited 2D culture of macrophages and demonstrated that high MW hyaluronic acid (>1000 kDa) promotes M2 polarization and inflammation resolution while low MW hyaluronic acid (<60 kDa) induces M1 polarization.[266,267]

Notably, the high MW hyaluronan might improve the immunosuppressive impact of Tregs. Bollyky *et al.* revealed that the high MW hyaluronan (1.5×10^6 kDa), in contrast to low MW hyaluronan (3 kDa), induces the transcription factor FOXP3 expression on human $CD4^+CD25^+$ Tregs and improves their capacity to limit the multiplication of responder cells. The effect was exclusively observed in activated $CD4^+CD25^+$ Tregs and was linked to the expression of CD44 isomers that exhibit a stronger affinity for high MW hyaluronan. Further, high MW hyaluronan directly suppressed effector T cells at higher concentrations.[268] Overall, the MW of hyaluronic acid serves as contextual signals for macrophages, Tregs, and T cells.

4.2.3.1.3.Chitosan

Chitosan, an osteoinductive and biocompatible polysaccharide derived from chitin, is widely used in bone implant research. Its immunomodulatory properties, along with those of its derivative chitooligosaccharide, support bone regeneration by influencing macrophage polarization.[269–272] For instance, chitosan-*graft*-polycaprolactone copolymers co-cultured with BMDMs attenuated pro-inflammatory cytokines secretion (IL-12 and IL-23) and increased M2 macrophage marker expression (Arg1). The observed effect was attributed to the chitosan, and the co-polymer with 50% w/w chitosan caused a four-fold higher increase in Arg1 expression than the co-polymer with 78% w/w chitosan.[272] *In vivo* experiments using mice implanted subcutaneously with the chitosan-*graft*-polycaprolactone scaffold also showed reduced pro-inflammatory cytokines and macrophages in the surrounding tissues by up to 65% with increasing chitosan content.[273] Another study demonstrated that the low concentration (4 mg ml^{-1}) and suitable polymerization degree of chitooligosaccharides polarize RAW 264.7 macrophages toward anti-inflammatory phenotypes and strengthen osteogenic and angiogenic processes in favor of bone regeneration without employing any inductive agent.[271]

Notably, the chitosan degree of acetylation affects its immunomodulatory effects. A chitosan scaffold with 5% acetylation promoted an anti-inflammatory response by increasing CD206-positive macrophages, elevating anti-inflammatory cytokines, and reducing pro-inflammatory cytokines. In contrast, a 15% acetylation scaffold induced a pro-inflammatory response by upregulating CCR7+ macrophages and increasing pro-inflammatory cytokine levels.[274] Similar findings demonstrated that decreasing the degree of acetylation contributes to the improvement of macrophage migration and adhesion to the chitosan surfaces and their polarization toward anti-inflammatory phenotypes *in vitro* and *in vivo*.[275] These data underscore the importance of chitosan and its derivative content and degree of acetylation in developed immunomodulatory bone tissue scaffolds.

4.2.3.1.4.Alginate

Alginates are highly adaptable materials with tunable properties. The influence of alginate-based biomaterials on macrophage phenotype and function has become a key factor in their design. Engineered alginate-based biomaterials through tuning their stiffness, topography, and hydrophilicity can facilitate macrophages' transition from the pro-inflammatory M1 phenotype to the anti-inflammatory M2 phenotype, ensuring an efficient resolution of the FBR and promoting bone regeneration.[276] By modifying parameters such as polymer structure, crosslinking type, and processing techniques, alginates can be engineered into various porous structures, including hydrogels, fibers, and beads, with sizes ranging from the nano- to macro-scale. Higher crosslinker concentrations lead to increased stiffness, reduced pore size, and altered scaffold morphology, influencing macrophage polarization and bone regeneration.[276–278] Additionally, incorporating materials like graphene oxide and polyvinyl alcohol enhances hydrophilicity, further optimizing alginate-based scaffolds for orthopedic applications.[279,280]

4.2.3.2. Synthetic polymers. Unlike naturally occurring polymers, synthetic polymers are created by artificial approaches. This allows for consistent quality between batches, cost-effective production, and easily adjustable physical and chemical characteristics. The subsequent discussion focuses on the immunomodulatory impacts of commonly used synthetic polymers in orthopedics.

4.2.3.2.1.Polyethylene glycol (PEG)

The remarkable tunability and reproducibility of PEG-based hydrogels have made them among the most popular synthetic biomaterials.[281] Known as "blank slates", they resist protein adsorption and elicit minimal physiological responses due to their water-binding capacity and high chain mobility.[282,283] Consequently, they are widely used in bone scaffolding and as coatings for implantable biomaterials to mitigate excessive inflammation and FBR.[284,285] PEG hydrogels possess intrinsic regenerative properties, as they can regulate local immune responses and influence the phenotypic changes of BMDMs. Lynn *et al.* cultured macrophages on PEG hydrogel disks with and without LPS stimulation. In the absence of LPS, there was an initial spike in IL-1β and TNF-α expression within 4 hours, followed by a decrease in pro-inflammatory gene expression and an increase in the IL-10/IL-12β ratio by 96 hours. With LPS, there was a more pronounced early upregulation of pro-inflammatory genes, followed by an increase in the M2 macrophage marker Arg1. These results suggest that PEG hydrogels promote a shift from an inflammatory to a pro-healing macrophage phenotype, which supports bone regeneration.[286] Of note, PEG hydrogel stiffness contributes to regulating immune reactions. Softer hydrogels (130 kPa) reduce macrophage activation and lessen the severity of FBR by lower-

ing pro-inflammatory cytokine levels (TNF-α, IL-1β, IL-6), while stiffer hydrogels (240 and 840 kPa) provoke stronger inflammatory responses.[287] This might explain the contradicting results by Lynn *et al.* demonstrating that PEG hydrogels instill robust inflammatory reactions and a thick layer of macrophages at the material interface. They found that RGD modification of PEG hydrogels could attenuate the inflammatory reactions and FBR.[92] The RGD cell adhesion ligand modulates the interaction of inflammatory cells with implants, particularly macrophages, by engaging integrin signaling, which helps reduce the production of inflammatory cytokines.[288,289]

Concerns about the immunogenicity of PEG have risen due to reports of high anti-PEG antibody levels in clinical studies.[290–292] Isaac *et al.* investigated this by immunizing mice against PEG and examining bone healing with BMP-2-loaded PEG hydrogels. PEG sensitization enhanced bone formation but led to abnormal porous bone structures and increased immune cell recruitment compared to non-sensitized mice. Notably, even non-immunized animals implanted with the hydrogel developed anti-PEG antibodies. These findings suggest that immune reactions against PEG could impact the effectiveness of PEG-based or PEG-coated bone implants, highlighting the need for further research.[293] PEG has also been shown to induce macrophage fusion *in vitro*, leading to the formation of osteoclast-like cells with bone resorptive activity. This suggests that PEG may enhance the osteoclastogenic function of macrophages, promoting cell fusion compared to spontaneous fusion without PEG.[294]

4.2.3.2.2.Polymethylmethacrylate (PMMA)

PMMA is known as a biocompatible, bioinert, and hydrophobic rigid thermoplastic polymer that offers exceptional mechanical fixation of implants; however, it might also affect macrophage activity at the bone–implant interface. PMMA has been shown to induce inflammatory macrophages, leading to low-grade surface and high-grade lacunar osteolysis, which can cause implant loosening.[295,296] PMMA particles are taken up by macrophages and provoke strong inflammatory responses, increasing bone resorption by mature osteoclasts.[297] Immune-based strategies have been introduced to improve cement osseointegration and address the inflammatory issues with PMMA. One such solution is incorporating enoxaparin into PMMA bone cement, which has been shown to induce macrophage M2 polarization and provide anti-inflammatory immune regulation. Fan *et al.* found that incorporating enoxaparin into PMMA cement significantly downregulated the TLR4/NF-κB signaling pathway in macrophages, promoting their M2 polarization, evidenced by decreased expression of CD86, TNF-α, IL-6, and iNOS, and increased expression of CD206, IL-10, and Arg1 in LPS-treated cells.[298] Modifying PMMA cement with MC has also been suggested to reduce FBR. This modification enhances the cement's hydrophilicity and provides an elastic modulus that complements the bone's mechanical performance under dynamic stress. Yang *et al.* implanted PMMA-MC and PMMA into a goat disc degeneration model. The MC helped reduce macrophage proliferation and fusion and significantly decreased the expression of fibroblast-stimulating growth factors like IGF-1, bFGF, and TGF-β. After three months, histological analysis showed that PMMA-MC was directly in contact with new bone, while PMMA was surrounded by fibrous tissue.[299] Moreover, mixing PMMA with bisphosphonates, such as etidronate, reduces bone resorption caused by PMMA particles. The mixed cement particles, when added to a co-culture of monocytes and UMR106 cells, led to significantly fewer lacunar pits and reduced numbers of tartrate-resistant acid phosphatase (TRAP)-positive cells, which are markers of osteoclast differentiation.[300] Various other strategies, such as modifying PMMA with borosilicate glass, calcium phosphate, and carbon nanotubes, have been introduced to enhance its osseointegration and provide osteogenic activity.[301–304]

4.2.3.2.3.Polyetheretherketone (PEEK)

PEEK is a popular orthopedic implant material due to its excellent biocompatibility, chemical stability, radiolucent properties, and elastic modulus similar to human bone.[305] However, as a bioinert material, smooth-surfaced PEEK faces challenges like fibrous encapsulation and poor osseointegration, leading to potential implant failure.[306,307] Creating porous PEEK has been shown to reduce fibrous responses and improve mechanical interlocking with bone, leading to better osteogenic differentiation and implant fixation.[307] The porous structure also enhances macrophage attachment, promoting their adhesion, diffusion, and polarization, which helps regulate the local immune microenvironment.[308,309] PEEK with a flat surface induced intense M1-mediated inflammation in a mouse air pouch model, while sulfonated PEEK (SP) with a 3D porous surface structure reduced cell infiltration, shifted macrophage M2 polarization, and decreased fibrous layer thickness compared to smooth PEEK (Fig. 11).[309] Porous PEEK scaffolds with a larger pore size (400 μm) promote better macrophage M2 polarization and enhance cytokine secretion related to osteogenesis and angiogenesis. They also exhibit superior biomechanical properties, osseointegration, and osteogenesis compared to scaffolds with smaller pores (200 μm).[310]

Another strategy to improve PEEK bioactivity is increasing surface hydrophilicity. Fukuda *et al.* prepared phosphate-modified PEEK with improved surface hydrophilicity but without surface topography or roughness alteration. The rough and hydrophilic PEEK considerably limited the phenotypic shift of LPS-stimulated RAW264.7 macrophages to an inflammatory phenotype, indicated by decreased TNF-α and increased IL-10 expression levels, and improved BMMSC proliferation, ALP activity, and bone-like nodule generation compared to rough and hydrophobic bare PEEK.[311] These data demonstrate the significance of the physicochemical properties of engineered PEEK in tuning local immune responses.

Chemical PEEK surface modification, for example, with inorganic ions, has also shown encouraging results. Calcium ion-modified PEEK was fabricated by Toita *et al.* through coating with poly(norepinephrine) and soaking in calcium hydroxide aqueous solution. LPS-primed RAW264.7 macrophages cultured on the modified PEEK were shifted towards

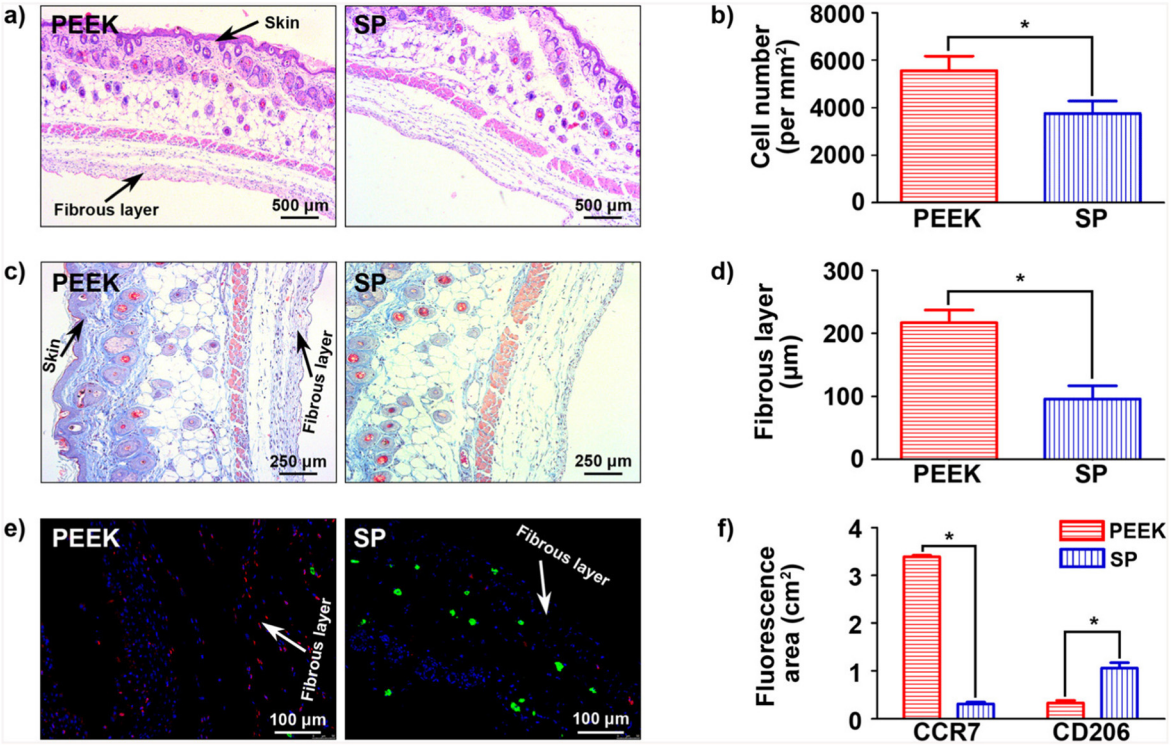

Fig. 11 SP-mediated immunomodulation in the air pouch model. (a) Illustration of the structure and layers of the air-pouch tissue after H&E staining; (b) infiltrated cells count; (c) illustration of the fibrous tissue after Masson trichrome staining; (d) the fibrous layer thicknesses; (e) illustrations showing macrophage phenotypes: CCR7-positive M1 cells (red) and CD206-positive M2 cells (green); (f) the fluorescence area representing the CCR7- and CD206-positive regions. * $p < 0.05$. Reproduced with permission.[309] Copyright 2019, Elsevier.

the M2 phenotype indicated by lower TNF-α and IL-1α but higher IL-10 production than those cultured on pristine PEEK. The calcium ion-modified PEEK consistently induced the proliferation and osteoblastic differentiation of pre-osteoblasts and human MSCs.[312] Liu *et al.* fabricated Zn-coated PEEK by incorporating a layer of Zn ions on sulfonated PEEK through a customized magnetron sputtering technique. The Zn-coated SPEEK instilled macrophage anti-inflammatory polarization and provoked osteogenic cytokine secretion. The osteogenic differentiation of BMMSCs was then improved, which led to better PEEK osseointegration.[313] PEEK modification by Sr, Cu, and Ag ions has also been reported to regulate local immune responses.[11]

Various coatings can enhance PEEK's surface properties to reduce inflammation and fibrous encapsulation while improving osseointegration. Ti dioxide coatings, applied *via* arc ion plating (AIP) or nanogranular structuring with polydopamine, have been shown to suppress inflammation, promote osteoblast adhesion, and improve implant-bone integration.[314,315] Plasma-sprayed Ti coatings also enhanced macrophage M2 polarization and reduced fibrous encapsulation, leading to better osseointegration and bone repair.[316,317] Additionally, hydroxyapatite coatings have demonstrated anti-inflammatory effects and improved osseointegration, though hydroxyapatite-PEEK blends may provide more stable anti-inflammatory benefits and superior mechanical properties.[318–320] This is probably due to the lack of chemical bonding between hydroxyapatite and PEEK, as well as the mechanical wear of the hydroxyapatite coating that weakens the anti-inflammatory function of the implant.[11,321]

Eventually, PEEK surface modification with functional groups can enhance implant osseointegration. Carboxyl-functionalized PEEK regulates integrin signaling, reduces macrophage inflammation, and promotes tissue repair by lowering TNF-α, IL-1β, and IL-6 expression. In contrast, amine-functionalized PEEK reduced MSC osteogenic differentiation but exhibited superior mineralization and bone binding. Combining different functional groups may optimize PEEK implants by reducing inflammation while enhancing bone integration.[322,323]

4.2.3.2.4.Other synthetic polymers

The synthesis of PLA-based scaffolds has shown significant promise in osteoimmunomodulation. PLA may influence local inflammation, as its degradation has been found to promote excessive M2 polarization in macrophages through STAT6 phosphorylation.[324] Functionalizing PLA with immunomodulatory agents such as chitosan and polydopamine can further enhance its osteoimmunomodulatory potential.[325] Additionally, PLA membranes engineered with bone-mimicking surface topographies using the soft lithography technique have demonstrated the ability to sequentially activate M1 and M2 macrophages, as previously discussed.[159] Furthermore,

PLA scaffolds can serve as a delivery platform for osteoimmunomodulatory applications. An injectable PLA porous microsphere has been developed, capable of forming calcium phosphate crystals on its surface through melatonin binding, followed by bionanomimetic mineralization. The controlled release of melatonin and calcium phosphate crystals facilitates macrophage M2 polarization, macrophage reprogramming, and enhanced osteogenesis.[326]

Polycaprolactone (PCL) and PCL-based scaffolds, approved by the FDA, are widely used in tissue engineering. However, due to their lack of bioactive agents, PCL alone is rarely employed for bone tissue engineering. The incorporation of a mineral phase into PCL might enhance its mechanical strength and bioactivity for orthopedic applications. Despite these benefits, this approach may disrupt macrophage responses and result in bone healing failure. Macrophage co-culture assays have shown that phagocytosis of the β-tricalcium phosphate (β-TCP)-integrated PCL scaffold degradation products induces oxidative stress and promotes inflammatory M1 polarization in macrophages.[181] However, PCL/PEG/hydroxyapatite bioactive scaffolds have been shown to influence macrophage polarization based on their pore size. Scaffolds with 582.1 ± 27.2 μm pores significantly reduced the FBR, promoted M2 macrophage infiltration, and enhanced new bone formation.[327] These data highlight the importance of considering both chemical composition and physicochemical properties when designing osteoimmunomodulatory bone implants. As another approach to improve PCL scaffold bioactivity, loading telmisartan into PCL/polyvinylpyrrolidone (PVP) electrospun scaffold enabled higher M2 macrophage upregulation and better bone regeneration.[328]

4.2.4 Bioceramics

4.2.4.1 Calcium phosphate (CP). Calcium phosphates (CPs) are the most extensively studied category of bioceramics incorporated into bone substitute materials. Numerous studies suggest that osteoimmunomodulation plays a key role in CPs' mechanism of action in facilitating bone regeneration. Chen *et al.* demonstrated that β-TCP powder extracts induce macrophage polarization toward the M2 phenotype through the calcium-sensing receptor pathway. This process was associated with upregulating BMP-2 and anti-inflammatory genes (IL-10 and IL-1rα) and downregulating pro-inflammatory genes (IL-1β and IL-6) that eventually provoked osteogenic differentiation of BMMSCs.[329] Additional research has yielded comparable results, showing that biphasic calcium phosphate (BCP) induces macrophage polarization toward the M2 phenotype by upregulating integrin αvβ expression, thereby enhancing the production of anti-inflammatory cytokines along with key growth factors like VEGF, BMP-2, and TGF-β1.[330,331] Shi *et al.* consistently demonstrated that CP coating on polycaprolactone scaffolds promotes implant osteointegration through M2 macrophage polarization *in vitro* and *in vivo*.[332] This collective upregulation is favorable for bone regeneration by supporting MSC recruitment and facilitating osteoblastic differentiation. Conflicting evidence also exists regarding BCP's role in promoting the expression of pro-inflammatory cytokines (IL-6, MCP-1, and TNF-α) in macrophages. However, this upregulation has not been linked to the suppression of MSC osteogenic differentiation, possibly due to the dose-dependent nature of inflammatory cytokine effects.[330,333]

4.2.4.2 Bioactive glasses (BGs). Bioactive glasses (BGs) are widely recognized for their biocompatibility and bioactivity, making them valuable materials for bone tissue engineering scaffolds and implant coatings. Extensive research has focused on their interactions with regenerative cells involved in bone repair, with growing insights into their immunomodulatory properties.[334] Gómez-Cerezo *et al.* synthesized a mesoporous BG (MBG-75S), which supported macrophage proliferation without promoting polarization toward the pro-inflammatory M1 phenotype. This *in vitro* observation suggests that MBG-75S may trigger the necessary innate immune response *in vivo* without causing excessive inflammation.[335] Montes-Casado *et al.* studied the *in vitro* interaction of MBG nanoparticles (MBGNs) with immune cells involved in both innate and adaptive immunity, including DCs, T cells, and B cells. Their findings indicated that MBGNs were non-cytotoxic, had no impact on cell viability or proliferation, and did not significantly alter the intracellular production or secretion of key pro- and anti-inflammatory cytokines (TNF-α, IFN-γ, IL-2, IL-6, IL-10) in activated immune cells.[336] However, when exposed to LPS, 45S5 BG notably decreased the secretion of pro-inflammatory cytokines IL-6 and TNF-α in macrophages.[337]

Unlike other inorganic biomaterials, BGs offer greater compositional flexibility, allowing the incorporation of bioactive ions to modulate inflammation.[338,339] For instance, MBGNs doped with Ce have been shown to suppress pro-inflammatory cytokines (TNF-α, IL-1β, and IL-6) in macrophages due to Ce's antioxidant properties.[340] Similarly, doping 58S BG with Zn and Cu significantly suppressed the expression of pro-inflammatory genes.[341] Additionally, surface functionalization with anti-inflammatory molecules has emerged as a strategy to further minimize inflammatory responses, enhancing BGs' potential for bone regeneration.[342]

5. Conclusion

The successful osseointegration of implants and bone regeneration largely depends on the interaction between implant materials and immune cells at bone defect sites. While various immune cells are involved in tissue regeneration and inflammatory responses to implants, significant research has focused on designing bone implants that encourage macrophages to adopt a pro-healing M2 phenotype (Fig. 12). Beyond using bone implants as delivery platforms for osteoimmunomodulatory therapies, it is essential to carefully adjust their properties to influence local immune responses positively. This review examined how the chemical composition and physicochemical characteristics of bone implants affect their interactions with immune cells. Irregularly shaped and rougher particles released from bone implants could induce stronger inflammation. Conflicting data on material stiffness highlights the

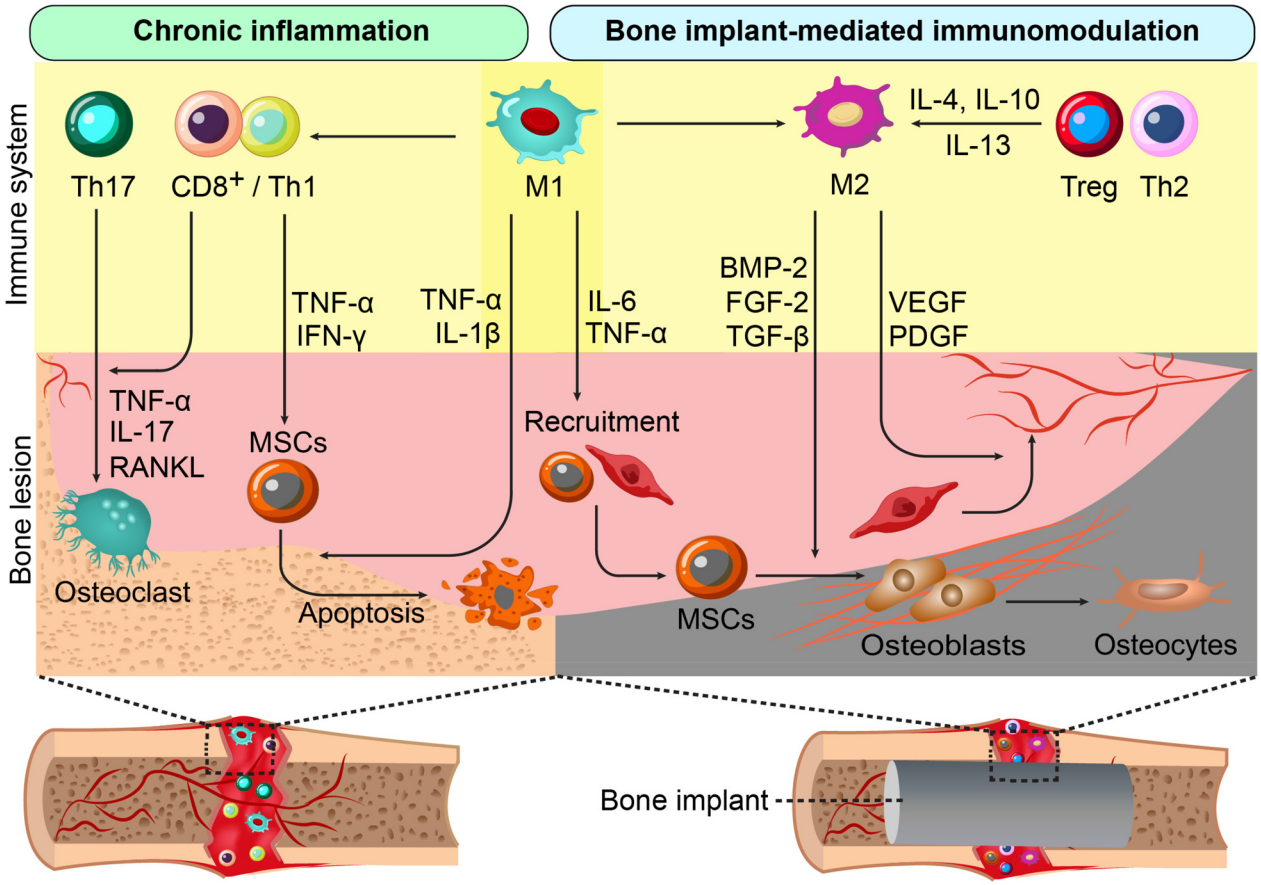

Fig. 12 Implant material-mediated osteoimmunomodulation. Impaired healing due to chronic inflammation induced by M1 macrophages, resulting in MSC apoptosis and osteoclast activation. Engineered bone implants promote macrophage M2 polarization and resolve inflammation, facilitating vascularization and new bone generation processes.

need for standardized investigations. Rough micro/nano topographies likely promote pro-healing macrophage polarization, and specific surface architectures, such as nanowires and nanotubes, could enhance immunomodulatory bone implants. Surface hydrophilicity helps regulate inflammation but may reduce protein adsorption if excessive. Similarly, positively charged surfaces support tissue regeneration by enhancing protein adsorption and immune cell interactions, though excessive charge can hinder cell proliferation. Regarding the chemical composition, non-biodegradable metallic implants like stainless steel, CoCrMo, and Ti alloys provide strong mechanical properties but are prone to corrosion, potentially triggering inflammation. Coatings and additive manufacturing offer solutions to mitigate these effects. Biodegradable metals such as Mg and Zn show promise in promoting pro-healing immune responses but degrade too rapidly. Natural polymers like MC and hyaluronic acid help reduce inflammation, while chitosan could enhance immunomodulatory scaffolds regarding its content and degree of acetylation. Synthetic polymers, including optimized PEEK and PEG, exhibit anti-inflammatory properties and support bone regeneration; however, PEG immunogenicity has raised concerns and PMMA induces inflammation. Eventually, bioceramics, particularly β-TCP and antioxidant-doped bioactive glasses, are promising for immunomodulatory bone implants. Optimizing bone implants based on these factors is crucial for developing advanced biomaterials with enhanced osteoimmunomodulatory potential. However, despite extensive preclinical research, the successful clinical translation of immunomodulatory bone biomaterials remains limited, likely due to an incomplete understanding of their interactions with the immune system.

To advance the clinical translation of immunomodulatory bone biomaterials, comprehensive investigations are required to elucidate how exactly immune cells interact with these materials, as well as their immunomodulatory payloads or coatings. These studies should provide a detailed understanding of the immune mechanisms involved in biomaterial interactions, including the specific molecular pathways and signaling mechanisms through which immune cells contribute to implant osseointegration, as well as bone formation/resorption. Furthermore, while current research primarily focuses on macrophage interactions, other key immune players have received less attention. A more in-depth analysis of these overlooked components may offer a more accurate prediction of immune responses to biomaterials, ultimately leading to the development of more effective osteoimmunomodulatory strat-

egies. Standardizing scaffold design methods could also help with better interpreting immune responses, as design variations often lead to inconsistent outcomes, making it challenging to compare study results and impede the effective translation of research findings into clinical practice.

Furthermore, considering multiple inherent or adopted characteristics simultaneously would allow for a more holistic interpretation of experimental data. Comprehensive research that integrates various contributing factors and employs consistent models is essential for advancing the development of clinically viable bone biomaterials. Standard examinations comparing immune responses to different implant materials under the same conditions are also needed to identify optimal materials for implant fabrication. For instance, research by Olivares-Navarrete *et al.* showed that 316L SS and PEEK implants elicited stronger inflammatory responses, characterized by high neutrophil and T cell infiltration, compared to Ti or TC4 alloy.[369] Finally, the development of advanced biomaterials incorporating nanomaterials and bioactive molecules to precisely target and modulate immune responses, along with conducting more translational research using improved animal models that closely mimic human immune responses, can significantly enhance osteoimmunomodulatory and regenerative capabilities.

Author contributions

Mehdi Sanati: conceptualization, data curation, formal analysis, investigation, validation, writing – original draft, writing – review & editing. Ines Pieterman: investigation, data curation, writing – original draft. Natacha Levy: investigation, data curation, writing – original draft. Tayebeh Akbari: formal analysis, software. Mohamadreza Tavakoli: data curation, writing – review & editing. Alireza Hassani Najafabadi: data curation, formal analysis, validation, writing – review & editing. Saber Amin Yavari: conceptualization, supervision, data curation, investigation, validation, writing – review & editing.

Data availability

No primary research results, software or code have been included and no new data were generated or analysed as part of this review.

Conflicts of interest

The authors declare no conflict of interest.

References

1 G. N. Duda, S. Geissler, S. Checa, S. Tsitsilonis, A. Petersen and K. Schmidt-Bleek, *Nat. Rev. Rheumatol.*, 2023, **19**, 78–95.
2 A. H. Schmidt, *Injury*, 2021, **52**, S18–S22.
3 A. Bandyopadhyay, I. Mitra, S. B. Goodman, M. Kumar and S. Bose, *Prog. Mater. Sci.*, 2023, **133**, 101053.
4 A. Szwed-Georgiou, P. Płociński, B. Kupikowska-Stobba, M. M. Urbaniak, P. Rusek-Wala, K. Szustakiewicz, P. Piszko, A. Krupa, M. Biernat and M. Gazińska, *ACS Biomater. Sci. Eng.*, 2023, **9**, 5222–5254.
5 G. Gautam, S. Kumar and K. Kumar, *Mater. Today: Proc.*, 2022, **50**, 2206–2217.
6 P. Ghelich, M. Kazemzadeh-Narbat, A. Hassani Najafabadi, M. Samandari, A. Memić and A. Tamayol, *Adv. NanoBiomed Res.*, 2022, **2**, 2100073.
7 F. Loi, L. A. Córdova, J. Pajarinen, T.-h. Lin, Z. Yao and S. B. Goodman, *Bone*, 2016, **86**, 119–130.
8 E. Gibon, Y. Takakubo, S. Zwingenberger, J. Gallo, M. Takagi and S. B. Goodman, *J. Biomed. Mater. Res., Part A*, 2023, **112**, 1172–1187.
9 J. He, G. Chen, M. Liu, Z. Xu, H. Chen, L. Yang and Y. Lv, *Mater. Sci. Eng., C*, 2020, **108**, 110411.
10 Q. Sun, Y. Zhou, A. Zhang, J. Wu, L. Tan and S. Guo, *J. Magnesium Alloys*, 2024, **12**(7), 2695–2710.
11 Z. Zhang, X. Zhang, Z. Zheng, J. Xin, S. Han, J. Qi, T. Zhang, Y. Wang and S. Zhang, *Mater. Today Bio*, 2023, 100748.
12 T. Khodaei, E. Schmitzer, A. P. Suresh and A. P. Acharya, *Bioact. Mater.*, 2023, **24**, 153–170.
13 B. Zhang, Y. Su, J. Zhou, Y. Zheng and D. Zhu, *Adv. Sci.*, 2021, **8**, 2100446.
14 S. S. Soni and C. B. Rodell, *Acta Biomater.*, 2021, **133**, 139–152.
15 J. Parkin and B. Cohen, *Lancet*, 2001, **357**, 1777–1789.
16 M. Ma, W. Jiang and R. Zhou, *Immunity*, 2024, **57**, 752–771.
17 J. Zindel and P. Kubes, *Annu. Rev. Pathol.: Mech. Dis.*, 2020, **15**, 493–518.
18 K. Hoebe, E. Janssen and B. Beutler, *Nat. Immunol.*, 2004, **5**, 971–974.
19 J. Han, A. N. Rindone and J. H. Elisseeff, *Adv. Mater.*, 2024, 2311646.
20 Z. Julier, A. J. Park, P. S. Briquez and M. M. Martino, *Acta Biomater.*, 2017, **53**, 13–28.
21 S. De Oliveira, E. E. Rosowski and A. Huttenlocher, *Nat. Rev. Immunol.*, 2016, **16**, 378–391.
22 C. J. Thomas and K. Schroder, *Trends Immunol.*, 2013, **34**, 317–328.
23 H. R. Manley, M. C. Keightley and G. J. Lieschke, *Front. Immunol.*, 2018, **9**, 426162.
24 V. Papayannopoulos, *Nat. Rev. Immunol.*, 2018, **18**, 134–147.
25 E. B. Okeke, C. Louttit, C. Fry, A. H. Najafabadi, K. Han, J. Nemzek and J. J. Moon, *Biomaterials*, 2020, **238**, 119836.
26 D. Azzouz, M. A. Khan and N. Palaniyar, *Cell Death Discovery*, 2021, **7**, 113.
27 S. L. Wong, M. Demers, K. Martinod, M. Gallant, Y. Wang, A. B. Goldfine, C. R. Kahn and D. D. Wagner, *Nat. Med.*, 2015, **21**, 815–819.

28 J. V. Dovi, L.-K. He and L. A. DiPietro, *J. Leukoc. Biol.*, 2003, **73**, 448–455.
29 M. C. Greenlee-Wacker, *Immunol. Rev.*, 2016, **273**, 357–370.
30 I. Kourtzelis, G. Hajishengallis and T. Chavakis, *Front. Immunol.*, 2020, **11**, 526246.
31 N. Lewkowicz, M. Klink, M. P. Mycko and P. Lewkowicz, *Immunobiology*, 2013, **218**, 455–464.
32 P. Ghelich, M. Samandari, A. Hassani Najafabadi, A. Tanguay, J. Quint, N. Menon, D. Ghanbariamin, F. Saeedinejad, F. Alipanah and R. Chidambaram, *Adv. Healthcare Mater.*, 2024, 2302836.
33 F. Ethuin, B. Gérard, J. E. Benna, A. Boutten, M.-A. Gougereot-Pocidalo, L. Jacob and S. Chollet-Martin, *Lab. Invest.*, 2004, **84**, 1363–1371.
34 X. Su, Y. Yu, Y. Zhong, E. G. Giannopoulou, X. Hu, H. Liu, J. R. Cross, G. Rätsch, C. M. Rice and L. B. Ivashkiv, *Nat. Immunol.*, 2015, **16**, 838–849.
35 G. S. Selders, A. E. Fetz, M. Z. Radic and G. L. Bowlin, *Regener. Biomater.*, 2017, **4**, 55–68.
36 W. Li, H.-M. Hsiao, R. Higashikubo, B. T. Saunders, A. Bharat, D. R. Goldstein, A. S. Krupnick, A. E. Gelman, K. J. Lavine and D. Kreisel, *JCI Insight*, 2016, **1**(12), e87315.
37 T. A. Wilgus, S. Roy and J. C. McDaniel, *Adv. Wound Care*, 2013, **2**, 379–388.
38 M. Braile, L. Cristinziano, S. Marcella, G. Varricchi, G. Marone, L. Modestino, A. L. Ferrara, A. De Ciuceis, S. Scala and M. R. Galdiero, *J. Leukoc. Biol.*, 2021, **109**, 621–631.
39 G. R. Grotendorst, G. Smale and D. Pencev, *J. Cell. Physiol.*, 1989, **140**, 396–402.
40 C. Sunderkötter, T. Nikolic, M. J. Dillon, N. Van Rooijen, M. Stehling, D. A. Drevets and P. J. Leenen, *J. Immunol.*, 2004, **172**, 4410–4417.
41 E. Melgarejo, M. Á. Medina, F. Sánchez-Jiménez and J. L. Urdiales, *Int. J. Biochem. Cell Biol.*, 2009, **41**, 998–1001.
42 J. Yang, L. Zhang, C. Yu, X.-F. Yang and H. Wang, *Biomark. Res.*, 2014, **2**, 1–9.
43 C. Schlundt, H. Fischer, C. H. Bucher, C. Rendenbach, G. N. Duda and K. Schmidt-Bleek, *Acta Biomater.*, 2021, **133**, 46–57.
44 R. de Waal Malefyt, J. Abrams, B. Bennett, C. G. Figdor and J. E. de Vries, *J. Exp. Med.*, 1991, **174**, 1209–1220.
45 N. McCartney-Francis, D. Mizel, H. Wong, L. Wahl and S. Wahl, *Growth Factors*, 1990, **4**, 27–35.
46 M. Murai, O. Turovskaya, G. Kim, R. Madan, C. L. Karp, H. Cheroutre and M. Kronenberg, *Nat. Immunol.*, 2009, **10**, 1178–1184.
47 H. Newman, Y. V. Shih and S. Varghese, *Biomaterials*, 2021, **277**, 121114.
48 R. Toita, J.-H. Kang and A. Tsuchiya, *Acta Biomater.*, 2022, **154**, 583–596.
49 X. Bai, D. Chen, Y. Dai, S. Liang, J. Guo, B. Dai, D. Zhang and L. Feng, *Nanomedicine*, 2021, **38**, 102457.
50 O. R. Mahon, D. C. Browe, T. Gonzalez-Fernandez, P. Pitacco, I. T. Whelan, S. Von Euw, C. Hobbs, V. Nicolosi, K. T. Cunningham and K. H. Mills, *Biomaterials*, 2020, **239**, 119833.
51 S. Reinke, S. Geissler, W. R. Taylor, K. Schmidt-Bleek, K. Juelke, V. Schwachmeyer, M. Dahne, T. Hartwig, L. Akyüz and C. Meisel, *Sci. Transl. Med.*, 2013, **5**, 177ra136.
52 C. Schlundt, S. Reinke, S. Geissler, C. H. Bucher, C. Giannini, S. Märdian, M. Dahne, C. Kleber, B. Samans and U. Baron, *Front. Immunol.*, 2019, **10**, 1954.
53 P. Stashenko, R. B. Gonçalves, B. Lipkin, A. Ficarelli, H. Sasaki and A. Campos-Neto, *Am. J. Pathol.*, 2007, **170**, 203–213.
54 K. Kang, S. M. Reilly, V. Karabacak, M. R. Gangl, K. Fitzgerald, B. Hatano and C.-H. Lee, *Cell Metab.*, 2008, **7**, 485–495.
55 F. Carbone, A. Nencioni, F. Mach, N. Vuilleumier and F. Montecucco, *Thromb. Haemostasis*, 2013, **110**, 501–514.
56 G. R. Kinsey, R. Sharma, L. Huang, L. Li, A. L. Vergis, H. Ye, S.-T. Ju and M. D. Okusa, *J. Am. Soc. Nephrol.*, 2009, **20**, 1744–1753.
57 F. R. D'Alessio, K. Tsushima, N. R. Aggarwal, E. E. West, M. H. Willett, M. F. Britos, M. R. Pipeling, R. G. Brower, R. M. Tuder and J. F. McDyer, *J. Clin. Invest.*, 2009, **119**, 2898–2913.
58 P. Lewkowicz, N. Lewkowicz, A. Sasiak and H. Tchórzewski, *J. Immunol.*, 2006, **177**, 7155–7163.
59 M. M. Tiemessen, A. L. Jagger, H. G. Evans, M. J. van Herwijnen, S. John and L. S. Taams, *Proc. Natl. Acad. Sci. U. S. A.*, 2007, **104**, 19446–19451.
60 L. S. Taams, J. M. van Amelsfort, M. M. Tiemessen, K. M. Jacobs, E. C. de Jong, A. N. Akbar, J. W. Bijlsma and F. P. Lafeber, *Hum. Immunol.*, 2005, **66**, 222–230.
61 F. Venet, A. Pachot, A.-L. Debard, J. Bohe, J. Bienvenu, A. Lepape, W. S. Powell and G. Monneret, *J. Immunol.*, 2006, **177**, 6540–6547.
62 L. W. Collison, C. J. Workman, T. T. Kuo, K. Boyd, Y. Wang, K. M. Vignali, R. Cross, D. Sehy, R. S. Blumberg and D. A. Vignali, *Nature*, 2007, **450**, 566–569.
63 A. Joetham, K. Takada, C. Taube, N. Miyahara, S. Matsubara, T. Koya, Y.-H. Rha, A. Dakhama and E. W. Gelfand, *J. Immunol.*, 2007, **178**, 1433–1442.
64 J. Weirather, U. D. Hofmann, N. Beyersdorf, G. C. Ramos, B. Vogel, A. Frey, G. Ertl, T. Kerkau and S. Frantz, *Circ. Res.*, 2014, **115**, 55–67.
65 T. Ono, K. Okamoto, T. Nakashima, T. Nitta, S. Hori, Y. Iwakura and H. Takayanagi, *Nat. Commun.*, 2016, **7**, 10928.
66 N. Charatcharoenwitthaya, S. Khosla, E. J. Atkinson, L. K. McCready and B. L. Riggs, *J. Bone Miner. Res.*, 2007, **22**, 724–729.
67 G. Mori, P. D'melio, R. Faccio and G. Brunetti, *J. Immunol. Res.*, 2013, **2013**, 720504.
68 S. Kotake, N. Udagawa, M. Hakoda, M. Mogi, K. Yano, E. Tsuda, K. Takahashi, T. Furuya, S. Ishiyama and K. J. Kim, *Arthritis Rheum.*, 2001, **44**, 1003–1012.
69 A. Bozec and M. M. Zaiss, *Curr. Osteoporos. Rep.*, 2017, **15**, 121–125.

70 M. M. Zaiss, R. Axmann, J. Zwerina, K. Polzer, E. Gückel, A. Skapenko, H. Schulze-Koops, N. Horwood, A. Cope and G. Schett, *Arthritis Rheum.*, 2007, **56**, 4104–4112.
71 A. A. Maghazachi, *The Chemokine System in Experimental and Clinical Hematology*, 2010, pp. 37–58.
72 M. Najar, M. Fayyad-Kazan, N. Meuleman, D. Bron, H. Fayyad-Kazan and L. Lagneaux, *Mol. Cell. Biochem.*, 2018, **447**, 111–124.
73 R. M. Petri, A. Hackel, K. Hahnel, C. A. Dumitru, K. Bruderek, S. B. Flohe, A. Paschen, S. Lang and S. Brandau, *Stem Cell Rep.*, 2017, **9**, 985–998.
74 O. DelaRosa, B. Sánchez-Correa, S. Morgado, C. Ramírez, B. del Río, R. Menta, E. Lombardo, R. Tarazona and J. G. Casado, *Stem Cells Dev.*, 2012, **21**, 1333–1343.
75 P. A. Sotiropoulou, S. A. Perez, A. D. Gritzapis, C. N. Baxevanis and M. Papamichail, *Stem Cells*, 2006, **24**, 74–85.
76 A. Tosello-Trampont, F. A. Surette, S. E. Ewald and Y. S. Hahn, *Front. Immunol.*, 2017, **8**, 301.
77 R. F. Sîrbulescu, C. K. Boehm, E. Soon, M. Q. Wilks, I. Ilieș, H. Yuan, B. Maxner, N. Chronos, C. Kaittanis and M. D. Normandin, *Wound Repair Regen.*, 2017, **25**, 774–791.
78 M. Pan, W. Hong, Y. Yao, X. Gao, Y. Zhou, G. Fu, Y. Li, Q. Guo, X. Rao and P. Tang, *Stem Cells Int.*, 2019, **2019**, 8150123.
79 Y. Han, Y. Jin, Y. Miao, T. Shi and X. Lin, *Int. Immunopharmacol.*, 2018, **62**, 147–154.
80 J. O. Manilay and M. Zouali, *Trends Mol. Med.*, 2014, **20**, 405–412.
81 M. Vinish, W. Cui, E. Stafford, L. Bae, H. Hawkins, R. Cox and T. Toliver-Kinsky, *Wound Repair Regener.*, 2016, **24**, 6–13.
82 S. J. Galli, M. Grimbaldeston and M. Tsai, *Nat. Rev. Immunol.*, 2008, **8**, 478–486.
83 T. Biedermann, M. Kneilling, R. Mailhammer, K. Maier, C. A. Sander, G. Kollias, S. L. Kunkel, L. Hültner and M. Röcken, *J. Exp. Med.*, 2000, **192**, 1441–1452.
84 S. Franz, S. Rammelt, D. Scharnweber and J. C. Simon, *Biomaterials*, 2011, **32**, 6692–6709.
85 B. O. O. Boni, L. Lamboni, T. Souho, M. Gauthier and G. Yang, *Mater. Horiz.*, 2019, **6**, 1122–1137.
86 S. Jhunjhunwala, *ACS Biomater. Sci. Eng.*, 2017, **4**, 1128–1136.
87 S. Yamashiro, H. Kamohara, J.-M. Wang, D. Yang, W.-H. Gong and T. Yoshimura, *J. Leukocyte Biol.*, 2001, **69**, 698–704.
88 J. Hahn, C. Schauer, C. Czegley, L. Kling, L. Petru, B. Schmid, D. Weidner, C. Reinwald, M. H. Biermann and S. Blunder, *FASEB J.*, 2019, **33**, 1401.
89 I. George Broughton, J. E. Janis and C. E. Attinger, *Plast. Reconstr. Surg.*, 2006, **117**, 12S–34S.
90 J. M. Fox, F. Kausar, A. Day, M. Osborne, K. Hussain, A. Mueller, J. Lin, T. Tsuchiya, S. Kanegasaki and J. E. Pease, *Sci. Rep.*, 2018, **8**, 9466.
91 J. A. Jones, D. T. Chang, H. Meyerson, E. Colton, I. K. Kwon, T. Matsuda and J. M. Anderson, *J. Biomed. Mater. Res., Part A*, 2007, **83**, 585–596.
92 A. D. Lynn, T. R. Kyriakides and S. J. Bryant, *J. Biomed. Mater. Res., Part A*, 2010, **93**, 941–953.
93 Z. Sheikh, P. J. Brooks, O. Barzilay, N. Fine and M. Glogauer, *Materials*, 2015, **8**, 5671–5701.
94 F. Eslami-Kaliji, N. Hedayat Nia, J. R. Lakey, A. M. Smink and M. Mohammadi, *Polymers*, 2023, **15**, 1313.
95 W. G. Brodbeck, M. MacEwan, E. Colton, H. Meyerson and J. M. Anderson, *J. Biomed. Mater. Res., Part A*, 2005, **74**, 222–229.
96 J. M. Anderson, *Biological Interactions on Materials Surfaces: Understanding and Controlling Protein, Cell, and Tissue Responses*, 2009, pp. 225–244.
97 A. P. Acharya, N. V. Dolgova, M. J. Clare-Salzler and B. G. Keselowsky, *Biomaterials*, 2008, **29**, 4736–4750.
98 V. Milleret, S. Buzzi, P. Gehrig, A. Ziogas, J. Grossmann, K. Schilcher, A. S. Zinkernagel, A. Zucker and M. Ehrbar, *Acta Biomater.*, 2015, **24**, 343–351.
99 J. Vitte, A.-M. Benoliel, A. Pierres and P. Bongrand, *eCells Mater. J.*, 2004, **30**, 52–63.
100 L. Zhang, Z. Cao, T. Bai, L. Carr, J.-R. Ella-Menye, C. Irvin, B. D. Ratner and S. Jiang, *Nat. Biotechnol.*, 2013, **31**, 553–556.
101 N. Caballero-Sánchez, S. Alonso-Alonso and L. Nagy, *FEBS J.*, 2024, **291**, 1597–1614.
102 B. Choi, C. Lee and J.-W. Yu, *Arch. Pharmacal Res.*, 2023, **46**, 78–89.
103 J. Lee, H. Byun, S. K. Madhurakkat Perikamana, S. Lee and H. Shin, *Adv. Healthcare Mater.*, 2019, **8**, 1801106.
104 Y. Wang, H. Zhang, Y. Hu, Y. Jing, Z. Geng and J. Su, *Adv. Funct. Mater.*, 2022, **32**, 2208639.
105 S. Metwally and U. Stachewicz, *Mater. Sci. Eng., C*, 2019, **104**, 109883.
106 S. Shirazi, S. Ravindran and L. F. Cooper, *Biomaterials*, 2022, **291**, 121903.
107 J. O. Abaricia, N. Farzad, T. J. Heath, J. Simmons, L. Morandini and R. Olivares-Navarrete, *Acta Biomater.*, 2021, **133**, 58–73.
108 R. Zhao, T. Shang, B. Yuan, X. Zhu, X. Zhang and X. Yang, *Bioact. Mater.*, 2022, **17**, 379–393.
109 P. Turon, L. J. Del Valle, C. Alemán and J. Puiggalí, *Appl. Sci.*, 2017, **7**, 60.
110 R. Wang, W. Liu, Q. Wang, G. Li, B. Wan, Y. Sun, X. Niu, D. Chen and W. Tian, *Biomater. Sci.*, 2020, **8**, 4426–4437.
111 F. Lebre, R. Sridharan, M. J. Sawkins, D. J. Kelly, F. J. O'Brien and E. C. Lavelle, *Sci. Rep.*, 2017, **7**, 2922.
112 D. J. Misiek, J. N. Kent and R. F. Carr, *J. Oral Maxillofac. Surg.*, 1984, **42**, 150–160.
113 B. F. Matlaga, L. P. Yasenchak and T. N. Salthouse, *J. Biomed. Mater. Res.*, 1976, **10**, 391–397.
114 M. V. Baranov, M. Kumar, S. Sacanna, S. Thutupalli and G. Van den Bogaart, *Front. Immunol.*, 2021, **11**, 607945.
115 J. A. Callejas, J. Gil, A. Brizuela, R. A. Pérez and B. M. Bosch, *Int. J. Mol. Sci.*, 2022, **23**, 7333.
116 A. Kurup, P. Dhatrak and N. Khasnis, *Mater. Today: Proc.*, 2021, **39**, 84–90.

117 T. Jiang, M.-T. Zheng, R.-M. Li and N.-J. Ouyang, *Mechanobiol. Med.*, 2024, 100046.
118 T. Jiang, X.-Y. Tang, Y. Mao, Y.-Q. Zhou, J.-J. Wang, R.-M. Li, X.-R. Xie, H.-M. Zhang, B. Fang and N.-J. Ouyang, *Acta Biomater.*, 2023, **168**, 159–173.
119 J. O. Abaricia, A. H. Shah and R. Olivares-Navarrete, *Biomaterials*, 2021, **271**, 120715.
120 Z. Yang, Z. Min and B. Yu, *Int. Rev. Immunol.*, 2020, **39**, 292–298.
121 M. Chen, Y. Zhang, P. Zhou, X. Liu, H. Zhao, X. Zhou, Q. Gu, B. Li, X. Zhu and Q. Shi, *Bioact. Mater.*, 2020, **5**, 880–890.
122 Z. Zhuang, Y. Zhang, S. Sun, Q. Li, K. Chen, C. An, L. Wang, J. J. van den Beucken and H. Wang, *ACS Biomater. Sci. Eng.*, 2020, **6**, 3091–3102.
123 Z. Liu, J. Liu, J. Li, Y. Li, J. Sun, Y. Deng and H. Zhou, *Front. Bioeng. Biotechnol.*, 2023, **11**, 1133547.
124 R. Hang, Z. Wang, H. Wang, Y. Zhang, Y. Zhao, L. Bai and X. Yao, *Biomater. Adv.*, 2023, **148**, 213356.
125 X.-T. He, R.-X. Wu, X.-Y. Xu, J. Wang, Y. Yin and F.-M. Chen, *Acta Biomater.*, 2018, **71**, 132–147.
126 F. Mei, Y. Guo, Y. Wang, Y. Zhou, B. C. Heng, M. Xie, X. Huang, S. Zhang, S. Ding and F. Liu, *Cell Proliferation*, 2024, e13640.
127 T. Okamoto, Y. Takagi, E. Kawamoto, E. J. Park, H. Usuda, K. Wada and M. Shimaoka, *Exp. Cell Res.*, 2018, **367**, 264–273.
128 J. Y. Hsieh, M. T. Keating, T. D. Smith, V. S. Meli, E. L. Botvinick and W. F. Liu, *APL Bioeng.*, 2019, **3**, 016103.
129 M. Saitakis, S. Dogniaux, C. Goudot, N. Bufi, S. Asnacios, M. Maurin, C. Randriamampita, A. Asnacios and C. Hivroz, *eLife*, 2017, **6**, e23190.
130 M. H. Chin, M. D. Norman, E. Gentleman, M.-O. Coppens and R. M. Day, *ACS Appl. Mater. Interfaces*, 2020, **12**, 47355–47367.
131 R. S. O'Connor, X. Hao, K. Shen, K. Bashour, T. Akimova, W. W. Hancock, L. C. Kam and M. C. Milone, *J. Immunol.*, 2012, **189**, 1330–1339.
132 L. Shi, J. Y. Lim and L. C. Kam, *Biomaterials*, 2023, **292**, 121928.
133 Y. Mori, M. Kamimura, K. Ito, M. Koguchi, H. Tanaka, H. Kurishima, T. Koyama, N. Mori, N. Masahashi and T. Aizawa, *Appl. Sci.*, 2024, **14**, 2259.
134 A. Bandyopadhyay, I. Mitra, J. D. Avila, M. Upadhyayula and S. Bose, *Int. J. Extreme Manuf.*, 2023, **5**, 032014.
135 L. Fan, S. Chen, M. Yang, Y. Liu and J. Liu, *Adv. Healthcare Mater.*, 2024, **13**, 2302132.
136 L. Zhang, B. Song, S.-K. Choi and Y. Shi, *Int. J. Mech. Sci.*, 2021, **197**, 106331.
137 K. M. Hotchkiss, G. B. Reddy, S. L. Hyzy, Z. Schwartz, B. D. Boyan and R. Olivares-Navarrete, *Acta Biomater.*, 2016, **31**, 425–434.
138 W. A. Soskolne, S. Cohen, L. Shapira, L. Sennerby and A. Wennerberg, *Clin. Oral Implants Res.*, 2002, **13**, 86–93.
139 I. Cockerill, Y. Su, J. H. Lee, D. Berman, M. L. Young, Y. Zheng and D. Zhu, *Nano Lett.*, 2020, **20**, 4594–4602.
140 J. O. Abaricia, A. H. Shah, R. M. Musselman and R. Olivares-Navarrete, *Biomater. Sci.*, 2020, **8**, 2289–2299.
141 P. G. Coelho, J. M. Granjeiro, G. E. Romanos, M. Suzuki, N. R. Silva, G. Cardaropoli, V. P. Thompson and J. E. Lemons, *J. Biomed. Mater. Res., Part B*, 2009, **88**, 579–596.
142 L. Zhao, S. Mei, P. K. Chu, Y. Zhang and Z. Wu, *Biomaterials*, 2010, **31**, 5072–5082.
143 P. G. Coelho, R. Jimbo, N. Tovar and E. A. Bonfante, *Dent. Mater.*, 2015, **31**, 37–52.
144 A. Klymov, L. Prodanov, E. Lamers, J. A. Jansen and X. F. Walboomers, *Biomater. Sci.*, 2013, **1**, 135–151.
145 M. Wang, F. Chen, Y. Tang, J. Wang, X. Chen, X. Li and X. Zhang, *Mater. Des.*, 2022, **213**, 110302.
146 T. Zhang, M. Jiang, X. Yin, P. Yao and H. Sun, *Sci. Rep.*, 2021, **11**, 18418.
147 Y. Yang, T. Zhang, M. Jiang, X. Yin, X. Luo and H. Sun, *J. Biomed. Mater. Res., Part A*, 2021, **109**, 1429–1440.
148 Y. Zhou, C. Tang, J. Deng, R. Xu, Y. Yang and F. Deng, *Biochem. Biophys. Res. Commun.*, 2021, **581**, 53–59.
149 T. U. Luu, S. C. Gott, B. W. Woo, M. P. Rao and W. F. Liu, *ACS Appl. Mater. Interfaces*, 2015, **7**, 28665–28672.
150 Y. Zhu, H. Liang, X. Liu, J. Wu, C. Yang, T. M. Wong, K. Y. Kwan, K. M. Cheung, S. Wu and K. W. Yeung, *Sci. Adv.*, 2021, **7**, eabf6654.
151 S. Jin, R. Yang, C. Chu, C. Hu, Q. Zou, Y. Li, Y. Zuo, Y. Man and J. Li, *Acta Biomater.*, 2021, **129**, 148–158.
152 Y. He, Z. Li, X. Ding, B. Xu, J. Wang, Y. Li, F. Chen, F. Meng, W. Song and Y. Zhang, *Bioact. Mater.*, 2022, **8**, 109–123.
153 K. Li, S. Liu, T. Hu, I. Razanau, X. Wu, H. Ao, L. Huang, Y. Xie and X. Zheng, *ACS Biomater. Sci. Eng.*, 2020, **6**, 969–983.
154 L. A. van Dijk, R. Duan, X. Luo, D. Barbieri, M. Pelletier, C. Christou, A. J. Rosenberg, H. Yuan, F. Barrèrre-de Groot and W. R. Walsh, *JOR Spine*, 2018, **1**, e1039.
155 L. A. van Dijk, D. Barbieri, F. Barrère-de Groot, H. Yuan, R. Oliver, C. Christou, W. R. Walsh and J. D. de Bruijn, *J. Biomed. Mater. Res., Part B*, 2019, **107**, 2080–2090.
156 R. Duan, L. Van Dijk, D. Barbieri, F. De Groot, H. Yuan and J. De Bruijn, *Eur. Cells Mater.*, 2019, **37**, 60–73.
157 H. W. Stempels, A. M. Lehr, D. Delawi, E. A. Hoebink, I. A. Wiljouw, D. H. Kempen, J. L. van Susante, M. C. Kruyt and D. C. S. R. Group, *Spine*, 2024, **49**(19), 1323–1331.
158 X. Dai, Y. Bai, B. C. Heng, Y. Li, Z. Tang, C. Lin, O. Liu, Y. He, X. Zhang and X. Deng, *J. Mater. Chem. B*, 2022, **10**, 1875–1885.
159 B. Özcolak, B. Erenay, S. Odabaş, K. D. Jandt and B. Garipcan, *Sci. Rep.*, 2024, **14**, 12721.
160 Y. Xie, C. Hu, Y. Feng, D. Li, T. Ai, Y. Huang, X. Chen, L. Huang and J. Tan, *Regener. Biomater.*, 2020, **7**, 233–245.
161 G. Li, P. Yang, X. Guo, N. Huang and R. Shen, *Cytokine*, 2011, **56**, 208–217.
162 L. Lv, Y. Xie, K. Li, T. Hu, X. Lu, Y. Cao and X. Zheng, *Adv. Healthcare Mater.*, 2018, **7**, 1800675.

163 M. A. Alfarsi, S. M. Hamlet and S. Ivanovski, *J. Biomed. Mater. Res., Part A*, 2014, **102**, 60–67.
164 S. M. Hamlet, R. S. Lee, H. J. Moon, M. A. Alfarsi and S. Ivanovski, *Clin. Oral Implants Res.*, 2019, **30**, 1085–1096.
165 Q. Li, A. Shen and Z. Wang, *RSC Adv.*, 2020, **10**, 16537–16550.
166 S. Gao, R. Lu, X. Wang, J. Chou, N. Wang, X. Huai, C. Wang, Y. Zhao and S. Chen, *J. Biomater. Appl.*, 2020, **34**, 1239–1253.
167 K. M. Hotchkiss, N. M. Clark and R. Olivares-Navarrete, *Biomaterials*, 2018, **182**, 202–215.
168 J. L. Drury and D. J. Mooney, *Biomaterials*, 2003, **24**, 4337–4351.
169 N. A. Peppas, J. Z. Hilt, A. Khademhosseini and R. Langer, *Adv. Mater.*, 2006, **18**, 1345–1360.
170 A. Al Madhoun, K. Meshal, N. Carrió, E. Ferrés-Amat, E. Ferrés-Amat, M. Barajas, A. L. Jiménez-Escobar, A. S. Al-Madhoun, A. Saber and Y. Abou Alsamen, *J. Funct. Biomater.*, 2024, **15**, 293.
171 M. Li, X. Chu, D. Wang, L. Jian, L. Liu, M. Yao, D. Zhang, Y. Zheng, X. Liu and Y. Zhang, *Biomaterials*, 2022, **282**, 121408.
172 J. Hunt, B. Flanagan, P. McLaughlin, I. Strickland and D. Williams, *J. Biomed. Mater. Res.*, 1996, **31**, 139–144.
173 E. Mariani, G. Lisignoli, R. M. Borzì and L. Pulsatelli, *Int. J. Mol. Sci.*, 2019, **20**, 636.
174 M. Bartneck, H. A. Keul, S. Singh, K. Czaja, J. Bornemann, M. Bockstaller, M. Moeller, G. Zwadlo-Klarwasser and J. Groll, *ACS Nano*, 2010, **4**, 3073–3086.
175 D. R. Getts, R. L. Terry, M. T. Getts, C. Deffrasnes, M. Müller, C. van Vreden, T. M. Ashhurst, B. Chami, D. McCarthy and H. Wu, *Sci. Transl. Med.*, 2014, **6**, 219ra217.
176 Z. Liu, J. Liu, J. Li, Y. Li, J. Sun, Y. Deng and H. Zhou, *Front. Bioeng. Biotechnol.*, 2023, **11**, 1133547.
177 Y. Yang, Y. Lin, R. Xu, Z. Zhang, W. Zeng, Q. Xu and F. Deng, *Int. J. Nanomed.*, 2022, **17**, 5117; M. A. Alfarsi, S. M. Hamlet and S. Ivanovski, *J. Biomed. Mater. Res. A.*, 2013, **102**(1), 60–67.
178 W. G. Brodbeck, J. Patel, G. Voskerician, E. Christenson, M. S. Shive, Y. Nakayama, T. Matsuda, N. P. Ziats and J. M. Anderson, *Proc. Natl. Acad. Sci. U. S. A.*, 2002, **99**, 10287–10292.
179 N. Eliaz, *Materials*, 2019, **12**, 407.
180 D. R. Bijukumar, S. Salunkhe, G. Zheng, M. Barba, D. J. Hall, R. Pourzal and M. T. Mathew, *Acta Biomater.*, 2020, **101**, 586–597.
181 H. Wu, X. Wei, Y. Liu, H. Dong, Z. Tang, N. Wang, S. Bao, Z. Wu, L. Shi and X. Zheng, *Bioact. Mater.*, 2023, **21**, 595–611.
182 C. C. Ude, C. J. Esdaille, K. S. Ogueri, H.-M. Kan, S. J. Laurencin, L. S. Nair and C. T. Laurencin, *Regener. Eng. Transl. Med.*, 2021, **7**, 247–261.
183 M. Li, J. Wu, W. Geng, P. Gao, Y. Yang, X. Li, K. Xu, Q. Liao and K. Cai, *Bioact. Mater.*, 2024, **31**, 355–367.
184 G. Heise, C. Black, R. Smith, B. Morrow and W. Mihalko, *Bone Joint J.*, 2020, **102**, 116–121.
185 M. Li, J. Wu, W. Geng, Y. Yang, X. Li, K. Xu, K. Li, Y. Li, Q. Duan and P. Gao, *Biomaterials*, 2023, **301**, 122262.
186 A. Bekmurzayeva, W. J. Duncanson, H. S. Azevedo and D. Kanayeva, *Mater. Sci. Eng., C*, 2018, **93**, 1073–1089.
187 M. K. Lodhi, K. M. Deen, M. Greenlee-Wacker and W. Haider, *Addit. Manuf.*, 2019, **27**, 8–19.
188 J. A. Moreto, R. V. Gelamo, M. V. da Silva, T. T. Steffen, C. J. F. de Oliveira, P. A. de Almeida Buranello and M. R. Pinto, *J. Mater. Sci.: Mater. Med.*, 2021, **32**, 1–6.
189 M. Ferreira, F. Mariani, N. Leite, R. Gelamo, I. Aoki, A. de Siervo, H. Pinto and J. Moreto, *Mater. Chem. Phys.*, 2024, **312**, 128610.
190 D. Sivaraj, K. Vijayalakshmi, A. Ganeshkumar and R. Rajaram, *Int. J. Pharm.*, 2020, **590**, 119946.
191 D. Pathote, D. Jaiswal, V. Singh and C. Behera, *Appl. Surf. Sci. Adv.*, 2023, **13**, 100365.
192 A. Sharifnabi, M. Fathi, B. E. Yekta and M. Hossainalipour, *Appl. Surf. Sci.*, 2014, **288**, 331–340.
193 B. Aksakal, M. Gavgali and B. Dikici, *J. Mater. Eng. Perform.*, 2010, **19**, 894–899.
194 A. Fratila, C. Jimenez-Marcos, J. C. Mirza-Rosca and A. Saceleanu, *Mater. Chem. Phys.*, 2023, **304**, 127867.
195 S. Xue, Y. Xu, S. Xu, Y. Zhong, G. Ruan, J. Ma, Y. Hu, C. Ding and W. Sang, *Chem. Eng. J.*, 2022, **435**, 135115.
196 J. L. Gilbert, S. Sivan, Y. Liu, S. B. Kocagöz, C. M. Arnholt and S. M. Kurtz, *J. Biomed. Mater. Res., Part A*, 2015, **103**, 211–223.
197 K. C. Miller, M. B. Holloway, B. R. Morrow, R. A. Smith and W. M. Mihalko, *J. Arthroplasty*, 2022, **37**, S355–S363.
198 M. N. Brown, L. H. Phan, D. M. Bryant, R. A. Smith, B. R. Morrow and W. M. Mihalko, *J. Arthroplasty*, 2024, **39**(9), S280–S285.
199 M. Alvarez-Vera, J. A. Ortega, I. Ortega-Ramos, H. Hdz-García, R. Muñoz-Arroyo, J. Díaz-Guillén, J. Acevedo-Dávila and M. Hernández-Rodriguez, *Wear*, 2021, **477**, 203819.
200 Y.-C. Lin, C.-C. Hu, W.-C. Liu, U. Dhawan, Y.-C. Chen, Y.-L. Lee, H.-W. Yen, Y.-J. Kuo and R.-J. Chung, *J. Mater. Chem. B*, 2024, **12**, 7814–7825.
201 B. Lohberger, N. Stuendl, D. Glaenzer, B. Rinner, N. Donohue, H. C. Lichtenegger, L. Ploszczanski and A. Leithner, *Sci. Rep.*, 2020, **10**, 1682.
202 V. Ragone, E. Canciani, C. A. Biffi, R. D'Ambrosi, R. Sanvito, C. Dellavia and E. Galliera, *Biomed. Microdevices*, 2019, **21**, 1–9.
203 C.-E. Tsai, J. Hung, Y. Hu, D.-Y. Wang, R. M. Pilliar and R. Wang, *J. Mech. Behav. Biomed. Mater.*, 2021, **114**, 104233.
204 P. D. Khan and S. H. Khahro, *Front. Bioeng. Biotechnol.*, 2024, **12**, 1400918.
205 E. Kandaswamy, M. Harsha and V. M. Joshi, *J. Trace Elem. Med. Biol.*, 2024, 127464.
206 C. Stolzer, M. Müller, M. Gosau, A. Henningsen, S. Fuest, F. Aavani and R. Smeets, *J. Oral Maxillofac. Surg.*, 2023, **81**, 308–317.

207 K. Y. Cheng, P. Gupta, H. Kanniyappan, H. Zahurullah, Y. Sun, M. Alhamad and M. T. Mathew, *Ann. Biomed. Eng.*, 2023, **51**, 2749–2761.
208 W. Kheder, A. Bouzid, T. Venkatachalam, I. M. Talaat, N. M. Elemam, T. K. Raju, S. Sheela, M. N. Jayakumar, A. A. Maghazachi and A. R. Samsudin, *Int. J. Mol. Sci.*, 2023, **24**, 11644.
209 M. A. Kurtz, K. Alaniz, P. W. Kurtz, A. C. Wessinger, A. Moreno-Reyes and J. L. Gilbert, *J. Biomed. Mater. Res., Part A*, 2024, **112**, 1250–1264.
210 C. Liu, Z. Yan, J. Yang, P. Wei, D. Zhang, Q. Wang, X. Zhang, Y. Hao and D. Yang, *ACS Appl. Mater. Interfaces*, 2024, **16**, 18503–18521.
211 A. O. Mace, M. A. Kurtz and J. L. Gilbert, *J. Funct. Biomater.*, 2024, **15**, 38.
212 M. A. Kurtz, A. C. Wessinger, A. Mace, A. Moreno-Reyes and J. L. Gilbert, *J. Biomed. Mater. Res., Part A*, 2023, **111**, 1538–1553.
213 A. Gudima, D. Hesselbarth, G. Li, V. Riabov, J. Michel, Q. Liu, C. Schmuttermaier, Z. Jiao, C. Sticht and A. Jawhar, *J. Leukocyte Biol.*, 2024, qiae072.
214 J. O. Abaricia, A. H. Shah, M. Chaubal, K. M. Hotchkiss and R. Olivares-Navarrete, *Biomaterials*, 2020, **243**, 119920.
215 D. Avery, L. Morandini, L. S. Sheakley, A. H. Shah, L. Bui, J. O. Abaricia and R. Olivares-Navarrete, *Biomaterials*, 2022, **289**, 121797.
216 D. Avery, L. Morandini, M. Gabriec, L. Sheakley, M. Peralta, H. J. Donahue, R. K. Martin and R. Olivares-Navarrete, *Acta Biomater.*, 2023, **169**, 605–624.
217 D. Avery, L. Morandini, L. Sheakley, M. Grabiec and R. Olivares-Navarrete, *Acta Biomater.*, 2024, **179**, 385–397.
218 C. Shuai, S. Li, S. Peng, P. Feng, Y. Lai and C. Gao, *Mater. Chem. Front.*, 2019, **3**, 544–562.
219 M. Rahman, N. K. Dutta and N. Roy Choudhury, *Front. Bioeng. Biotechnol.*, 2020, **8**, 564.
220 W. Qiao, K. H. Wong, J. Shen, W. Wang, J. Wu, J. Li, Z. Lin, Z. Chen, J. P. Matinlinna and Y. Zheng, *Nat. Commun.*, 2021, **12**, 2885.
221 V. Manescu, I. Antoniac, A. Antoniac, D. Laptoiu, G. Paltanea, R. Ciocoiu, I. V. Nemoianu, L. G. Gruionu and H. Dura, *Biomimetics*, 2023, **8**, 618.
222 H. B. Amara, D. C. Martinez, F. A. Shah, A. J. Loo, L. Emanuelsson, B. Norlindh, R. Willumeit-Römer, T. Plocinski, W. Swieszkowski and A. Palmquist, *Bioact. Mater.*, 2023, **26**, 353–369.
223 J. Sugimoto, A. M. Romani, A. M. Valentin-Torres, A. A. Luciano, C. M. Ramirez Kitchen, N. Funderburg, S. Mesiano and H. B. Bernstein, *J. Immunol.*, 2012, **188**, 6338–6346.
224 N.-Y. Su, T.-C. Peng, P.-S. Tsai and C.-J. Huang, *J. Surg. Res.*, 2013, **185**, 726–732.
225 M. P. Kwesiga, A. A. Gillette, F. Razaviamri, M. E. Plank, A. L. Canull, Z. Alesch, W. He, B. P. Lee and R. J. Guillory II, *Bioact. Mater.*, 2023, **23**, 261–273.
226 M. Costantino, A. Schuster, H. Helmholz, A. Meyer-Rachner, R. Willumeit-Römer and B. Luthringer-Feyerabend, *Acta Biomater.*, 2020, **101**, 598–608.
227 L. Liang, D. Song, K. Wu, Z. Ouyang, Q. Huang, G. Lei, K. Zhou, J. Xiao and H. Wu, *Biomater. Res.*, 2022, **26**, 17.
228 M. Bessa-Gonçalves, C. Ribeiro-Machado, M. Costa, C. Ribeiro, J. Barbosa, M. Barbosa and S. Santos, *Acta Biomater.*, 2023, **155**, 667–683.
229 Y. Sun, H. Yu, H. Peng, X. Kang, Z. Peng, X. Dong, W. Wang, Y. Song and X. Zhang, *J. Mater. Sci. Technol.*, 2023, **139**, 113–119.
230 F. Witte, *Acta Biomater.*, 2010, **6**, 1680–1692.
231 A. Zhang, X. Wang, Z. Zhang, X. Zhang, J. Wang, Y. Liu, Y. Chen, J. Chen, T. Chen and Y. Wang, *Chem. Eng. J.*, 2024, 152761.
232 F. Kiani, C. Wen and Y. Li, *Acta Biomater.*, 2020, **103**, 1–23.
233 A. Mahato, M. De, P. Bhattacharjee, V. Kumar, P. Mukherjee, G. Singh, B. Kundu, V. K. Balla and S. K. Nandi, *J. Mater. Sci.: Mater. Med.*, 2021, **32**, 55.
234 A. H. Md Yusop, M. F. Ulum, A. Al Sakkaf, D. Hartanto and H. Nur, *Biotechnol. J.*, 2021, **16**, 2100255.
235 B. Wegener, A. Sichler, S. Milz, C. Sprecher, K. Pieper, W. Hermanns, V. Jansson, B. Nies, B. Kieback and P. E. Müller, *Sci. Rep.*, 2020, **10**, 9141.
236 B. Wegener, M. Behnke, S. Milz, V. Jansson, C. Redlich, W. Hermanns, C. Birkenmaier, K. Pieper, T. Weißgärber and P. Quadbeck, *Sci. Rep.*, 2021, **11**, 12035.
237 N. Putra, K. Borg, P. Diaz-Payno, M. Leeflang, M. Klimopoulou, P. Taheri, J. Mol, L. Fratila-Apachitei, Z. Huan and J. Chang, *Acta Biomater.*, 2022, **148**, 355–373.
238 J. H. Brock and V. Mulero, *Proc. Nutr. Soc.*, 2000, **59**, 537–540.
239 G. Weiss, *Eur. J. Clin. Invest.*, 2002, **32**, 70–78.
240 B. J. Cherayil, *Immunol. Res.*, 2011, **50**, 1–9.
241 P. Handa, S. Thomas, V. Morgan-Stevenson, B. D. Maliken, E. Gochanour, S. Boukhar, M. M. Yeh and K. V. Kowdley, *J. Leukocyte Biol.*, 2019, **105**, 1015–1026.
242 B. Jia, H. Yang, Z. Zhang, X. Qu, X. Jia, Q. Wu, Y. Han, Y. Zheng and K. Dai, *Bioact. Mater.*, 2021, **6**, 1588–1604.
243 Z.-Z. Shi, X.-X. Gao, H.-J. Zhang, X.-F. Liu, H.-Y. Li, C. Zhou, Y.-X. Yin and L.-N. Wang, *Bioact. Mater.*, 2020, **5**, 210–218.
244 M. Yamaguchi and M. N. Weitzmann, *Mol. Cell. Biochem.*, 2011, **355**, 179–186.
245 J. Tan, S. Li, C. Sun, G. Bao, M. Liu, Z. Jing, H. Fu, Y. Sun, Q. Yang and Y. Zheng, *Adv. Healthcare Mater.*, 2024, **13**, 2302305.
246 H. Ji, G. Shen, H. Liu, Y. Liu, J. Qian, G. Wan and E. Luo, *Bioact. Mater.*, 2024, **38**, 422–437.
247 H. Qiang, C. Hou, Y. Zhang, X. Luo, J. Li, C. Meng, K. Liu, Z. Lv, X. Chen and F. Liu, *Regener. Biomater.*, 2023, **10**, rbad051.
248 J. Zhang, Q. Wu, C. Yin, X. Jia, Z. Zhao, X. Zhang, G. Yuan, H. Hu and Q. Zhao, *J. Leukocyte Biol.*, 2021, **110**, 485–496.
249 X. Chen, M. Wang, F. Chen, J. Wang, X. Li, J. Liang, Y. Fan, Y. Xiao and X. Zhang, *Acta Biomater.*, 2020, **103**, 318–332.

250 X. Sun, Z. Li, X. Wang, J. He and Y. Wu, *Adv. Sci.*, 2024, **11**, 2306062.
251 J. R. Alhamdi, T. Peng, I. M. Al-Naggar, K. L. Hawley, K. L. Spiller and L. T. Kuhn, *Biomaterials*, 2019, **196**, 90–99.
252 X. Wang, A. Liu, Z. Zhang, D. Hao, Y. Liang, J. Dai, X. Jin, H. Deng, Y. Zhao and P. Wen, *Adv. Sci.*, 2024, **11**, 2307329.
253 S. Li, H. Yang, X. Qu, Y. Qin, A. Liu, G. Bao, H. Huang, C. Sun, J. Dai and J. Tan, *Nat. Commun.*, 2024, **15**, 3131.
254 L. Guo, Z. Liang, L. Yang, W. Du, T. Yu, H. Tang, C. Li and H. Qiu, *J. Controlled Release*, 2021, **338**, 571–582.
255 K. Eswar, S. Mukherjee, P. Ganesan and A. K. Rengan, *Eur. Polym. J.*, 2023, **188**, 111935.
256 A. Liu, S. Jin, C. Fu, S. Cui, T. Zhang, L. Zhu, Y. Wang, S. G. Shen, N. Jiang and Y. Liu, *Int. J. Oral Sci.*, 2020, **12**, 33.
257 S.-S. Jin, D.-Q. He, D. Luo, Y. Wang, M. Yu, B. Guan, Y. Fu, Z.-X. Li, T. Zhang and Y.-H. Zhou, *ACS Nano*, 2019, **13**, 6581–6595.
258 Y. Sun, S. Liu, Y. Fu, X.-X. Kou, D.-Q. He, G.-N. Wang, C.-C. Fu, Y. Liu and Y.-H. Zhou, *J. Biomed. Nanotechnol.*, 2016, **12**, 2029–2040.
259 J. Shao, L. Weng, J. Li, H. Lin, H. Wang and J. Lin, *ACS Biomater. Sci. Eng.*, 2022, **8**, 610–619.
260 P. Zhai, X. Peng, B. Li, Y. Liu, H. Sun and X. Li, *Int. J. Biol. Macromol.*, 2020, **151**, 1224–1239.
261 S. Garantziotis and R. C. Savani, *Am. J. Physiol.: Cell Physiol.*, 2022, **323**, C202–C214.
262 H. Deng, J. Wang and R. An, *Front. Pharmacol.*, 2023, **14**, 1131001.
263 S. P. Hart, A. G. Rossi, C. Haslett and I. Dransfield, *PLoS One*, 2012, **7**, e33142.
264 S. Vivers, I. Dransfield and S. P. Hart, *Clin. Sci.*, 2002, **103**, 441–449.
265 J. E. Rayahin, J. S. Buhrman, Y. Zhang, T. J. Koh and R. A. Gemeinhart, *ACS Biomater. Sci. Eng.*, 2015, **1**, 481–493.
266 C.-H. Lee, C.-F. Chiang, F.-C. Kuo, S.-C. Su, C.-L. Huang, J.-S. Liu, C.-H. Lu, C.-H. Hsieh, C.-C. Wang and C.-H. Lee, *Int. J. Mol. Sci.*, 2021, **22**, 11917.
267 Q. Shi, L. Zhao, C. Xu, L. Zhang and H. Zhao, *Molecules*, 2019, **24**, 1766.
268 P. L. Bollyky, J. D. Lord, S. A. Masewicz, S. P. Evanko, J. H. Buckner, T. N. Wight and G. T. Nepom, *J. Immunol.*, 2007, **179**, 744–747.
269 M. R. Leedy, H. J. Martin, P. A. Norowski, J. A. Jennings, W. O. Haggard and J. D. Bumgardner, *Chitosan for biomaterials II*, 2011, pp. 129–165.
270 T. Takeuchi, M. Oyama and T. Hatanaka, *BioTech*, 2024, **13**, 6.
271 X. Huang, M. Chen, H. Wu, Y. Jiao and C. Zhou, *ACS Biomater. Sci. Eng.*, 2020, **6**, 1614–1629.
272 L. Papadimitriou, M. Kaliva, M. Vamvakaki and M. Chatzinikolaidou, *ACS Biomater. Sci. Eng.*, 2017, **3**, 1341–1349.
273 M. J. Moore, Y. T. Lam, M. Santos, R. P. Tan, N. Yang, J. Hung, Z. Li, K. A. Kilian, J. Rnjak-Kovacina and J. B. Pitts, *ACS Biomater. Sci. Eng.*, 2023, **9**, 3320–3334.
274 D. P. Vasconcelos, A. C. Fonseca, M. Costa, I. F. Amaral, M. A. Barbosa, A. P. Águas and J. N. Barbosa, *Biomaterials*, 2013, **34**, 9952–9959.
275 Y. von Boxberg, S. Soares, C. Giraudon, L. David, M. Viallon, A. Montembault and F. Nothias, *J. Biomed. Mater. Res., Part A*, 2022, **110**, 773–787.
276 Y. Li, Z. Xu, J. Wang, X. Pei, J. Chen and Q. Wan, *Int. J. Biol. Macromol.*, 2023, **230**, 123246.
277 M. Ghorbani, E. Vasheghani-Farahani, N. Azarpira, S. Hashemi-Najafabadi and A. Ghasemi, *Biomater. Adv.*, 2023, **153**, 213565.
278 P. Rosiak, I. Latanska, P. Paul, W. Sujka and B. Kolesinska, *Molecules*, 2021, **26**, 7264.
279 A. Hurtado, A. A. Aljabali, V. Mishra, M. M. Tambuwala and Á. Serrano-Aroca, *Int. J. Mol. Sci.*, 2022, **23**, 4486.
280 M. M. Saraiva, M. d. S. Campelo, J. F. Camara Neto, A. B. N. Lima, G. d. A. Silva, A. T. d. F. F. Dias, N. M. P. S. Ricardo, D. L. Kaplan and M. E. N. P. Ribeiro, *J. Biomed. Mater. Res., Part B*, 2023, **111**, 220–233.
281 J. Zhu, *Biomaterials*, 2010, **31**, 4639–4656.
282 G. Pasut and F. M. Veronese, *J. Controlled Release*, 2012, **161**, 461–472.
283 M. Roberts, M. Bentley and J. Harris, *Adv. Drug Delivery Rev.*, 2002, **54**, 459–476.
284 S. Sun, Y. Cui, B. Yuan, M. Dou, G. Wang, H. Xu, J. Wang, W. Yin, D. Wu and C. Peng, *Front. Bioeng. Biotechnol.*, 2023, **11**, 1117647.
285 M. D. Swartzlander, C. A. Barnes, A. K. Blakney, J. L. Kaar, T. R. Kyriakides and S. J. Bryant, *Biomaterials*, 2015, **41**, 26–36.
286 A. D. Lynn and S. J. Bryant, *Acta Biomater.*, 2011, **7**, 123–132.
287 A. K. Blakney, M. D. Swartzlander and S. J. Bryant, *J. Biomed. Mater. Res., Part A*, 2012, **100**, 1375.
288 A. Cam and E. G. de Mejia, *Mol. Nutr. Food Res.*, 2012, **56**, 1569–1581.
289 C. Moon, J. R. Han, H.-J. Park, J. S. Hah and J. L. Kang, *Respir. Res.*, 2009, **10**, 1–15.
290 P. E. Lipsky, L. H. Calabrese, A. Kavanaugh, J. S. Sundy, D. Wright, M. Wolfson and M. A. Becker, *Arthritis Res. Ther.*, 2014, **16**, 1–8.
291 Y. Ju, W. S. Lee, E. H. Pilkington, H. G. Kelly, S. Li, K. J. Selva, K. M. Wragg, K. Subbarao, T. H. Nguyen and L. C. Rowntree, *ACS Nano*, 2022, **16**, 11769–11780.
292 S. Ye, *Nat. Rev. Bioeng.*, 2024, 1–1.
293 A. H. Isaac, S. Y. Recalde Phillips, E. Ruben, M. Estes, V. Rajavel, T. Baig, C. Paleti, K. Landsgaard, R. H. Lee and T. Guda, *Nat. Commun.*, 2024, **15**, 3283.
294 A. Murillo, C. A. Guerrero, O. Acosta and C. A. Cardozo, *Biol. Res.*, 2010, **43**, 205–224.
295 J. Quinn, C. Joyner, J. Triffitt and N. Athanasou, *J. Bone Jt. Surg., Br. Vol.*, 1992, **74**, 652–658.

296 X. Cai, R. Chen, K. Ma, F. Wang, Y. Zhou, Y. Wang and T. Jiang, *Appl. Mater. Today*, 2020, **18**, 100454.
297 H. Zhang, B. F. Ricciardi, X. Yang, Y. Shi, N. P. Camacho and M. P. Bostrom, *Acta Orthop.*, 2008, **79**, 281–288.
298 W. Fan, D. Fu, L. Zhang, Z. Xiao, X. Shen, J. Chen and X. Qi, *J. Orthop. Surg. Res.*, 2023, **18**, 380.
299 L. Yang, J. Kong, Z. Qiu, T. Shang, S. Chen, R. Zhao, M. G. Raucci, X. Yang and Z. Wu, *Regener. Biomater.*, 2020, **7**, 181–193.
300 A. Sabokbar, Y. Fujikawa, D. W. Murray and N. A. Athanasou, *Ann. Rheum. Dis.*, 1998, **57**, 614–618.
301 Y. Xia, H. Wang, Y. Li and C. Fu, *Front. Mater.*, 2022, **9**, 929618.
302 S. Aghyarian, E. Bentley, T. N. Hoang, I. M. Gindri, V. Kosmopoulos, H. K. Kim and D. C. Rodrigues, *ACS Biomater. Sci. Eng.*, 2017, **3**, 2267–2277.
303 S. Soleymani Eil Bakhtiari, H. R. Bakhsheshi-Rad, S. Karbasi, M. Tavakoli, M. Razzaghi, A. F. Ismail, S. RamaKrishna and F. Berto, *Polymers*, 2020, **12**, 1469.
304 H. Zhang, Y. Cui, X. Zhuo, J. Kim, H. Li, S. Li, H. Yang, K. Su, C. Liu and P. Tian, *ACS Appl. Mater. Interfaces*, 2022, **14**, 51711–51727.
305 R. Ma and T. Tang, *Int. J. Mol. Sci.*, 2014, **15**, 5426–5445.
306 L. Wang, H. He, X. Yang, Y. Zhang, S. Xiong, C. Wang, X. Yang, B. Chen and Q. Wang, *Mater. Today Adv.*, 2021, **12**, 100162.
307 F. B. Torstrick, A. S. Lin, D. Potter, D. L. Safranski, T. A. Sulchek, K. Gall and R. E. Guldberg, *Biomaterials*, 2018, **185**, 106–116.
308 Z. Chen, S. Ni, S. Han, R. Crawford, S. Lu, F. Wei, J. Chang, C. Wu and Y. Xiao, *Nanoscale*, 2017, **9**, 706–718.
309 R. Wei, J. Wu and Y. Li, *Mater. Sci. Eng., C*, 2019, **104**, 109948.
310 X. Yang, J. Gao, S. Yang, Y. Wu, H. Liu, D. Su and D. Li, *Int. J. Bioprint.*, 2023, **9**(5), 755.
311 N. Fukuda, A. Tsuchiya, R. Toita, K. Tsuru, Y. Mori and K. Ishikawa, *Colloids Surf., B*, 2019, **173**, 36–42.
312 R. Toita, A. Rashid, K. Tsuru and K. Ishikawa, *J. Mater. Chem. B*, 2015, **3**, 8738–8746.
313 W. Liu, J. Li, M. Cheng, Q. Wang, K. W. Yeung, P. K. Chu and X. Zhang, *Adv. Sci.*, 2018, **5**, 1800749.
314 H.-K. Tsou, M.-H. Chi, Y.-W. Hung, C.-J. Chung and J.-L. He, *BioMed Res. Int.*, 2015, **2015**, 328943.
315 P. Xian, Y. Chen, S. Gao, J. Qian, W. Zhang, A. Udduttula, N. Huang and G. Wan, *Surf. Coat. Technol.*, 2020, **401**, 126282.
316 W. R. Walsh, N. Bertollo, C. Christou, D. Schaffner and R. J. Mobbs, *Spine J.*, 2015, **15**, 1041–1049.
317 Y. Yang, H. Zhang, S. Komasa, T. Kusumoto, S. Kuwamoto, T. Okunishi, Y. Kobayashi, Y. Hashimoto, T. Sekino and J. Okazaki, *Int. J. Mol. Sci.*, 2022, **23**, 612.
318 S. Tang, P. Cheang, M. AbuBakar, K. Khor and K. Liao, *Int. J. Fatigue*, 2004, **26**, 49–57.
319 X. Liu, L. Ouyang, L. Chen, Y. Qiao, X. Ma, G. Xu and X. Liu, *Regener. Biomater.*, 2022, **9**, rbab076.
320 B.-D. Hahn, D.-S. Park, J.-J. Choi, J. Ryu, W.-H. Yoon, J.-H. Choi, J.-W. Kim, C.-W. Ahn, H.-E. Kim and B.-H. Yoon, *Appl. Surf. Sci.*, 2013, **283**, 6–11.
321 D. Almasi, S. Izman, M. Assadian, M. Ghanbari and M. A. Kadir, *Appl. Surf. Sci.*, 2014, **314**, 1034–1040.
322 E. Buck, S. Lee, Q. Gao, S. D. Tran, F. Tamimi, L. S. Stone and M. Cerruti, *ACS Biomater. Sci. Eng.*, 2022, **8**, 1506–1521.
323 E. Buck, S. Lee, L. S. Stone and M. Cerruti, *ACS Appl. Mater. Interfaces*, 2021, **13**, 7021–7036.
324 S. Wang, M. Lu, Y. Cao, Z. Tao, Z. Sun, X. Liu, J. Liu and S. Liu, *Composites, Part B*, 2023, **253**, 110520.
325 H. Yu, Y. Li, Y. Pan, H. Wang, W. Wang, X. Ren, H. Yuan, Z. Lv, Y. Zuo and Z. Liu, *J. Nanobiotechnol.*, 2023, **21**, 110.
326 Y. Huang, Y. Xu, Z. Huang, J. Mao, Y. Hui, M. Rui, X. Jiang, J. Wu, Z. Ding and Y. Feng, *J. Mater. Chem. B*, 2024, **12**, 7367–7383.
327 W. Li, F. Dai, S. Zhang, F. Xu, Z. Xu, S. Liao, L. Zeng, L. Song and F. Ai, *ACS Appl. Mater. Interfaces*, 2022, **14**, 20693–20707.
328 S. Wu, J. Ma, J. Liu, C. Liu, S. Ni, T. Dai, Y. Wang, Y. Weng, H. Zhao and D. Zhou, *ACS Appl. Mater. Interfaces*, 2022, **14**, 15942–15955.
329 Z. Chen, C. Wu, W. Gu, T. Klein, R. Crawford and Y. Xiao, *Biomaterials*, 2014, **35**, 1507–1518.
330 X. Chen, J. Wang, X. Zhu, X. Yang, Y. Fan and X. Zhang, *RSC Adv.*, 2016, **6**, 102134–102141.
331 H. Liu, Q. Wu, S. Liu, L. Liu, Z. He, Y. Liu, Y. Sun, X. Liu and E. Luo, *Biomaterials*, 2024, **304**, 122406.
332 Y. Shi, W. Tao, W. Yang, L. Wang, Z. Qiu, X. Qu, J. Dang, J. He and H. Fan, *J. Nanobiotechnol.*, 2024, **22**, 47.
333 J. Wang, D. Liu, B. Guo, X. Yang, X. Chen, X. Zhu, Y. Fan and X. Zhang, *Acta Biomater.*, 2017, **51**, 447–460.
334 K. Zheng, W. Niu, B. Lei and A. R. Boccaccini, *Acta Biomater.*, 2021, **133**, 168–186.
335 N. Gómez-Cerezo, L. Casarrubios, I. Morales, M. Feito, M. Vallet-Regí, D. Arcos and M. Portolés, *J. Colloid Interface Sci.*, 2018, **528**, 309–320.
336 M. Montes-Casado, A. Sanvicente, L. Casarrubios, M. J. Feito, J. M. Rojo, M. Vallet-Regí, D. Arcos, P. Portolés and M. T. Portolés, *Int. J. Mol. Sci.*, 2020, **21**, 8291.
337 M. Bosetti, L. Hench and M. Cannas, *J. Biomed. Mater. Res.*, 2002, **60**, 79–85.
338 S. Fiorilli, G. Molino, C. Pontremoli, G. Iviglia, E. Torre, C. Cassinelli, M. Morra and C. Vitale-Brovarone, *Materials*, 2018, **11**, 678.
339 K. Zheng, Y. Fan, E. Torre, P. Balasubramanian, N. Taccardi, C. Cassinelli, M. Morra, G. Iviglia and A. R. Boccaccini, *Part. Part. Syst. Charact.*, 2020, **37**, 2000054.
340 K. Zheng, E. Torre, A. Bari, N. Taccardi, C. Cassinelli, M. Morra, S. Fiorilli, C. Vitale-Brovarone, G. Iviglia and A. R. Boccaccini, *Mater. Today Bio*, 2020, **5**, 100041.
341 E. A. Varmette, J. R. Nowalk, L. M. Flick and M. M. Hall, *J. Biomed. Mater. Res., Part A*, 2009, **90**, 317–325.

342 C. Wu, Z. Chen, Q. Wu, D. Yi, T. Friis, X. Zheng, J. Chang, X. Jiang and Y. Xiao, *Biomaterials*, 2015, **71**, 35–47.
343 X. Zhao, X. Zhou, H. Sun, H. Shi, Y. Song, Q. Wang, G. Zhang and D. Xu, *Front. Immunol.*, 2022, **13**, 1001526.
344 D.-W. Zhao, C. Liu, K.-Q. Zuo, P. Su, L.-B. Li, G.-Y. Xiao and L. Cheng, *Chem. Eng. J.*, 2021, **408**, 127362.
345 N. F. Nuswantoro, M. Manjas, N. Suharti, D. Juliadmi, N. Kasuma, Y. Yusuf, Y. W. Sari, M. Niinomi and T. Akahori, *J. Mater. Res. Technol.*, 2024, **30**, 6210–6217.
346 X. Xu, Y. Lu, S. Li, S. Guo, M. He, K. Luo and J. Lin, *Mater. Sci. Eng., C*, 2018, **90**, 198–210.
347 D. Xu, J. Qian, X. Guan, L. Ren, K. Yang, X. Huang, S. Zhang, Y. Chai, X. Wu and H. Wu, *Front. Bioeng. Biotechnol.*, 2021, **8**, 620629.
348 C. Peng, T. Izawa, L. Zhu, K. Kuroda and M. Okido, *ACS Appl. Mater. Interfaces*, 2019, **11**, 45489–45497.
349 Q. Wang, L. Xu, R. Willumeit-Römer and B. J. Luthringer-Feyerabend, *Acta Biomater.*, 2021, **133**, 268–279.
350 L. Chang, Y. Zhong, L. Zhou, S. Zhu, L. Wang, S. Zhu and S. Guan, *Mater. Chem. Phys.*, 2024, **315**, 128980.
351 D. W. Zhao, C. M. Du, K. Q. Zuo, Y. X. Zhao, X. Q. Xu, Y. B. Li, S. Tian, H. R. Yang, Y. P. Lu and L. Cheng, *Adv. Healthcare Mater.*, 2023, **12**, 2202537.
352 C. Meng, X. Luo, J. Li, Y. Zhang, Z. Lv, C. Hou, K. Liu and F. Liu, *Int. J. Biol. Macromol.*, 2024, **269**, 131800.
353 Y. Xuan, L. Li, M. Ma, J. Cao and Z. Zhang, *Front. Bioeng. Biotechnol.*, 2022, **9**, 781268.
354 M. Halperin-Sternfeld, A. Pokhojaev, M. Ghosh, D. Rachmiel, R. Kannan, I. Grinberg, M. Asher, M. Aviv, P. X. Ma and I. Binderman, *J. Clin. Periodontol.*, 2023, **50**, 200–219.
355 P. Kazimierczak, M. Koziol and A. Przekora, *Int. J. Mol. Sci.*, 2021, **22**, 1109.
356 A. Soriente, I. Fasolino, A. Gomez-Sánchez, E. Prokhorov, G. G. Buonocore, G. Luna-Barcenas, L. Ambrosio and M. G. Raucci, *J. Biomed. Mater. Res., Part A*, 2022, **110**, 266–272.
357 Y. Shu, Y. Yu, S. Zhang, J. Wang, Y. Xiao and C. Liu, *Biomater. Sci.*, 2018, **6**, 2496–2507.
358 B. Sun, H. Wang, B. Xiao, H. Yan, H. Wu, R. Zhang, Y. Zhang, W. Yuan, X. Wang and C. Shi, *Chem. Eng. J.*, 2023, **476**, 146743.
359 X. Zhao, J. Gao, H. Han, X. Lou, H. Ma, X. Su, L. Zhang, J. Tian, B. Lei and Y. Zhang, *Chem. Eng. J.*, 2023, **474**, 145609.
360 A. Gao, Q. Liao, L. Xie, G. Wang, W. Zhang, Y. Wu, P. Li, M. Guan, H. Pan and L. Tong, *Biomaterials*, 2020, **230**, 119642.
361 X. Liu, X. Li, S. Huo, L. Lu, C. Zhou and Z. Li, *Colloids Surf., B*, 2023, **230**, 113523.
362 X. Chen, L. Zhou, D. Wu, W. Huang, Y. Lin, B. Zhou and J. Chen, *BioMed Res. Int.*, 2020, **2020**, 2327034.
363 J. Wang, Y. Xue, Y. Wang, C. Liu, S. Hu, H. Zhao, Q. Gu, H. Yang, L. Huang and X. Zhou, *npj Regener. Med.*, 2023, **8**, 6.
364 D.-W. Zhao, K.-Q. Zuo, K. Wang, Z.-Y. Sun, Y.-P. Lu, L. Cheng, G.-Y. Xiao and C. Liu, *Mater. Sci. Eng., C*, 2021, **118**, 111512.
365 H. Zhao, X. Wang, W. Zhang, L. Wang, C. Zhu, Y. Huang, R. Chen, X. Chen, M. Wang and G. Pan, *Front. Bioeng. Biotechnol.*, 2021, **9**, 780609.
366 S. Huo, F. Wang, Z. Lyu, Q. Hong, J. Wei, Y. Wang, J. Zhang and B. Yue, *Chem. Eng. J.*, 2021, **426**, 130806.
367 S. Jin, R. Yang, C. Hu, S. Xiao, Y. Zuo, Y. Man, Y. Li and J. Li, *ACS Appl. Mater. Interfaces*, 2023, **15**, 7804–7820.
368 Y. Cao, L. Xiao, Y. Cao, A. Nanda, C. Xu and Q. Ye, *Biochem. Biophys. Res. Commun.*, 2019, **512**, 889–895.
369 D. Avery, L. Morandini, N. Celt, L. Bergey, J. Simmons, R. K. Martin, H. J. Donahue and R. Olivares-Navarrete, *Acta Biomater.*, 2023, **161**, 285–297.

